



University of Tennessee, Knoxville
**TRACE: Tennessee Research and Creative
Exchange**

Doctoral Dissertations

Graduate School

12-2000

Speeds of invasion for models with Allee effects

Mei-Hui Wang

Follow this and additional works at: https://trace.tennessee.edu/utk_graddiss

Recommended Citation

Wang, Mei-Hui, "Speeds of invasion for models with Allee effects. " PhD diss., University of Tennessee, 2000.

https://trace.tennessee.edu/utk_graddiss/8445

This Dissertation is brought to you for free and open access by the Graduate School at TRACE: Tennessee Research and Creative Exchange. It has been accepted for inclusion in Doctoral Dissertations by an authorized administrator of TRACE: Tennessee Research and Creative Exchange. For more information, please contact trace@utk.edu.

To the Graduate Council:

I am submitting herewith a dissertation written by Mei-Hui Wang entitled "Speeds of invasion for models with Allee effects." I have examined the final electronic copy of this dissertation for form and content and recommend that it be accepted in partial fulfillment of the requirements for the degree of Doctor of Philosophy, with a major in Mathematics.

Mark Kot, Major Professor

We have read this dissertation and recommend its acceptance:

Suzanne Lenhart, Thomas Hallam, Yueh-er Kuo

Accepted for the Council:

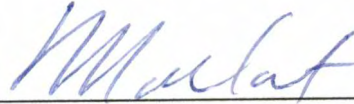
Carolyn R. Hodges

Vice Provost and Dean of the Graduate School

(Original signatures are on file with official student records.)

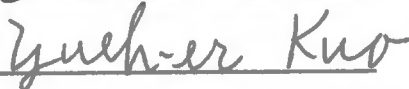
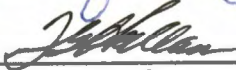
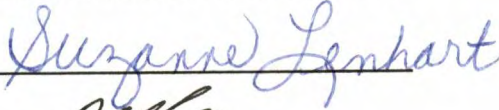
To the Graduate Council:

I am submitting herewith a dissertation written by Mei-Hui Wang entitled "Speeds of Invasion for Models with Allee Effects." I have examined the final copy of this dissertation for form and content and recommend that it be accepted in partial fulfillment of the requirements for the degree of Doctor of Philosophy, with a major in Mathematics.



Mark Kot, Major Professor

We have read this thesis
and recommend its acceptance:



Accepted for the Council:



Associate Vice Chancellor and
Dean of the Graduate School

Speeds of Invasion for Models with Allee Effects

A Dissertation
Presented for the
Doctoral Degree
The University of Tennessee, Knoxville

Mei-Hui Wang
December 2000

Acknowledgments

There are many people whom I appreciate for making my time at University of Tennessee so meaningful. I am particularly grateful to professor Mark Kot for his support and advice. He has read a number of revisions of this dissertation and given me lots of beneficial suggestions. I am also thankful to professors Suzanne Lenhart, Yueh-er Kuo, and Thomas Hallam for their discussions and assistance.

It is a pleasure to acknowledge Doctors Michael Neubert, Bill Fagan, Mark Lewis, and Pauline van den Driessche for suggestions and discussions. I am grateful to the Department of Mathematics and the National Science Foundation (DMS-9973212) for their financial support.

Lastly, I would like to thank my husband, Jin-Ping Gwo for his encouragement.

Abstract

Models that describe the spread of invading organisms often assume no Allee effect. In contrast, abundant observational data provide evidence for Allee effects. In chapter 1, I study an invasion model based on an integrodifference equation with an Allee effect. I derive a general result for the sign of the speed of invasion. I then examine a special, linear-constant, Allee growth function and introduce a numerical scheme that allows me to estimate the speed of traveling wave solutions. In chapter 2, I study an invasion model based on a reaction-diffusion equation with an Allee effect. I use a special, piecewise-linear, Allee population growth rate. This function allows me to obtain traveling wave solutions and to compute wave speeds for a full range of Allee effects, including weak Allee effects. Some investigators claim that linearization fails to give the correct speed of invasion if there is an Allee effect. I show that the minimum speed for a sufficiently weak Allee may be the same as that derived by means of linearization. In chapters 3 and 4, I extend a discrete-time analog of the Lotka-Volterra competition equations to an integrodifference-competition model and analyze this model by investigating traveling wave solutions. The speed of wave is calculated as a function of the model parameters by linearization. I also show that the linearization may fail to give the correct speed for the competition model with strongly interacting competitors because of the introduction of a “weak Allee effect”. A linear-constant approximation to the resulting Allee growth function is

introduced to estimate the speed under this weak Allee effect. I also analyze the back of the wave for the competition model. Some sufficient conditions that guarantee no oscillation behind the wave are given.

Contents

1	Integrodifference Equations, Allee Effects, and Invasions	1
1.1	Introduction	1
1.2	A general result	5
1.3	Estimating invasion speed:	
	a numerical scheme	14
	1.3.1 Traveling wave solutions	16
1.4	Other numerical examples	24
1.5	Discussion	27
2	Speeds of Invasion in a Model with Strong or Weak Allee Effects	32
2.1	Introduction	32
2.2	The model	37
2.3	Traveling wave solutions	38
	2.3.1 Strong Allee effect ($b < 0$)	42
	2.3.2 Weak Allee effect ($0 < b < 1$)	46
2.4	General case	52
2.5	Conclusion and discussion	56

3	Integrodifference Equations and Competition Models, I	59
3.1	Introduction	59
3.2	The model	60
3.3	Traveling waves	65
3.3.1	The front and the speed of the wave	65
3.3.2	The behavior behind the wave	79
4	Integrodifference Equations and Competition Models, II	91
4.1	Traveling waves	91
4.1.1	The behavior behind the wave	92
4.2	Discussion	111
	Bibliography	114
	Appendix	129
	Vita	135

List of Tables

2.1	Wave speeds c and minimum speeds c^* for population growth rate (2.2.2)	52
2.2	Minimum speeds c^* and possible speeds c for population growth rate (2.4.1)	53
2.3	Traveling wave solutions u and the slowest heteroclinic connections u^* for (2.4.1)	54

List of Figures

1.1	Representative strong and weak Allee growth functions	3
1.2	The sum of area A and area B = 1	12
1.3	The area below the growth function and above the 45° line equals the area above the growth function and below the 45° line	13
1.4	A rational growth function and its traveling wave solutions for various choices of the parameter B	15
1.5	The Linear-constant Allee growth function	16
1.6	The speed c as a function of λ for the Laplace distribution	22
1.7	The error in λ for different orders of power series (1.3.10c) for the Laplace distribution	23
1.8	The speed c as a function of λ for the Laplace, normal, expo- nential square root, and Cauchy kernels	25
1.9	The slope λ as a function of the upper limit of integration L for the Cauchy distribution	28
1.10	The slope λ as a function of the upper limit of integration L for the exponential square root distribution	29

2.1	Representative strong, weak, and no-Allee-effect population growth rates and the corresponding per capita growth rates . . .	33
2.2	The piecewise-linear Allee population growth rate	39
2.3	The phase plane for traveling wave solutions of function (2.2.2) with $b < 0$	43
2.4	The minimum speed c^* as a function of b	44
2.5	The traveling wave solution for various choices of the parameter b and speed c	45
2.6	The phase planes for traveling wave solutions of function (2.2.2) with $b > 0$	47
2.7	The minimum speed c^* as a function of the parameter a (b) for various choices of b (a)	55
3.1	The speed c^* as a function of $\lambda_1/[1 + (\lambda_1 - 1)\beta_{12}]$ for IDEs (3.2.13) with the Laplace kernels (3.3.16)	69
3.2	The observed speed \bar{c} for IDEs (3.2.13) with the Laplace kernels (3.3.16)	70
3.3	The observed speed \bar{c} for IDEs (3.2.13) with kernels (3.3.27) and (3.3.28)	72
3.4	Weak Allee growth rate (3.3.41c)	75
3.5	The observed speed \bar{c} of IDEs (3.2.13) with kernels (3.3.52) . . .	78
3.6	Growth function F in (3.3.41c) and its linear-constant approximation F^*	80

3.7	The root s^* of equation (3.3.99)	88
3.8	The traveling wave solution for IDEs (3.2.13) with Laplace kernels (3.3.16)	89
3.9	The traveling wave solution for IDEs (3.2.13) with kernels (3.3.27) and (3.3.28)	90
4.1	The traveling wave solution for IDEs (3.2.13) with two same Laplace kernels (4.1.31)	101
4.2	The traveling wave solution for IDEs (3.2.13) with kernels (4.1.44)	103
4.3	The traveling wave solution for IDEs (3.2.13) with kernels (4.1.104) and (4.1.105)	112

Chapter 1

Integrodifference Equations, Allee Effects, and Invasions

1.1 Introduction

Ecologists are increasingly concerned with the effects of invading organisms [23, 42, 76, 94]. Thus, there is keen interest in models that can predict the rates of spread of invaders. Most invasion models have per capita growth rates that decrease with density. For these models, one can determine the speed of invasion from a linearized version of the original model [75, 99]. At the same time, many natural populations exhibit Allee effects [1, 2] or depensation [19] and show an increase in the per capita growth rate at low densities. This complicates matters: linearization may fail to give the correct speed of invasion if there is an Allee effect.

Allee effects may be weak or strong. Consider the density-dependent difference equation

$$N_{t+1} = f(N_t), \tag{1.1.1}$$

where N_t is the population size in generation t . I will assume that the growth function $f(N_t)$ satisfies

$$f(0) = 0, \quad f(1) = 1, \quad (1.1.2)$$

so that there is a trivial equilibrium at the origin and a nontrivial equilibrium that has been normalized to one. I will also assume that there is, at most, one other equilibrium between zero and one. Under these assumptions, the population exhibits a strong Allee effect if there exists a range of N_t , in the interval of $[0, 1]$, such that

$$f(N_t) > f'(0)N_t, \quad 0 \leq f'(0) < 1, \quad (1.1.3)$$

and a weak Allee effect if there exists a range of N_t , in the interval of $[0, 1]$, such that

$$f(N_t) > f'(0)N_t, \quad f'(0) > 1. \quad (1.1.4)$$

A strong Allee effect introduces a population threshold. The population must surpass this threshold to grow. Figure 1.1 shows representative strong and weak Allee growth functions.

Allee effects can arise from a shortage of mates [45, 46, 63, 74, 100], lack of effective pollination [33, 62], population fragmentation [34, 64], or many other causes. Allee effects can slow down or stall an invasion [66, 67].

In this chapter, I will analyze integrodifference equations (IDEs) with Allee effects. IDEs are models for populations with discrete, nonoverlapping generations and well-defined growth and dispersal stages. In the simplest

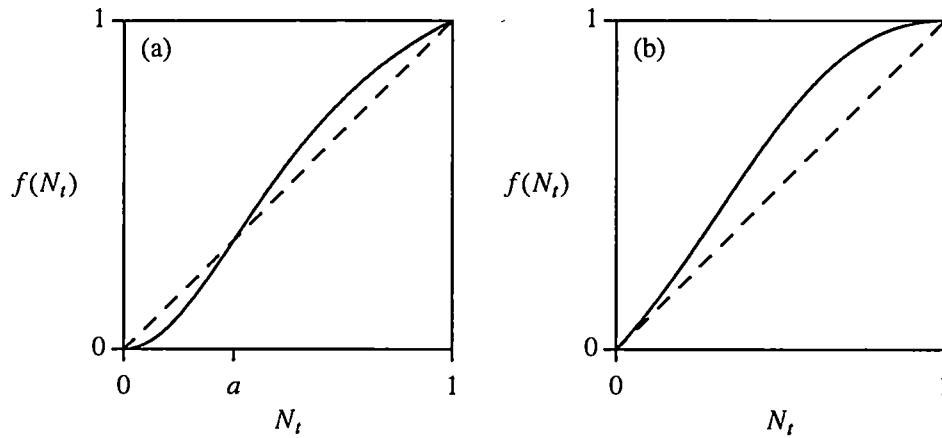


Figure 1.1: Representative strong and weak Allee growth functions

The strong Allee growth function in subfigure (a) has population threshold a , and satisfies the conditions that $f(N_t) > f'(0)N_t$, $0 \leq f'(0) < 1$, for a range of N_t in $[0, 1]$. The weak Allee growth function in subfigure (b) has no population threshold, but there is a range of N_t in $[0, 1]$ such that $f(N_t) > f'(0)N_t$ with $f'(0) > 1$.

case,

$$N_{t+1}(x) = \int_{-\infty}^{+\infty} k(x-y)f(N_t(y)) dy, \quad (1.1.5)$$

where $N_t(x)$ is the population density, in space, of a species at generation t . Time is discrete, space is continuous. The function $f(N_t(x))$ describes the growth of a species during its sedentary stage. The redistribution kernel $k(x-y)$ is the probability density function for dispersal from a source at y . Neubert et al. [77] describe how dispersal kernels can arise from mechanistic models of dispersal. The integral tallies dispersal from all sources y .

Interest in IDEs in ecology has been increasing [3, 6, 15, 16, 20, 36, 37, 38, 39, 41, 57, 58, 59, 60, 65, 77, 79, 99, 100]. One reason is that IDEs can handle an extremely wide variety of dispersal distributions. IDEs can have traveling wave solutions [39, 58, 70, 71, 72, 103, 104] similar to those of reaction-diffusion equations. However, they can also give rise to accelerating invasions [20, 60].

Despite this keen interest, there has been little work on Allee effects and IDEs. Lewis and Veit [100] used an IDE with an Allee effect to describe the dynamics of the House Finch invasion in eastern North America. Their model was quite general, but they relied on numerical simulations. In contrast, Kot et al. [60] took an analytic approach, but focused on an extremely narrow limiting case. In this chapter, I extend the work of Kot et al. [60]. I also hope to complement recent work on Allee effects in reaction-diffusion models [21, 66].

In section 1.2, I derive a general result on the sign of the speed of invasion

in the presence of an Allee effect. I follow this, in section 1.3, with an iterative scheme for estimating the rate of spread for a linear–constant Allee growth function. I use this scheme, in section 1.4, to estimate the rates of spread for both thin and fat-tailed dispersal kernels. I discuss the implications of my results in section 1.5.

1.2 A general result

In this section, I derive conditions that determine whether a traveling wave solution advances or retreats. I assume that the dynamics of a population is described by the IDE

$$N_{t+1}(x) = \int_{-\infty}^{+\infty} k(x-y)f(N_t(y)) dy, \quad (1.2.1)$$

where the kernel $k(x-y)$ is a bounded and symmetric probability density function that satisfies

$$\int_{-\infty}^{+\infty} k(z) dz = 1. \quad (1.2.2)$$

I also assume that the growth function is infinitely smooth ($f \in C^\infty$), increases with density,

$$f'(N) > 0, \quad (1.2.3)$$

and satisfies

$$f(N) \geq 0, \quad f(0) = 0, \quad f(1) = 1. \quad (1.2.4)$$

I am thus ignoring the possibility of overcompensation. Since f is strictly increasing, I can define its inverse f^{-1} .

Under these assumptions, it is reasonable to look for traveling wave solutions

$$N_{t+1}(x) = N_t(x - c) \quad (1.2.5)$$

that satisfy

$$\lim_{x \rightarrow -\infty} N_t(x) = 1, \quad \lim_{x \rightarrow +\infty} N_t(x) = 0 \quad (1.2.6)$$

[58, 70, 71, 72, 103, 104]. The number c is the speed of the wave. If $c > 0$, the wave front moves toward low densities, and the population always approaches the carrying capacity; the invader is successful. On the other hand, if $c < 0$, the wave front moves toward high densities, and the population eventually goes extinct everywhere.

The traveling waves satisfy

$$N(x - c) = \int_{-\infty}^{+\infty} k(x - y) f(N(y)) dy, \quad (1.2.7)$$

where I have now taken the liberty of dropping the subscripts on the N_t 's. I will assume that these waves are infinitely smooth, $N(x) \in C^\infty$, and strictly decreasing, $N'(x) < 0$. I will also assume that

$$\lim_{x \rightarrow -\infty} \frac{d^i N}{dx^i} = \lim_{x \rightarrow +\infty} \frac{d^i N}{dx^i} = 0, \quad i = 1, 2, \dots \quad (1.2.8)$$

and that there exists a positive number M such that

$$\left| \frac{d^i f(N(x))}{dx^i} \right| \leq M \text{ for all } x \text{ and } i = 1, 2, \dots \quad (1.2.9)$$

Lui [72] discusses conditions that guarantee the existence of traveling waves for models with Allee effects.

Based on the above assumptions, I derive the following result:

Theorem 1.1. For the traveling wave solutions of IDE (1.2.1),

$$c < 0 \iff \int_0^1 [f(N) - N] dN < 0, \quad (1.2.10)$$

$$c > 0 \iff \int_0^1 [f(N) - N] dN > 0, \quad (1.2.11)$$

and

$$c = 0 \iff \int_0^1 [f(N) - N] dN = 0. \quad (1.2.12)$$

Here, \iff means "if and only if".

Proof : If I subtract $N(x)$ from both sides of traveling-wave equation (1.2.7) and let $z \equiv x - y$, I obtain

$$N(x - c) - N(x) = \int_{-\infty}^{+\infty} k(x - y) f(N(y)) dy - N(x) \quad (1.2.13)$$

$$= \int_{-\infty}^{+\infty} k(z) f(N(x - z)) dz - N(x). \quad (1.2.14)$$

Let me write $f(N(x - z))$ as the sum of an odd and an even function in z ,

$$f(N(x - z)) = f_o(x, z) + f_e(x, z), \quad (1.2.15)$$

where

$$f_o(x, z) = \frac{1}{2}[f(N(x - z)) - f(N(x + z))], \quad (1.2.16)$$

$$f_e(x, z) = \frac{1}{2}[f(N(x - z)) + f(N(x + z))]. \quad (1.2.17)$$

Since $f(N(x - z))$ and $f(N(x + z))$ are bounded by zero and one, and because the kernel integrates to one, equation (1.2.2), the integrals of $k(z)f(N(x - z))$,

$k(z)f_o(x, z)$, and $k(z)f_e(x, z)$ with respect to z each exist and

$$\int_{-\infty}^{+\infty} k(z)f(N(x-z)) dz = \int_{-\infty}^{+\infty} k(z)f_o(x, z) dz + \int_{-\infty}^{+\infty} k(z)f_e(x, z) dz. \quad (1.2.18)$$

The first integral on the right hand side of equation (1.2.18) equals zero because $k(z)f_o(x, z)$ is an odd function in z . It follows that

$$N(x-c) - N(x) = \int_{-\infty}^{+\infty} k(z)f_e(x, z) dz - N(x). \quad (1.2.19)$$

If I multiply equation (1.2.19) by $df(N(x))/dx$ and integrate with respect to x from $-\infty$ to $+\infty$, I get

$$\int_{-\infty}^{+\infty} [N(x-c) - N(x)] \frac{df}{dx} dx = \int_{-\infty}^{+\infty} \int_{-\infty}^{+\infty} k(z)f_e(x, z) \frac{df}{dx} dz dx - \int_{-\infty}^{+\infty} N(x) \frac{df}{dx} dx, \quad (1.2.20)$$

where

$$\frac{df}{dx} \equiv \frac{df(N(x))}{dx}. \quad (1.2.21)$$

Since f is a strictly increasing function of N and N is a strictly decreasing function of x , the derivative of f with respect to x is negative. The integrand $k(z)f_e(x, z)df/dx$ is thus of one sign. By Tonelli's Theorem [105], I can switch the order of integration in the first integral on the right hand side of equation (1.2.20).

Let me expand $f_e(x, z)$ as a Taylor series in z ,

$$f_e(x, z) = f(N(x)) + \sum_{i=1}^{\infty} \frac{z^{2i}}{(2i)!} \frac{d^{2i}f(N(x))}{dx^{2i}}. \quad (1.2.22)$$

It follows that

$$\int_{-\infty}^{+\infty} [N(x-c) - N(x)] \frac{df}{dx} dx = \int_{-\infty}^{+\infty} [f(N(x)) - N(x)] \frac{df}{dx} dx + \int_{-\infty}^{+\infty} \int_{-\infty}^{+\infty} \sum_{i=1}^{\infty} J_i(x, z) dx dz. \quad (1.2.23)$$

where

$$J_i(x, z) \equiv k(z) \frac{z^{2i}}{(2i)!} \frac{d^{2i} f}{dx^{2i}} \frac{df}{dx} \quad (1.2.24)$$

and

$$\frac{d^{2i} f}{dx^{2i}} \equiv \frac{d^{2i} f(N(x))}{dx^{2i}}. \quad (1.2.25)$$

I will now show that the second integral on the right hand side of equation (1.2.23) vanishes. The bound (1.2.9) guarantees that $\{J_i(x, z)\}$ is a sequence of integrable functions in x . Moreover, for fixed z ,

$$\sum_{i=1}^{\infty} \int_{-\infty}^{+\infty} |J_i(x, z)| dx = \sum_{i=1}^{\infty} \int_{-\infty}^{+\infty} k(z) \frac{z^{2i}}{(2i)!} \left| \frac{d^{2i} f}{dx^{2i}} \right| \left| \frac{df}{dx} \right| dx \quad (1.2.26)$$

$$\leq \sum_{i=1}^{\infty} M k(z) \frac{z^{2i}}{(2i)!} \int_{-\infty}^{+\infty} \left| \frac{df}{dx} \right| dx \quad (1.2.27)$$

$$\leq M k(z) \sum_{i=1}^{\infty} \frac{z^{2i}}{(2i)!} \quad (1.2.28)$$

$$\leq M k(z) [\cosh(z) - 1] < \infty. \quad (1.2.29)$$

Thus, by the Levi Theorem for series [8]

$$\int_{-\infty}^{+\infty} \int_{-\infty}^{+\infty} \sum_{i=1}^{\infty} J_i(x, z) dx dz = \int_{-\infty}^{+\infty} \sum_{i=1}^{\infty} \int_{-\infty}^{+\infty} J_i(x, z) dx dz \quad (1.2.30)$$

or

$$\int_{-\infty}^{+\infty} \int_{-\infty}^{+\infty} \sum_{i=1}^{\infty} J_i(x, z) dx dz = \int_{-\infty}^{+\infty} \sum_{i=1}^{\infty} k(z) \frac{z^{2i}}{(2i)!} S_i dz, \quad (1.2.31)$$

where

$$S_i \equiv \int_{-\infty}^{+\infty} \frac{d^{2i} f}{dx^{2i}} \frac{df}{dx} dx. \quad (1.2.32)$$

However, all of the S_i vanish by integration by parts,

$$S_1 = \int_{-\infty}^{+\infty} \frac{d^2 f}{dx^2} \frac{df}{dx} dx = \frac{1}{2} \left(\frac{df}{dx} \right)^2 \Big|_{-\infty}^{+\infty} = \frac{1}{2} \left(\frac{df}{dN} \frac{dN}{dx} \right)^2 \Big|_{-\infty}^{+\infty} = 0, \quad (1.2.33)$$

$$S_2 = \int_{-\infty}^{+\infty} \frac{d^4 f}{dx^4} \frac{df}{dx} dx = \left(\frac{d^3 f}{dx^3} \frac{df}{dx} \right) \Big|_{-\infty}^{+\infty} - \int_{-\infty}^{+\infty} \frac{d^3 f}{dx^3} \frac{d^2 f}{dx^2} dx \quad (1.2.34)$$

$$= 0 - \frac{1}{2} \left(\frac{d^2 f}{dx^2} \right)^2 \Big|_{-\infty}^{+\infty} = 0, \quad (1.2.35)$$

$$S_i = \int_{-\infty}^{+\infty} \frac{d^{2i} f}{dx^{2i}} \frac{df}{dx} dx \quad (1.2.36)$$

$$= \left(\frac{d^{2i-1} f}{dx^{2i-1}} \frac{df}{dx} \right) \Big|_{-\infty}^{+\infty} - \int_{-\infty}^{+\infty} \frac{d^{2i-1} f}{dx^{2i-1}} \frac{d^2 f}{dx^2} dx \quad (1.2.37)$$

$$= \dots = (-1)^{i-1} \int_{-\infty}^{+\infty} \frac{d^{i+1} f}{dx^{i+1}} \frac{d^i f}{dx^i} dx \quad (1.2.38)$$

$$= \frac{(-1)^{i-1}}{2} \left(\frac{d^i f}{dx^i} \right)^2 \Big|_{-\infty}^{+\infty} = 0, \quad i \geq 3. \quad (1.2.39)$$

Notice that the above calculations require

$$\lim_{x \rightarrow -\infty} \frac{d^i f}{dx^i} = \lim_{x \rightarrow +\infty} \frac{d^i f}{dx^i} = 0, \quad i = 1, 2, \dots, \quad (1.2.40)$$

which can be deduced from asymptotic boundary condition (1.2.8) using the chain rule.

Since the integrals in equation (1.2.31) equal zero, integral equation (1.2.23) reduces to

$$\int_{-\infty}^{+\infty} [N(x-c) - N(x)] \frac{df}{dx} dx = \int_{-\infty}^{+\infty} [f(N(x)) - N(x)] \frac{df}{dx} dx \quad (1.2.41)$$

or

$$\int_{-\infty}^{+\infty} [N(x-c) - N(x)] \frac{df}{dx} dx = \int_1^0 [f(N) - N] \frac{df}{dN} dN. \quad (1.2.42)$$

Setting $y \equiv f(N)$ gives me that

$$\int_1^0 [f(N) - N] \frac{df}{dN} dN = - \int_0^1 y dy + \int_0^1 f^{-1}(y) dy. \quad (1.2.43)$$

Since the sum of the two areas bounded by

$$y = 1, \quad N = 0, \quad y = f(N) \quad (1.2.44)$$

and

$$y = 0, \quad N = 1, \quad y = f(N) \quad (1.2.45)$$

equals one (see Figure 1.2), I have

$$\int_0^1 f^{-1}(y) dy = 1 - \int_0^1 f(N) dN. \quad (1.2.46)$$

It follows that

$$\int_{-\infty}^{+\infty} [N(x-c) - N(x)] \frac{df}{dx} dx = - \int_0^1 N dN + 1 - \int_0^1 f(N) dN \quad (1.2.47)$$

or

$$\int_{-\infty}^{+\infty} [N(x-c) - N(x)] \frac{df}{dx} dx = \int_0^1 [N - f(N)] dN. \quad (1.2.48)$$

Since N is a strictly decreasing function of x and the derivative of f with respect to x is negative, I have

$$c > 0 \iff N(x-c) - N(x) > 0 \text{ on } (-\infty, \infty) \quad (1.2.49)$$

$$\iff \int_{-\infty}^{+\infty} [N(x-c) - N(x)] \frac{df}{dx} dx < 0 \quad (1.2.50)$$

$$\iff \int_0^1 [f(N) - N] dN > 0. \quad (1.2.51)$$

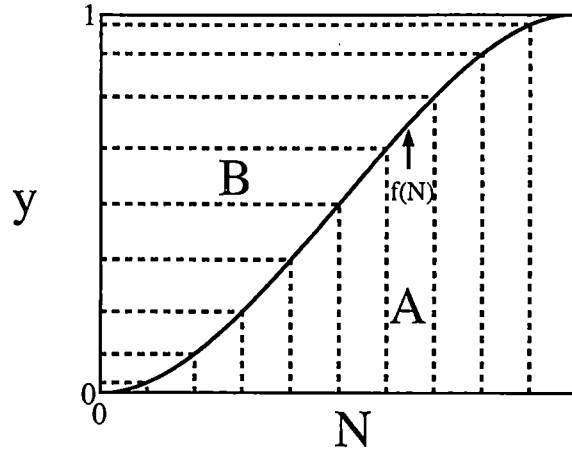


Figure 1.2: The sum of area A and area B = 1

Note: Area A is the area bounded by (1.2.45) and area B is the area bounded by (1.2.44).

Similarly, I can show that result (1.2.10) for the negative sign of the speed and result (1.2.12) for the steady-state solution hold. \square

Theorem 1.1 implies that the wave is advancing if and only if

$$\int_0^1 [f(N) - N] dN > 0, \quad (1.2.52)$$

and that it is retreating if and only if

$$\int_0^1 [f(N) - N] dN < 0. \quad (1.2.53)$$

The wave is a steady state if the area below the growth function and above the 45° line equals the area above the growth function and below the 45° line,

$$\int_0^1 [f(N) - N] dN = 0 \quad (1.2.54)$$

(see Figure 1.3).

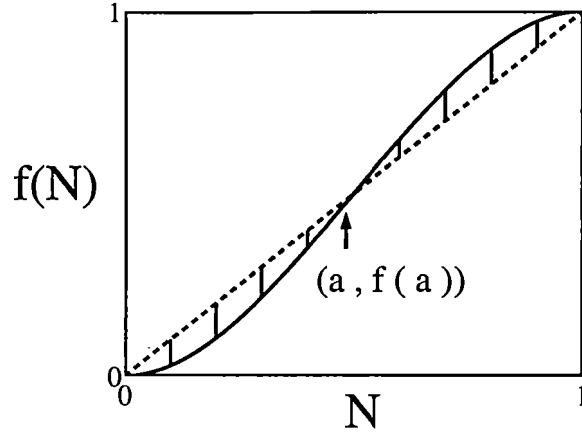


Figure 1.3: The area below the growth function and above the 45° line equals the area above the growth function and below the 45° line

Example 1.2.1. Consider IDE (1.2.1) with growth function

$$f(N) = \frac{BN^2}{1 + (B-1)N^2}, \quad (1.2.55)$$

where $B > 2$. Under the assumptions at the beginning of this section, I can determine the sign of the speed c of the wave solution for various choices of B .

Since

$$\int_0^1 [f(N) - N] dN = \frac{B}{B-1} \left(1 - \frac{\tan^{-1}(\sqrt{B-1})}{\sqrt{B-1}} \right) - \frac{1}{2}, \quad (1.2.56)$$

I conclude that $c > 0$ if and only if

$$\frac{B}{B-1} \left(1 - \frac{\tan^{-1}(\sqrt{B-1})}{\sqrt{B-1}} \right) > \frac{1}{2}, \quad (1.2.57)$$

or

$$B > 3.2952 \dots \quad (1.2.58)$$

I also have $c < 0$ for $B < 3.2952\dots$ and $c = 0$ for $B = 3.2952\dots$. Figure 1.4 shows the growth functions and traveling wave solutions for $B = 5.0, 3.2952,$ and $2.\bar{3}$. □

1.3 Estimating invasion speed: a numerical scheme

Theorem 1.1 determines the direction of a traveling wave solution of IDE (1.2.1) with an Allee effect. The theorem does not give me the actual speed. Unfortunately, even estimating the speed for most Allee growth functions is difficult. In this section, I develop a numerical scheme to estimate the invasion speed for a particularly simple growth function [78]:

$$f(N_t) = \begin{cases} \lambda N_t, & N_t < a, \\ 1, & N_t > a, \end{cases} \quad (1.3.1a)$$

where

$$0 \leq \lambda \leq \frac{1}{a}, \quad 0 < a < 1 \quad (1.3.1b)$$

(see Figure 1.5).

Notice that $f(N_t)$ has a strong Allee effect if

$$0 \leq \lambda < 1, \quad (1.3.2)$$

a weak Allee effect if

$$1 < \lambda < \frac{1}{a}, \quad (1.3.3)$$

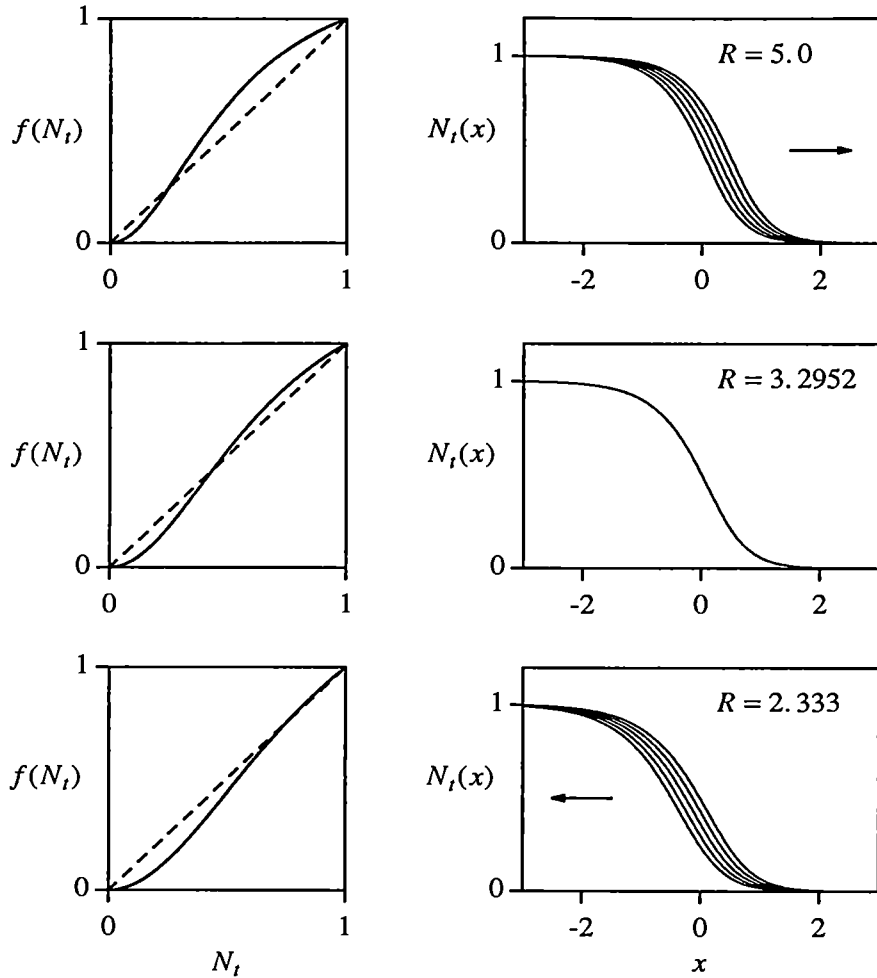


Figure 1.4: A rational growth function and its traveling wave solutions for various choices of the parameter B

The growth function, equation (1.2.55), is shown on the left for $B = 5$ (top), $B = 3.2952$ (middle), and $B = 7/3$ (bottom). The traveling wave solutions for these parameters are shown on the right. If the area between the growth function and the 45° line is positive (top), the waves move to the right. If this area is negative (bottom), the waves move to the left. If this area is zero (middle), the traveling wave is a steady-state cline. The waves were simulated by integrating IDE (1.1.5) with 2^{13} mesh points and an FFT-assisted implementation of the trapezoidal rule. The kernel was the Laplace distribution, equation (1.3.11), with $\alpha = 3$. Each panel shows five iterates of the traveling wave.

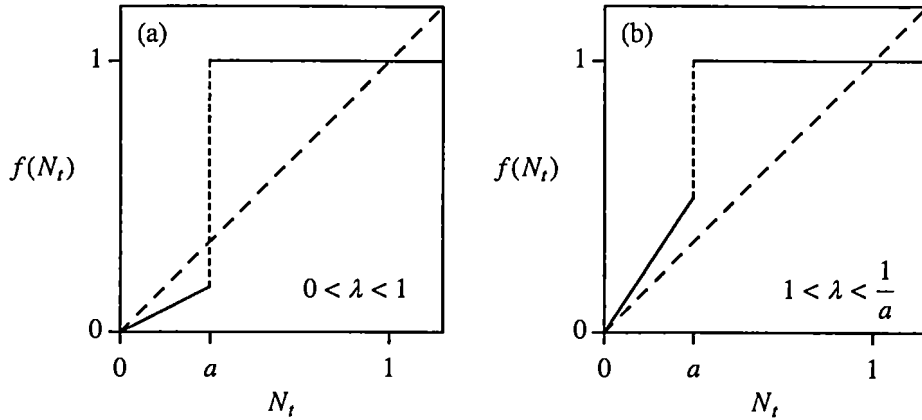


Figure 1.5: The Linear-constant Allee growth function

The growth function is defined by equations (1.3.1a) and (1.3.1b); it consists of a linear ramp of slope λ and a constant top. The function has (a) a strong Allee effect for $0 \leq \lambda < 1$ and (b) a weak Allee effect for $1 < \lambda < 1/a$. There is no Allee effect for $\lambda = 1/a$.

and no Allee effect if

$$\lambda = \frac{1}{a}. \quad (1.3.4)$$

I study IDE (1.2.1) with a symmetric kernel and the linear-constant Allee growth function (1.3.1). I introduce a numerical scheme for estimating the speed of the traveling wave solutions.

1.3.1 Traveling wave solutions

To estimate the speed of invasion, I look for a traveling wave solution. Suppose this traveling wave is moving to the right and that it attains the threshold value a at $x = 0$ and time t . Traveling-wave equation (1.2.7) and equation

(1.3.1a) imply that the traveling wave satisfies

$$N(x - c) = \lambda \int_0^{\infty} k(x - y)N(y)dy + G(x), \quad (1.3.5a)$$

$$N(0) = a, \quad (1.3.5b)$$

where

$$G(x) \equiv 1 - \int_{-\infty}^x k(z)dz. \quad (1.3.5c)$$

I have, once again, dropped the subscript on N_t . Equation (1.3.5a) is a Wiener–Hopf integral-difference equation [32]. If $c = 0$, then equation (1.3.5a) is a one-sided or Wiener–Hopf integral equation of the second kind [43, 88].

For the case $\lambda = 0$, system (1.3.5) reduces to

$$N(x) = G(x + c), \quad (1.3.6a)$$

$$G(c) = a. \quad (1.3.6b)$$

I may thus conclude that the traveling wave solution takes the shape of the function $G(x)$ and that the speed c is given by equation (1.3.6b), or

$$c = G^{-1}(a) \quad (1.3.7)$$

(see [60] for details).

For the case $\lambda \neq 0$, I will try to solve system (1.3.5) by considering a Neumann series [88] of the form

$$N(x) = \sum_{i=0}^{\infty} \lambda^i u_i(x). \quad (1.3.8)$$

After substituting this series into system (1.3.5) and matching powers of λ , I obtain

$$u_0(x) = G(x + c), \quad (1.3.9a)$$

$$u_i(x) = \int_0^\infty k(x + c - y)u_{i-1}(y) dy, \quad i = 1, 2, \dots, \quad (1.3.9b)$$

$$a = G(c) + u_1(0)\lambda + u_2(0)\lambda^2 + \dots \quad (1.3.9c)$$

It is difficult to apply numeric methods directly to equation (1.3.9b) because of the infinite upper limit of integration. For Wiener–Hopf equations, numerical analysts commonly use a finite-section approximation [7, 11, 44, 96]. This approximation allows me to replace the infinite upper limit of integration with an appropriate positive finite number L , so that iterative method (1.3.9) becomes

$$u_0(x) = G(x + c), \quad (1.3.10a)$$

$$u_i(x) = \int_0^L k(x + c - y)u_{i-1}(y) dy, \quad i = 1, 2, \dots, \quad (1.3.10b)$$

$$a = G(c) + u_1(0)\lambda + u_2(0)\lambda^2 + \dots \quad (1.3.10c)$$

The accuracy of this method is sensitive to the choice of L .

If I choose a value of c , I can iterate equation (1.3.10b) starting with the function $G(x + c)$. For the integration, I use a fast-Fourier-transform-assisted [6] implementation of the trapezoidal rule. For each iteration, I evaluate $u_i(x)$ at the origin to get the next coefficient in equation (1.3.10c). Equation (1.3.10c) gives the relationship between the speed c and λ . Since all of the u_i are positive, Descartes's rule of signs guarantees that equation

(1.3.10c) has a single positive root λ for fixed c . I determine this root and solve for λ as a function of c (or, equivalently, for c as a function of λ) numerically using Brent's method [89].

Even though this is a numerical scheme, I can calculate the successive iterates, $u_i(x)$, analytically for at least one choice of the kernel $k(x)$. This kernel lets me test the effectiveness of Dr. Kot's code.

Example 1.3.1. Consider the Laplace kernel

$$k(x) = \frac{1}{2}\alpha e^{-\alpha|x|}, \quad (1.3.11)$$

with

$$G(x) = \begin{cases} \frac{1}{2}e^{-\alpha x}, & x \geq 0, \\ 1 - \frac{1}{2}e^{\alpha x}, & x < 0. \end{cases} \quad (1.3.12)$$

For the case $\lambda = 0$, I have

$$N(x) = G(x+c) = \begin{cases} \frac{1}{2}e^{-\alpha(x+c)}, & x \geq 0, \\ 1 - \frac{1}{2}e^{\alpha(x+c)}, & x < 0, \end{cases} \quad (1.3.13)$$

and

$$c = G^{-1}(a) = \begin{cases} \frac{1}{\alpha} \ln 2(1-a), & a > \frac{1}{2}, \\ -\frac{1}{\alpha} \ln(2a), & a < \frac{1}{2}. \end{cases} \quad (1.3.14)$$

For Laplace kernel (1.3.11) with $\lambda \neq 0$, equation (1.3.5a) can be rewritten

$$\begin{aligned} N(x) &= \lambda \int_0^{x+c} \frac{1}{2}\alpha e^{-\alpha(x+c-y)} N(y) dy \\ &\quad + \lambda \int_{x+c}^{+\infty} \frac{1}{2}\alpha e^{\alpha(x+c-y)} N(y) dy + G(x+c), \end{aligned} \quad (1.3.15)$$

for $x > -c$, and

$$N(x) = \lambda \int_0^{+\infty} \frac{1}{2} \alpha e^{\alpha(x+c-y)} N(y) dy + G(x+c), \quad (1.3.16)$$

for $x < -c$. The solution on the interval $(-\infty, -c)$ is determined by the solution on the right-half real line ($x > 0$).

After applying algorithm (1.3.10) to equation (1.3.15), I obtain

$$u_0(x) = \frac{1}{2} e^{-\alpha(x+c)}, \quad (1.3.17a)$$

$$u_i(x) = \int_0^{x+c} \frac{1}{2} \alpha e^{-\alpha(x+c-y)} u_{i-1}(y) dy + \int_{x+c}^{+\infty} \frac{1}{2} \alpha e^{\alpha(x+c-y)} u_{i-1}(y) dy \quad i = 1, 2, \dots, \quad (1.3.17b)$$

$$a = G_1(c) + u_1(0)\lambda + u_2(0)\lambda^2 + \dots \quad (1.3.17c)$$

for $x > -c$.

To second order in λ , I have

$$N(x) = \frac{1}{2} e^{-\alpha(x+c)} + \frac{\lambda}{8} [1 + 2\alpha(x+c)] e^{-\alpha(x+2c)} + \frac{\lambda^2}{16} [(1 + 3\alpha c + 3\alpha^2 c^2) + 2\alpha(1 + 2\alpha c)x + \alpha^2 x^2] e^{-\alpha(x+3c)} \quad (1.3.18)$$

for $x > -c$. Equation (1.3.17c) now reduces to

$$a = \frac{1}{2} e^{-\alpha c} + \frac{\lambda}{8} (1 + 2\alpha c) e^{-2\alpha c} + \frac{\lambda^2}{16} (1 + 3\alpha c + 3\alpha^2 c^2) e^{-3\alpha c}. \quad (1.3.19)$$

By using equation (1.3.19), I can plot the speed c as a function of λ for various choices of a .

Figure 1.6 shows the numerical data for order λ and order λ^2 on top of the corresponding analytic curves that I get from equation (1.3.19). The agreement is quite good. I have also plotted the curves for the order λ^{20} and order λ^{500} power series. I expect the different-order curves to agree for small λ and to diverge for large λ , and this is indeed so. These results suggest that my numerical scheme is self-consistent. How accurate, however, are the various curves? I can get some feel for their accuracy for $\lambda = 1/a$.

For $\lambda = 1/a$, there is no Allee effect and I can compute the true speed. Since the Laplace kernel has the moment generating function

$$M(s) = \int_{-\infty}^{+\infty} k(z)e^{sz} dz, \quad (1.3.20)$$

the true speed c can be obtained from the parametric equations

$$c = \frac{M'(s)}{M(s)}, \quad \lambda = \frac{e^{sM'(s)/M(s)}}{M(s)} \quad (1.3.21)$$

(see [60]). For the case

$$a = 0.5, \quad \lambda = 2.0, \quad \alpha = 1.0, \quad (1.3.22)$$

the speed is $c = 1.898985\dots$ I can now use my numerical scheme to estimate λ for various orders of the power series in equation (1.3.10c). Since $\lambda = 2.0$, I can compute the difference between the numerically estimated λ and the true λ (see Figure 1.7). The error decays as the reciprocal of order. □

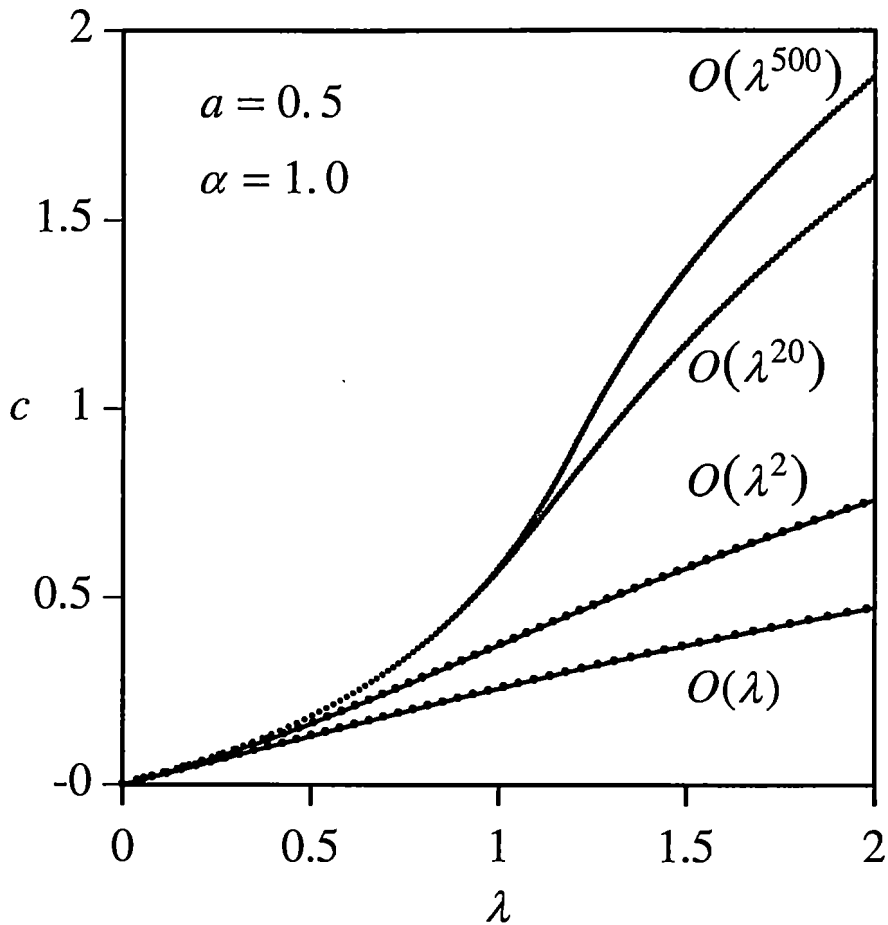


Figure 1.6: The speed c as a function of λ for the Laplace distribution

I chose $\alpha = 1$ and Allee threshold $a = 0.5$. The speeds were obtained numerically, using iterative scheme (1.3.10). The plot shows numerical data of order λ and λ^2 atop the corresponding analytical curves from equation (1.3.19). The order λ^{20} and order λ^{500} numerical data are also plotted. Integrations were performed using an FFT-assisted implementation of the trapezoidal rule with 2^{13} mesh points and an upper limit of integration of $L = 50$.

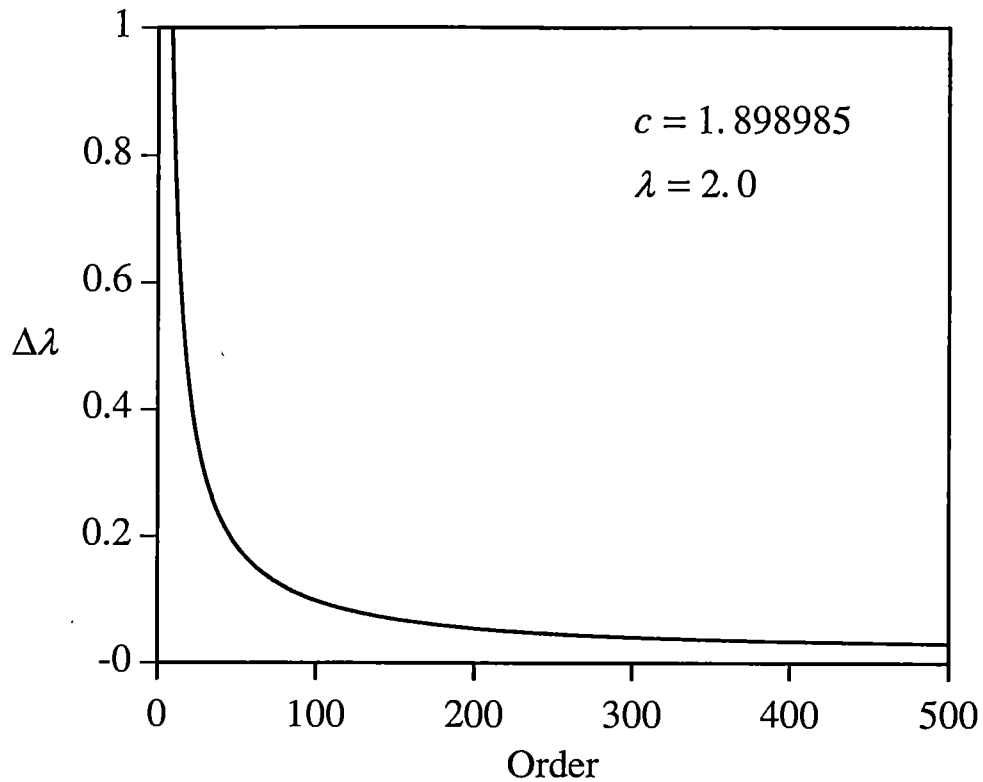


Figure 1.7: The error in λ for different orders of power series (1.3.10c) for the Laplace distribution

The figure is for the Laplace distribution with $\alpha = 1.0$, an Allee threshold of $a = 0.5$, and the speed $c = 1.898985\dots$. The true value is $\lambda = 2.0$ (see equation (1.3.21)). Estimates of λ were obtained by iterating and solving equations (1.3.10) numerically using 2^{13} mesh points and an upper limit of integration of $L = 50$.

1.4 Other numerical examples

Few kernels are as tractable as the Laplace distribution. I must rely on numerical procedures for most distributions. In this section, I use my iterative scheme to estimate the speeds for thin-tailed and fat-tailed redistribution kernels. I use “thin-tailed” for kernels such as the normal distribution and the Laplace distribution that have moment generating functions. I use “fat-tailed” for kernels such as the exponential square root distribution and the Cauchy distribution that do not have moment generating functions.

Example 1.4.1. *Consider the normal distribution*

$$k(x) = \frac{1}{\sqrt{2\pi}\sigma} e^{-x^2/2\sigma^2} \quad (1.4.1)$$

with

$$G(x) = \frac{1}{\sqrt{2\pi}\sigma} \int_x^\infty e^{-z^2/2\sigma^2} dz = \frac{1}{2} \operatorname{erfc}\left(\frac{x}{\sqrt{2}\sigma}\right). \quad (1.4.2)$$

I show $c(\lambda)$ for the normal distribution and $a = 0.5$ in Figure 1.8. \square

Example 1.4.2. *Consider the exponential square root distribution*

$$k(x) = \frac{\alpha^2}{4} e^{-\alpha\sqrt{|x|}} \quad (1.4.3)$$

with

$$G(x) = \frac{1}{2}(1 + \alpha\sqrt{x})e^{-\alpha\sqrt{x}} \quad (1.4.4)$$

for $x > 0$.

This distribution has moments of all integer order, but no moment generating function. This distribution gives rise to accelerating invasions in the

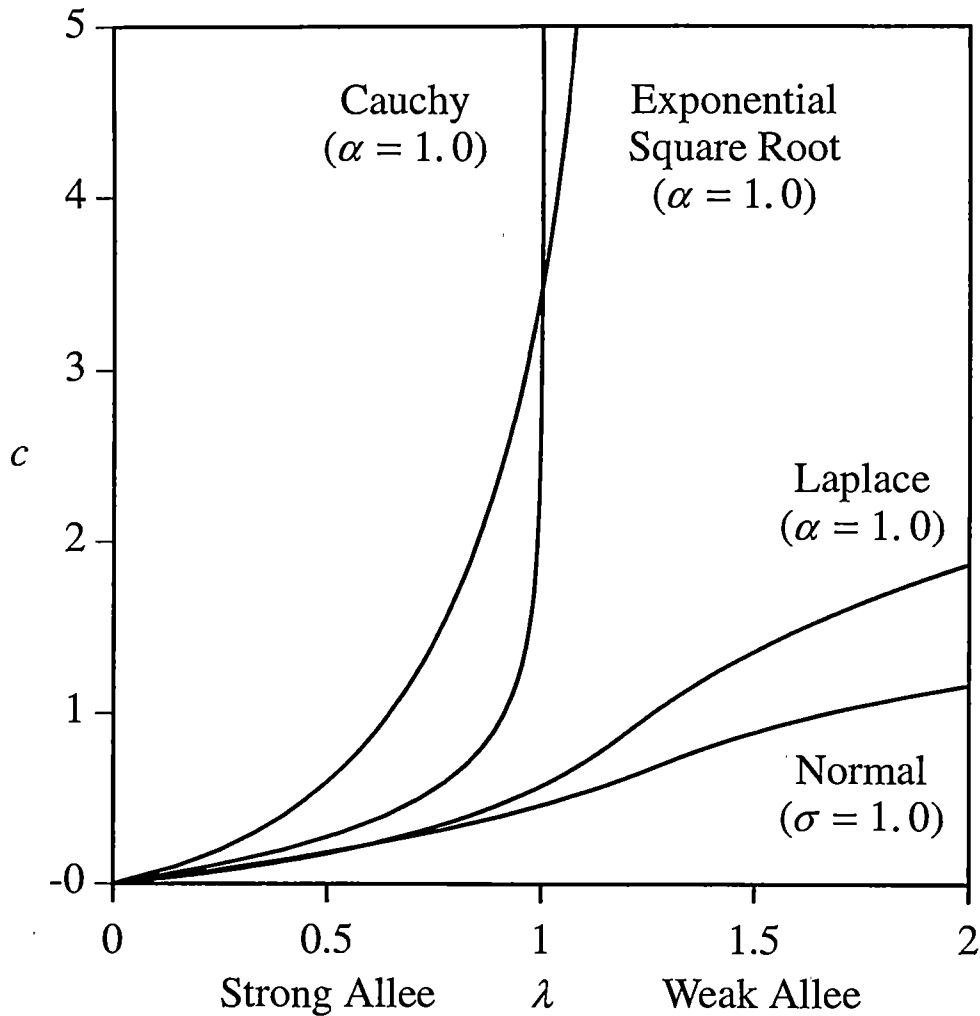


Figure 1.8: The speed c as a function of λ for the Laplace, normal, exponential square root, and Cauchy kernels

The parameters α and σ were chosen as $\alpha = 1.0$ (Laplace), $\sigma = 1.0$ (normal), $\alpha = 1.0$ (exponential square root), and $\alpha = 1.0$ (Cauchy). The Allele threshold is $a = 0.5$ for all kernels. The curves were computed using iterative scheme (1.3.10) with 2^{14} mesh points, and upper limits of integration of $L = 50$, $L = 30$, $L = 400$, and $L = 6000$. The thin-tailed Laplace and normal distributions generate finite-speed traveling waves for all positive λ . The speed diverges to infinity for the fat-tailed exponential square root distribution for some $\lambda > 1$ and for the fat-tailed Cauchy distributions at or near $\lambda = 1$.

absence of an Allee effect [60]. Figure 1.8 shows a monotonic increase in the wave speed with increasing λ for $a = 0.5$. The speed appears to diverge to infinity for some λ greater than one. I am, however, suspicious of some of my large λ numerical results, for reasons to be discussed. \square

Example 1.4.3. *Consider the the Cauchy distribution*

$$k(x) = \frac{1}{\pi} \frac{\alpha}{(\alpha^2 + x^2)} \quad (1.4.5)$$

with

$$G(x) = \frac{1}{2} - \frac{1}{\pi} \tan^{-1} \left(\frac{x}{\alpha} \right) \quad (1.4.6)$$

for $x > 0$.

The Cauchy distribution is the classic example of a fat-tailed distribution that lacks all moments. This distribution, like the square root distribution gives rise to accelerating invasions in the absence of an Allee effect. In Figure 1.8, I see that the speed c increases with the net reproductive rate λ and that it diverges at or near one for $a = 0.5$. \square

The two fat-tailed distributions show similar large- λ behavior for other choices of the threshold level a : the speed for the Cauchy distribution continues to diverge at or near one. Similarly, the speed for the exponential square root distribution continues to diverge for some λ greater than one.

The choice of L is critical for my numerical results. If I choose an L too large, numerical instabilities arise. Conversely, if L is too small, I expect a large error from neglecting too much of the integral. Consider the Cauchy distribution. If I fix the speed c , the Allee threshold a , the order of the power

series, and the number of mesh points n of integration, I see, in Figure 1.9, the effect of L on λ .

For the Laplace kernel and the normal distribution, I easily chose upper limits L from the plateaus of the curves $\lambda(L)$. I chose $L = 50$ for the Laplace distribution and $L = 30$ for the normal distribution. Figure 1.10 shows the influence of L on λ for the exponential square root distribution with speeds $c = 2.0$ and $c = 5.0$. The first curve reaches a plateau prior to the onset of oscillations. If I increase the speed to $c = 5.0$, I lose my plateau. For the exponential square root distribution, I could not find a good choice of L for my iterative scheme. I chose $L = 400$.

1.5 Discussion

Allee effects can slow down [66] or reverse [67] traveling wave solutions of reaction-diffusion equations. For integrodifference equations (IDEs), Allee effects can play an additional role: they can turn accelerating invasions into constant-speed invasions [60]. In this chapter, I have tried to broaden my understanding of the effects of Allee effects on simple IDEs.

I have followed two complementary paths. In section 1.2, I have derived a simple formula for the sign of the speed of a traveling wave solution for a general, single-species IDE. This formula resembles a well-known result for the generalized Nagumo [17] or bistable [54] reaction-diffusion equation. My result holds for redistribution kernels that are bounded and symmetric. It suggests that the ultimate success of a sufficiently large invasion is indepen-

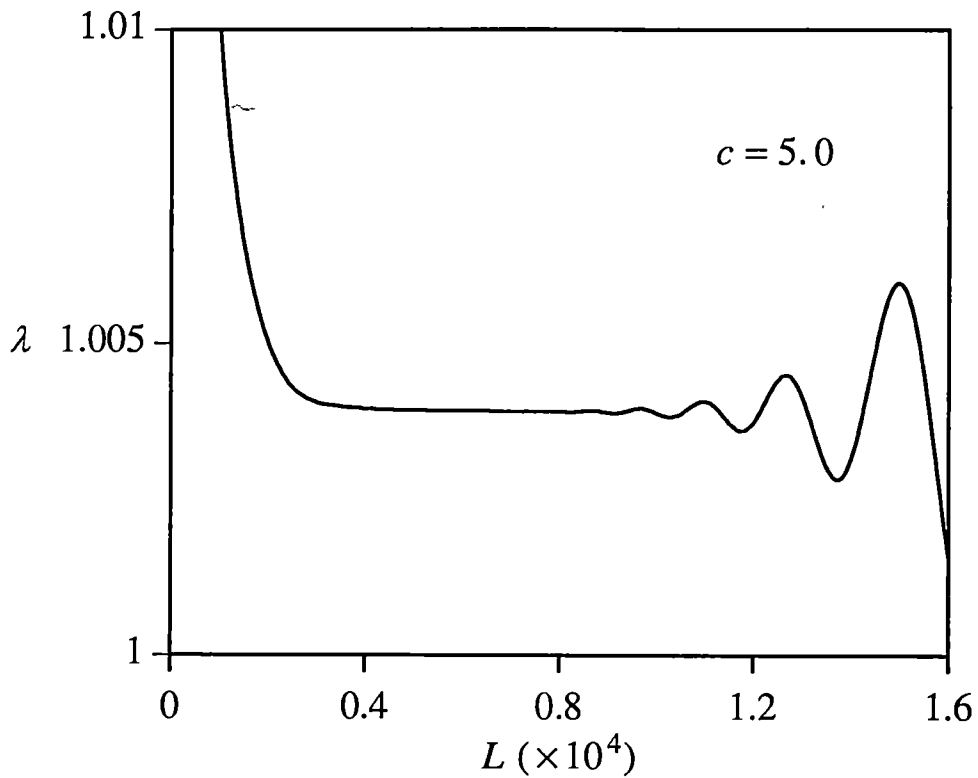


Figure 1.9: The slope λ as a function of the upper limit of integration L for the Cauchy distribution

The plot shows the effect of the upper limit of integration on the value of λ produced using numerical scheme (1.3.10) for order 500 with 2^{14} mesh points, speed $c = 5.0$, and an Allee threshold of $a = 0.5$. As L increases, the slope λ approaches a plateau. For larger values of L , the slope oscillates due to a numerical instability. Care must be taken to choose a value of L from the plateau.

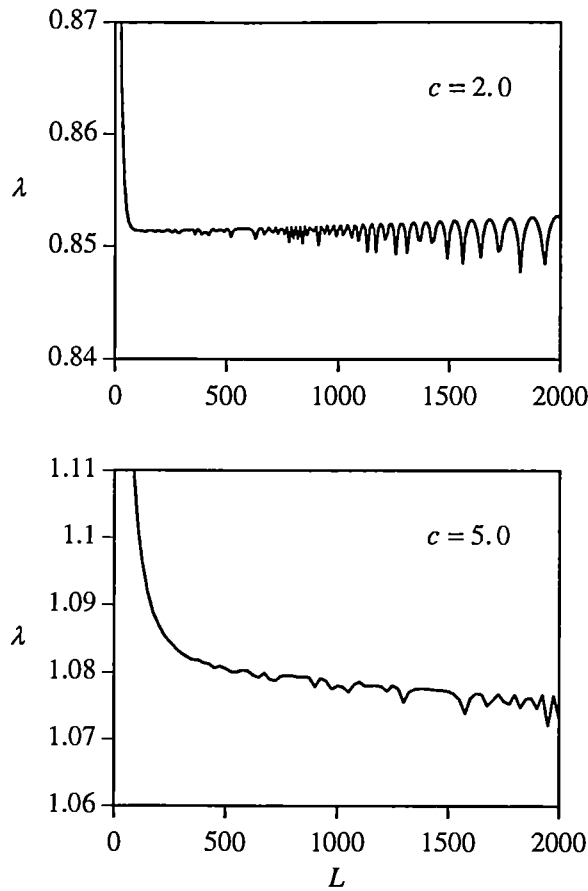


Figure 1.10: The slope λ as a function of the upper limit of integration L for the exponential square root distribution

The speed c was chosen as $c = 2.0$ for the top and $c = 5.0$ for the bottom. The plots show the effects of the upper limit of integration on the value of λ produced using numerical scheme (1.3.11) for order 500 with 2^{14} mesh points and an Allee threshold of $a = 0.5$. For $c = 2.0$, the curve rapidly reaches a plateau before succumbing to a numerical instability. For $c = 5.0$, there is no obvious plateau. In this case, it may be difficult to choose an appropriate upper limit of integration.

dent of the exact redistribution kernel and depends only on the form of the growth function. Loosely speaking, if the area of increase exceeds the area of decrease, à la equation (1.2.11), traveling waves will be waves of invasion.

While the exact form of a symmetric kernel does not have an obvious effect on the ultimate success of a sufficiently large invasion, it does have a profound influence on the speed with which that invasion occurs. In section 1.3, I developed a numerical scheme for estimating the speed of invasion for a linear-constant growth function. This function shows all the important properties of more general Allee growth functions and can exhibit the full range of strong and weak Allee effects. The use of this growth function establishes an intimate tie between traveling wave speeds for integrodifference equations with Allee effects and the theory of Wiener-Hopf integral and integral-difference equations.

In section 1.4, I used my numerical scheme to estimate the speed of invasion for various thin-tailed and fat-tailed redistribution kernels in the presence of both strong and weak Allee effects. For two fat-tailed examples, a strong Allee effect could always turn an accelerating invasion into a constant-speed invasion (or retreat). A weak Allee effect might or might not turn an accelerating invasion into a constant-speed invasion. For the Cauchy distribution, which has no moments, the wave speed diverges to infinity at or near the boundary, $\lambda = 1$, between strong and weak Allee effect. For the exponential square root distribution, which has moments, but no moment generating function, the wave speed diverges for some $\lambda > 1$. Thin-tailed distributions

were better behaved and always gave rise to finite speeds.

These results have some interesting consequences. Hosono [48] has shown that an inferior competitor can introduce a weak Allee effect into the growth rate of a superior competition. This suggests that an inferior competitor might be able to turn the accelerating invasion of a superior competitor into a constant-speed invasion for some kernels, but not for others. I hope to determine if this is true in future research.

Chapter 2

Speeds of Invasion in a Model with Strong or Weak Allee Effects

2.1 Introduction

Biological invasions [1–4] have long been of interest. Invading organisms play important roles in both economy and ecology. One significant way to understand these invasions is to estimate rates of spread. Most invasion models assume no Allee effect: per capita growth rates decrease with density (see subfigure 2.1B). One can determine the speed of invasion for models without Allee effects by linearization [75, 99]. In contrast, abundant observational data [4, 25, 33, 46, 61, 62, 63, 64, 97] provide evidence for an increase in the per capita growth rate at low densities (see figures 2.1D and 2.1F). Odum [81] first referred to this phenomenon as “Allee’s Principle”, and it is now called an Allee effect [1, 2] or depensation [19]. I will show, by example, that linearization may still give the correct speed of invasion for sufficiently weak

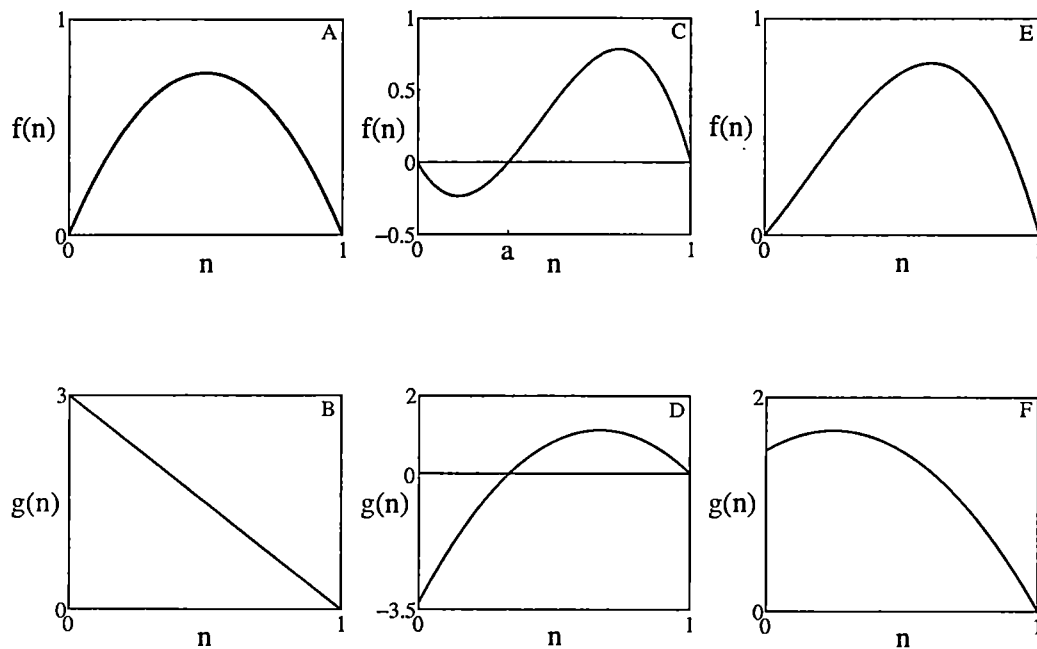


Figure 2.1: Representative strong, weak, and no-Allee-effect population growth rates and the corresponding per capita growth rates

The no-Allee-effect population growth rate in subfigure A satisfies the condition that $f(n) \leq f'(0)n$, for all n in $[0, 1]$. The corresponding no-Allee-effect per capita growth rate g in subfigure B decreases with density. The strong-Allee population growth rate in subfigure C has a population threshold a , and satisfies the conditions that $f(n) > f'(0)n$, $f'(0) < 0$, for a range of n in $[0, 1]$. The corresponding strong-Allee-effect per capita growth rate g in subfigure D increases with density at low densities, commencing with a negative value. The weak-Allee population growth rate in subfigure E has no population threshold, but there is a range of n in $[0, 1]$ such that $f(n) > f'(0)n$ with $f'(0) > 0$. The corresponding weak-Allee per capita growth rate g in subfigure F starts with a positive value and increases with density at low densities.

Allee effects.

Most people regard the strong Allee effect as the Allee effect and ignore the weak Allee effect [5, 21, 22, 33, 34, 46, 60, 66, 67, 69, 85, 100]. In fact, Allee effects may be weak or strong. Consider a population that is governed by

$$\frac{dn}{dt} = f(n), \quad (2.1.1)$$

where n is the population size at time t . I will assume that the growth function $f(n)$ satisfies

$$f(0) = 0, \quad f(1) = 0, \quad (2.1.2)$$

so that there is a trivial equilibrium at the origin and a nontrivial equilibrium that has been normalized to one. I will also assume that there is, at most, one other equilibrium between zero and one. Under these assumptions, the population exhibits a strong Allee effect if there exists a range of n in the interval of $[0, 1]$, such that

$$f(n) > f'(0)n, \quad f'(0) < 0, \quad (2.1.3)$$

and a weak Allee effect if there exists a range of n , in the interval of $[0, 1]$, such that

$$f(n) > f'(0)n, \quad f'(0) > 0. \quad (2.1.4)$$

The difference between the strong and weak Allee effects lies in the sign of the slope of the growth function at the origin or, equivalently, in the sign of the per capita growth rate when the population is rare. A positive sign

implies that the Allee effect is weak, while a negative sign indicates the effect is strong. A strong Allee effect introduces a population threshold. The population must surpass this threshold to grow. In contrast, a population with a weak Allee effect does not have a threshold. Figure 2.1 shows representative strong, weak, and no-Allee-effect population growth rates and the corresponding per capita growth rates. Clark [19] and several other investigators refer to a strong Allee effect as critical depensation and a weak Allee effect as noncritical depensation. Notice that the definitions of strong and weak Allee effects in this chapter differ from those of [45].

One of the earliest examples of a weak Allee effect is found in experimental work on flour beetles of the genus *Tribolium* [1, 2, 18, 55, 73, 86]. These studies showed that the per capita growth rate of beetles reaches its maximum at an intermediate population size and that this rate is positive when the population is rare. Two other examples of a weak Allee effect occur in the experimental work of Robertson [91] and Petersen [87] on *Enchelys farcimen* and *Paramecium caudatum*. Robertson [91] found that when two *Enchelys farcimen* individuals were placed together in a restricted amount of culture medium, the early rate of reproduction, following a period of readjustment, was over twice that when a single *Enchelys farcimen* individual was so treated. Petersen [87] obtained the same results for *Paramecium caudatum* using larger volumes of culture medium. Turchin and Kareiva [97] also provided experimental data that highlighted a weak Allee effect for aphid colony size. These Allee effects are weak because the populations do not

exhibit any thresholds. Numerous examples of weak Allee effects can also be found in [1, 2].

In this chapter, I will analyze a reaction-diffusion equation with an Allee effect. Reaction-diffusion equations describe populations with growth and dispersal. In the simplest case,

$$n_t = f(n) + n_{xx}, \quad (2.1.5)$$

where $n(t, x)$ denote the population density of a species at time t and position x , $f(n)$ is the population growth rate. Time and space are both continuous. A classic example is Fisher's equation [28], with no Allee effect, where

$$f(n) = n(1 - n). \quad (2.1.6)$$

This equation was first proposed by Fisher [28] for a progressive wave of gene increase due to a locally favorable mutation for a uniformly distributed population in one dimensional space. It was then applied by Skellam [95] to the study of population dispersal. This equation has traveling wave solutions $n(x - ct)$ for all velocities $c \geq 2 \equiv c^*$ [28, 56].

Interest in wave speeds for Allee effects has been increasing [9, 10, 21, 26, 27, 35, 41, 60, 66, 67, 92, 93, 100, 102]. Cruickshank et al. [21] developed a numerical method to determine velocities for reaction-diffusion models with strong Allee effects. However, their model of European fox rabies has a particularly low carrying capacity so that the speed under strong Allee effects is not much different from that computed from threshold-free models. Lewis

and Kareiva [66] used a partial differential equation model to examine the influences of a strong Allee effect on local population dynamics, but relied on numerical investigations. Lewis and Veit [67] used a general integrodifference equation (IDE) model with an Allee effect to describe the dynamics of the House Finch invasion in eastern North America, but gave only numerical simulations. In contrast, Kot et al. [60] analytically investigated an IDE model with a Allee effect, but focused on an extremely narrow limiting case.

Despite this increasing interest, most work does not distinguish between strong and weak Allee effects (but see [19, 102]). Most people take the strong Allee effect as “the Allee effect” and neglect the weak Allee effect. In this chapter, I extend a model of Jones and Sleeman [49] to include both strong and weak Allee effects. I analytically solve for the traveling wave solutions and compute the wave speeds for a full range of Allee effects. The transition from strong Allee effect to no-Allee effect through the weak Allee effect region gives the most interesting results. I also hope to complement recent work of Wang et al. [102] on integrodifference equations.

2.2 The model

Jones and Sleeman [49] (see also [13]) considered the following piecewise-linear approximation to the Fisher equation:

$$f(n) = \begin{cases} n, & 0 \leq n \leq \frac{1}{2}, \\ 1 - n, & \frac{1}{2} \leq n \leq 1. \end{cases} \quad (2.2.1)$$

Reaction-diffusion equation (2.1.5) with population growth rate (2.2.1) has a minimum wave speed of $c^* = 2$. For any wave speed $c \geq 2$, one can solve for the exact traveling wave solution.

I generalize equation (2.2.1) by incorporating strong and weak Allee effects,

$$f(n) = \begin{cases} bn, & 0 \leq n \leq \frac{1}{2}, \\ 1 - n, & \frac{1}{2} < n < 1, \end{cases} \quad (2.2.2)$$

where

$$b < 1 \quad (2.2.3)$$

(see Figure 2.2). Notice that $f(n)$ has a strong Allee effect if

$$b < 0, \quad (2.2.4)$$

and a weak Allee effect if

$$0 < b < 1. \quad (2.2.5)$$

I am interested in the speeds and shapes of traveling wave solutions.

2.3 Traveling wave solutions

To estimate the speed of invasion for reaction-diffusion equation (2.1.5) with population growth rate (2.2.2), I consider a traveling wave solution of the form

$$n(x, t) \equiv u(z), \quad z = x - ct, \quad (2.3.1)$$

where c is the speed of the wave. I assume that the population goes to zero in front of the wave,

$$\lim_{z \rightarrow +\infty} u(z) = 0, \quad (2.3.2)$$

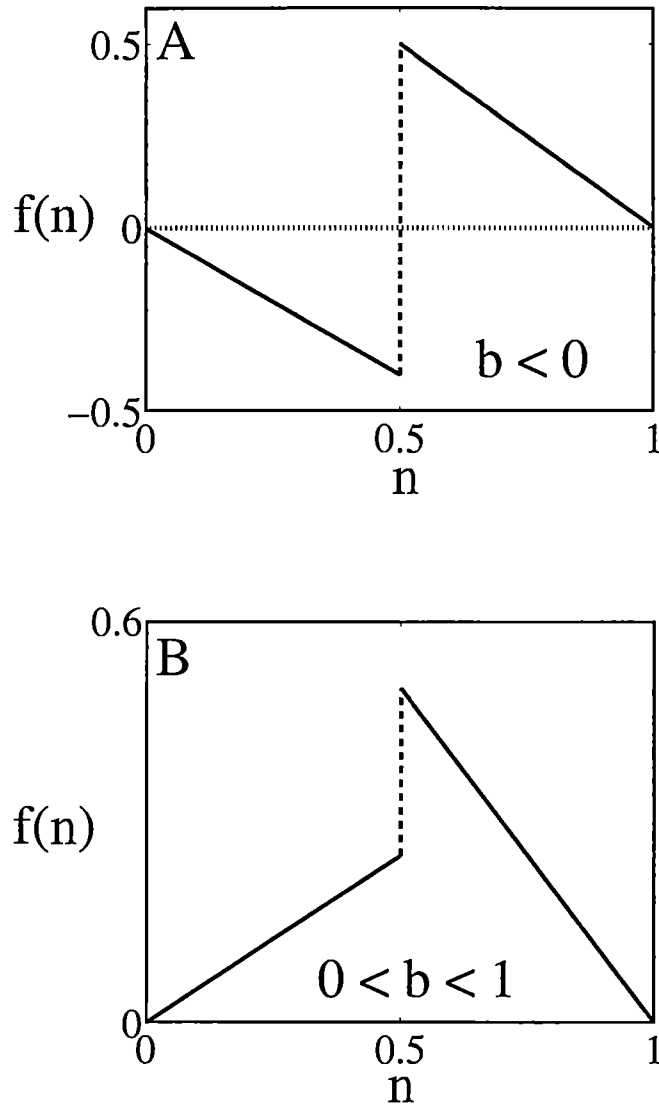


Figure 2.2: The piecewise-linear Allee population growth rate

The population growth rate is defined by equations (2.2.2) and (2.2.3); it consists of two linear ramps of slopes b and -1 . The function has A: a strong Allee effect for $b < 0$ and B: a weak Allee effect for $0 < b < 1$. There is no Allee effect for $b = 1$.

that it approaches its carrying capacity behind the wave,

$$\lim_{z \rightarrow -\infty} u(z) = 1, \quad (2.3.3)$$

and that the wave is centered at the origin,

$$u(0) = \frac{1}{2}. \quad (2.3.4)$$

I determine the speed of invasion using standard methods [17]. For a simple traveling wave, (2.3.1), reaction-diffusion equation (2.1.5) reduces to

$$u'' + cu' + f(u) = 0, \quad (2.3.5)$$

where primes denote differentiation with respect to z . Multiplying equation (2.3.5) by u' and integrating from $z = -\infty$ to $z = +\infty$ gives me

$$\frac{1}{2}u'^2 \Big|_{-\infty}^{+\infty} + c \int_{-\infty}^{+\infty} u'^2 dz + \int_{-\infty}^{+\infty} f(s) \frac{ds}{dz} dz = 0. \quad (2.3.6)$$

Since u' goes to 0 as z goes to $-\infty$ or $+\infty$, I conclude that

$$c = \frac{\int_0^1 f(s) ds}{\int_{-\infty}^{+\infty} u'^2 dz}. \quad (2.3.7)$$

Since $\int_{-\infty}^{+\infty} u'^2 dz$ is positive, the wave speed c has the same sign as the integral $\int_0^1 f(s) ds$.

I now define $v(z) \equiv u'(z)$ for differential equation (2.3.5) so that

$$u' = v, \quad v' = -cv - f(u). \quad (2.3.8)$$

I wish to find a heteroclinic orbit that lies in the lower-half (u, v) phase plane, that connects $(1, 0)$ to $(0, 0)$, and that remains in the strip $0 \leq u \leq 1$. There is

no such orbit if the critical points $(0, 0)$ and $(1, 0)$ are centers or foci. Finally, I assume that the wave solution satisfies the flux-continuity condition

$$\lim_{z \rightarrow 0^+} v(z) = \lim_{z \rightarrow 0^-} v(z). \quad (2.3.9)$$

The linearization about $(0, 0)$ gives the characteristic equation

$$\begin{vmatrix} -\lambda & 1 \\ -b & -c - \lambda \end{vmatrix} = \lambda^2 + c\lambda + b = 0. \quad (2.3.10)$$

The two eigenvalues are thus

$$\lambda_1 = \frac{-c + \sqrt{c^2 - 4b}}{2}, \quad \lambda_2 = \frac{-c - \sqrt{c^2 - 4b}}{2}. \quad (2.3.11)$$

If $b < 0$, the critical point $(0, 0)$ is a saddle point. If $b > 0$, speed formula (2.3.7) guarantees that c is positive. I need $c \geq 2\sqrt{b}$ for real eigenvalues. (Complex eigenvalues lead to oscillatory solutions about $(0, 0)$ that violate $u \geq 0$.) I thus restrict my attention to the case $c \geq 2\sqrt{b}$. This implies that the critical point $(0, 0)$ is a stable node.

The linearization about $(1, 0)$, in turn, gives the characteristic equation

$$\begin{vmatrix} -\lambda & 1 \\ 1 & -c - \lambda \end{vmatrix} = \lambda^2 + c\lambda - 1 = 0 \quad (2.3.12)$$

with eigenvalues

$$\lambda_3 = \frac{-c + \sqrt{c^2 + 4}}{2}, \quad \lambda_4 = \frac{-c - \sqrt{c^2 + 4}}{2}. \quad (2.3.13)$$

The critical point $(1, 0)$ is thus a saddle point.

Notice that differential equation (2.3.5) has the general solution

$$u(z) = \begin{cases} A_1 e^{\lambda_1 z} + A_2 e^{\lambda_2 z}, & z \geq 0, \\ 1 + A_3 e^{\lambda_3 z} + A_4 e^{\lambda_4 z}, & z \leq 0, \end{cases} \quad (2.3.14)$$

for $c^2 \neq 4b$, and

$$u(z) = \begin{cases} D_1 e^{-\frac{c}{2}z} + D_2 z e^{-\frac{c}{2}z}, & z \geq 0, \\ 1 + D_3 e^{\lambda_3 z} + D_4 e^{\lambda_4 z}, & z \leq 0, \end{cases} \quad (2.3.15)$$

for $c^2 = 4b$. The coefficients $A_1, A_2, A_3, A_4, D_1, D_2, D_3, D_4$ are determined by centering condition (2.3.4), boundary conditions (2.3.2), (2.3.3), and flux-continuity condition (2.3.9).

In the next two subsections, I will consider two possible heteroclinic connections.

2.3.1 Strong Allee effect ($b < 0$)

For the strong Allee case, $b < 0$, the critical points $(0, 0)$ and $(1, 0)$ are both saddle points (see Figure 2.3). For each $b < 0$, there is one and only one speed c that gives rise to a heteroclinic connection from $(1, 0)$ to $(0, 0)$. The proof is similar to that of Theorem 4.76 in [17] and to that of Theorem 4.15 in [27].

I now derive the unique speed c and the corresponding traveling wave solution. Since $b < 0$, equation (2.3.14) is the general solution and

$$\lambda_1 > 0, \quad \lambda_2 < 0, \quad \lambda_3 > 0, \quad \lambda_4 < 0. \quad (2.3.16)$$

Centering condition (2.3.4) and asymptotic boundary conditions (2.3.2) and (2.3.3) guarantee that

$$A_1 = 0, \quad A_2 = \frac{1}{2}, \quad A_3 = -\frac{1}{2}, \quad A_4 = 0, \quad (2.3.17)$$

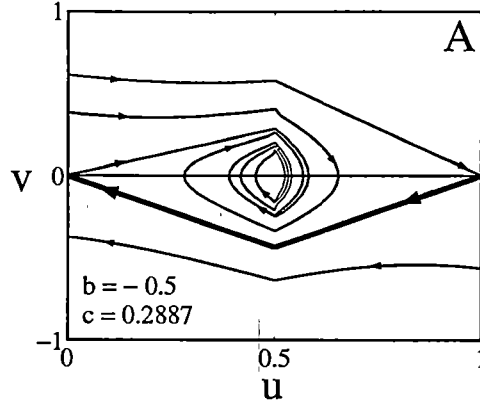


Figure 2.3: The phase plane for traveling wave solutions of function (2.2.2) with $b < 0$

Note: The phase plane for the strong Allee case, $b = -0.5$ and $c = 0.2887$, shows that the two critical points $(0, 0)$ and $(1, 0)$ are both saddle points.

and that solution (2.3.14) reduces to

$$u(z) = \begin{cases} \frac{1}{2}e^{\frac{-c - \sqrt{c^2 - 4b}}{2}z}, & z \geq 0, \\ 1 - \frac{1}{2}e^{\frac{-c + \sqrt{c^2 + 4}}{2}z}, & z \leq 0. \end{cases} \quad (2.3.18)$$

Applying flux-continuity condition (2.3.9) to equation (2.3.18), I obtain

$$-c - \sqrt{c^2 - 4b} = c - \sqrt{c^2 + 4}, \quad (2.3.19)$$

which gives the unique speed

$$c = \frac{1 + b}{\sqrt{2(1 - b)}} \quad (2.3.20)$$

(see Figure 2.4) and the wave solution

$$u(z) = \begin{cases} \frac{1}{2}e^{-\sqrt{\frac{1-b}{2}}z}, & z \geq 0, \\ 1 - \frac{1}{2}e^{\sqrt{\frac{1-b}{2}}z}, & z \leq 0 \end{cases} \quad (2.3.21)$$

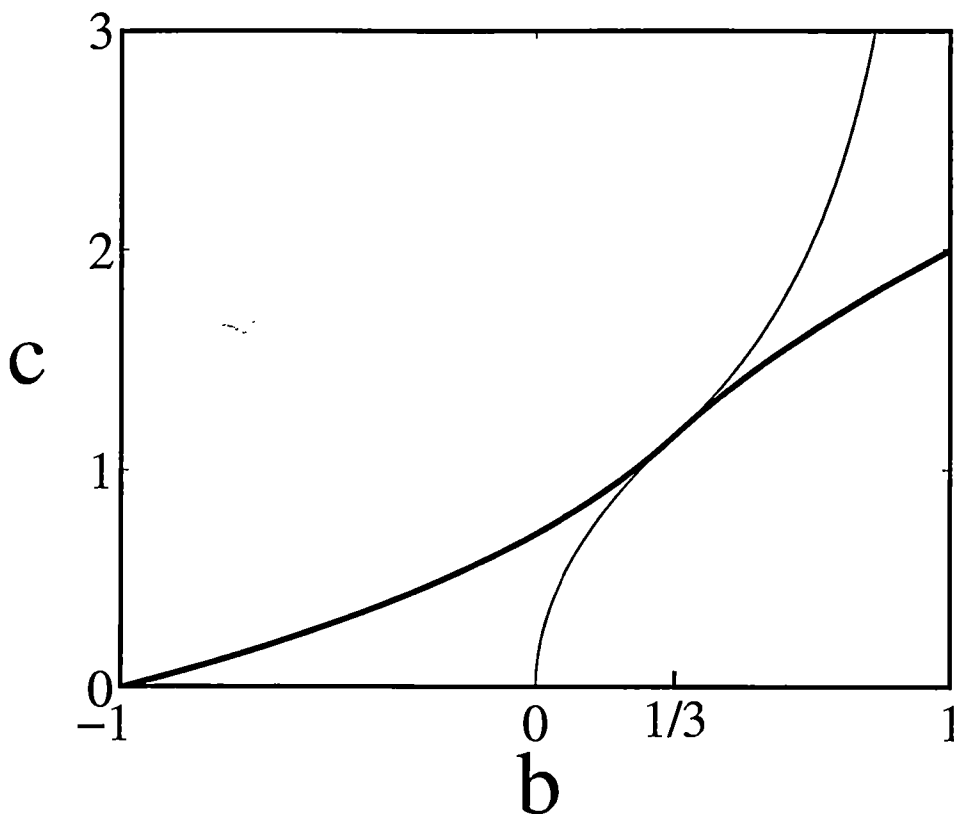


Figure 2.4: The minimum speed c^* as a function of b

The minimum speed c^* is the unique speed (2.3.20) for $b < 0$, for which there is a strong Allee effect. The minimum speed c^* for an insufficiently weak Allee case with $0 < b < 1/3$ satisfies (2.3.39). This formula is the same as (2.3.20) for the speed of strong Allee case. The minimum speed c^* for a sufficiently weak Allee effect with $1/3 \leq b < 1$ satisfies (2.3.30). This formula is the same as the formula that results from linearization. The thick curve is the minimum speed c^* . The thin curve on top of the thick curve corresponds to speed formula (2.3.39) for $1/3 \leq b < 1$, while the thin curve below the thick curve corresponds to speed formula (2.3.30) for $0 < b < 1/3$.

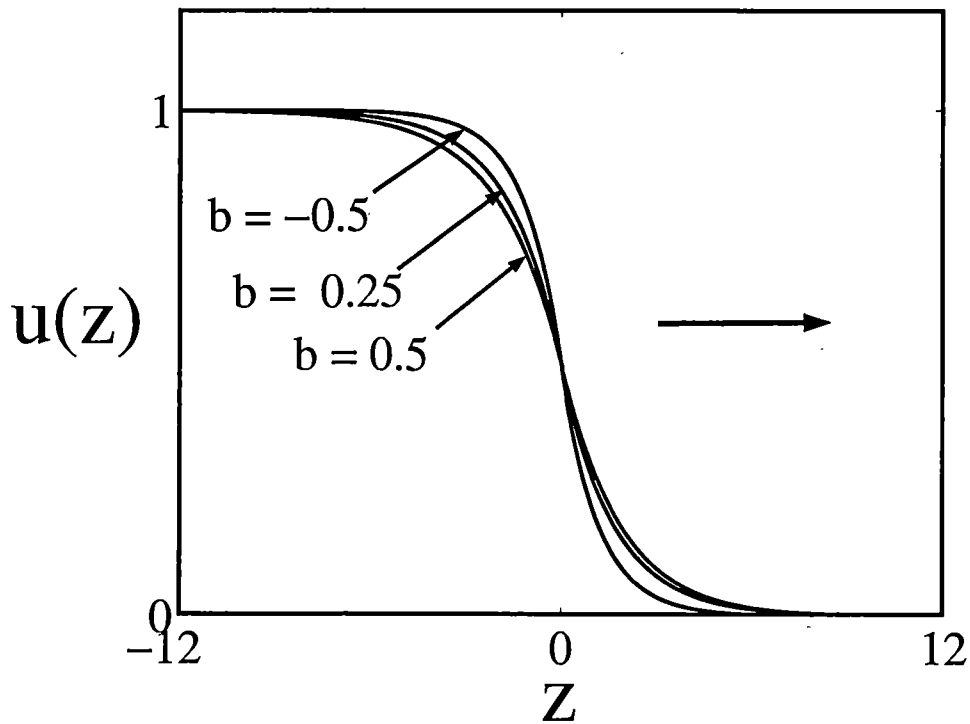


Figure 2.5: The traveling wave solution for various choices of the parameter b and speed c

The traveling wave solution is shown on the left-top (right-bottom) for the strong Allee case with $b = -0.5$ and $c = 0.2887$, left-middle (right-middle) for the insufficiently weak Allee case with $b = 0.25$ and $c = c^* = 1.0206$, and left-bottom (right-top) for the sufficiently weak Allee effect with $b = 0.5$ and $c = c^* = 1.4142$. The traveling wave solutions for all three cases are moving to the right.

(see Figure 2.5).

Equation (2.3.20) for the speed is quite different from the formula that results from linearization. Linearization does not give the correct speed of invasion for this simple example of a strong Allee effect.

2.3.2 Weak Allee effect ($0 < b < 1$)

For the weak Allee case, $0 < b < 1$, $(0, 0)$ is a stable node, while $(1, 0)$ is a saddle point (see Figure 2.6). I would like to determine the traveling wave solutions and the minimum wave speed c^* for various choices of b .

Following the proof of Theorem 4.68 in [17] or of Theorem 4.15 in [27], I can show that there is a speed $c^* \in [2\sqrt{b}, 2]$ such that a connection from 1 to 0 exists if and only if $c \geq c^*$.

Since $b > 0$, I need $c \geq 2\sqrt{b}$ in order to have real eigenvalues at the origin. For $c \geq 2\sqrt{b}$, eigenvalue formulae (2.3.11) and (2.3.13) imply that

$$\lambda_1 < 0, \lambda_2 < 0, \lambda_3 > 0, \lambda_4 < 0. \quad (2.3.22)$$

Double eigenvalues ($c = 2\sqrt{b}$)

For the special case $c = 2\sqrt{b}$, equation (2.3.15) is the general solution. Centering condition (2.3.4) and asymptotic boundary conditions (2.3.2) and (2.3.3) guarantee that

$$D_1 = \frac{1}{2}, \quad D_3 = -\frac{1}{2}, \quad D_4 = 0, \quad (2.3.23)$$

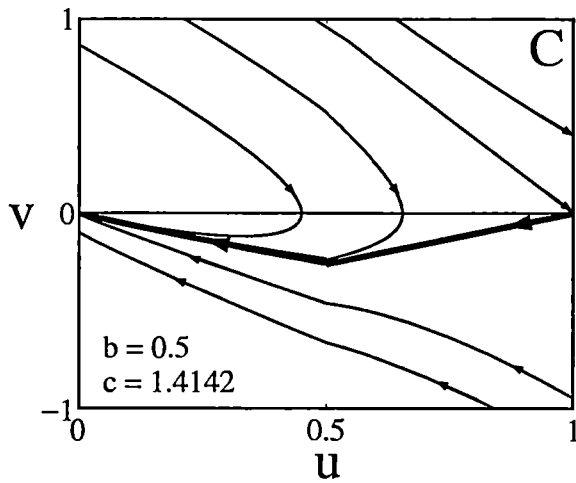
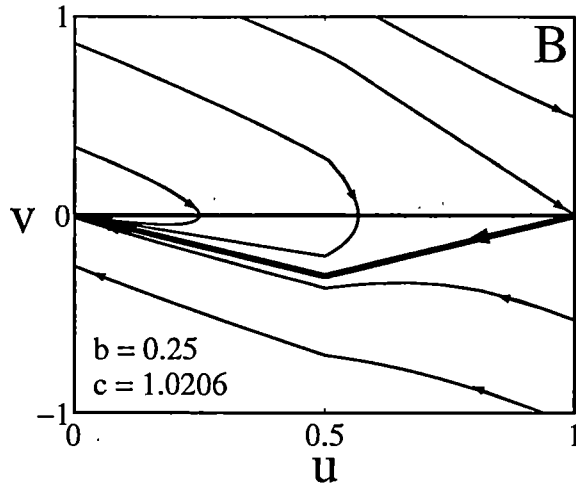


Figure 2.6: The phase planes for traveling wave solutions of function (2.2.2) with $b > 0$

The phase plane B for the insufficiently weak Allee case, $b = 0.25$ and $c = 1.0206$, shows that the critical point $(0, 0)$ is a stable node and the critical point $(1, 0)$ is a saddle point. The phase plane C for the sufficiently weak Allee effect, $b = 0.5$ and $c = 1.4142$, shows that the critical point $(0, 0)$ is a stable node and the critical point $(1, 0)$ is a saddle point.

so that solution (2.3.15) reduces to

$$u(z) = \begin{cases} \frac{1}{2}e^{-\sqrt{b}z} + D_2ze^{-\sqrt{b}z}, & z \geq 0, \\ 1 - \frac{1}{2}e^{(\sqrt{b+1}-\sqrt{b})z}, & z \leq 0. \end{cases} \quad (2.3.24)$$

Imposing flux-continuity condition (2.3.9) upon equation (2.3.24), I thus obtain

$$-\frac{\sqrt{b}}{2} + D_2 = \frac{\sqrt{b} - \sqrt{b+1}}{2}, \quad (2.3.25)$$

or

$$D_2 = -\frac{\sqrt{b+1}}{2} + \sqrt{b}. \quad (2.3.26)$$

It follows that

$$u(z) = \begin{cases} \frac{1}{2}e^{-\sqrt{b}z} + \left(\sqrt{b} - \frac{\sqrt{b+1}}{2}\right)ze^{-\sqrt{b}z}, & z \geq 0, \\ 1 - \frac{1}{2}e^{(\sqrt{b+1}-\sqrt{b})z}, & z \leq 0, \end{cases} \quad (2.3.27)$$

for $c = 2\sqrt{b}$ (see Figure 2.5).

Since solution (2.3.27) can be written as

$$u(z) = e^{-\sqrt{b}z} \left(\frac{1}{2} + D_2z \right), \quad (2.3.28)$$

for $c = 2\sqrt{b}$ and $z \geq 0$, the coefficient D_2 must be nonnegative to prevent negative value of u . Since

$$D_2 = -\frac{\sqrt{b+1}}{2} + \sqrt{b} \geq 0 \quad (2.3.29)$$

if and only if $1/3 \leq b < 1$, I conclude that the minimum speed is

$$c_1^* = 2\sqrt{b} \quad (2.3.30)$$

(see Figure 2.4) and the slowest heteroclinic connection is thus (2.3.27) for $1/3 \leq b < 1$. In addition, the minimum wave speed $c^* \equiv c_2^* > 2\sqrt{b}$ for $0 < b < 1/3$.

Distinct eigenvalues ($c > 2\sqrt{b}$)

I now simplify the general wave solution for any speed $c > 2\sqrt{b}$. For the case $c > 2\sqrt{b}$, equation (2.3.14) gives the general solution. Centering condition (2.3.4) and asymptotic boundary conditions (2.3.2) and (2.3.3) guarantee that

$$A_3 = -\frac{1}{2}, \quad A_4 = 0, \quad A_1 + A_2 = \frac{1}{2}, \quad (2.3.31)$$

so that solution (2.3.14) reduces to

$$u(z) = \begin{cases} A_1 e^{\frac{-c+\sqrt{c^2-4b}}{2}z} + \left(\frac{1}{2} - A_1\right) e^{\frac{-c-\sqrt{c^2-4b}}{2}z}, & z \geq 0, \\ 1 - \frac{1}{2}e^{\frac{-c+\sqrt{c^2+4}}{2}z}, & z \leq 0. \end{cases} \quad (2.3.32)$$

Applying flux-continuity condition (2.3.9) to equation (2.3.32) implies that

$$\begin{aligned} & A_1 \left(\frac{-c + \sqrt{c^2 - 4b}}{2} \right) + \left(\frac{1}{2} - A_1 \right) \left(\frac{-c - \sqrt{c^2 - 4b}}{2} \right) \\ &= \left(-\frac{1}{2} \right) \left(\frac{-c + \sqrt{c^2 + 4}}{2} \right). \end{aligned} \quad (2.3.33)$$

It follows that

$$A_1 = \frac{\sqrt{c^2 - 4b} - \sqrt{c^2 + 4} + 2c}{4\sqrt{c^2 - 4b}}, \quad (2.3.34)$$

$$A_2 = \frac{\sqrt{c^2 - 4b} + \sqrt{c^2 + 4} - 2c}{4\sqrt{c^2 - 4b}}, \quad (2.3.35)$$

and

$$u(z) = \begin{cases} A_1 e^{\frac{-c+\sqrt{c^2-4b}}{2}z} + A_2 e^{\frac{-c-\sqrt{c^2-4b}}{2}z}, & z \geq 0, \\ 1 - \frac{1}{2}e^{\frac{-c+\sqrt{c^2+4}}{2}z}, & z \leq 0, \end{cases} \quad (2.3.36)$$

for any $c > 2\sqrt{b}$ (see Figure 2.5).

I now determine the minimum speed and the slowest heteroclinic connection for $0 < b < 1/3$. Since $c \geq c_*^* > 2\sqrt{b}$, the traveling wave solution is

(2.3.36). Since wave solution (2.3.36) can be written as

$$u(z) = e^{-\frac{c}{2}z} \left[A_1 e^{\frac{\sqrt{c^2-4b}}{2}z} + \left(\frac{1}{2} - A_1 \right) e^{-\frac{\sqrt{c^2-4b}}{2}z} \right], \quad (2.3.37)$$

for $z \geq 0$ and $c > 2\sqrt{b}$, A_1 must be nonnegative to prevent negative value for u .

I now consider the two cases $A_1 = 0$ and $A_1 > 0$.

Case 1. $A_1 = 0$.

In this case, I have from definition (2.3.34) of A_1 that

$$2c = \sqrt{c^2 + 4} - \sqrt{c^2 - 4b}. \quad (2.3.38)$$

This equation has a solution for c if and only if $0 < b \leq 1/3$ and the speed c is

$$c \equiv c_2^* = \frac{1+b}{\sqrt{2(1-b)}}. \quad (2.3.39)$$

Case 2. $A_1 > 0$.

In this case, I have from definition (2.3.34) of A_1 that

$$2c > \sqrt{c^2 + 4} - \sqrt{c^2 - 4b}. \quad (2.3.40)$$

Since $0 < b < 1$ and $c > 2\sqrt{b}$, the numbers on both sides of inequality (2.3.40) are positive so that I can square both sides of inequality (2.3.40) to obtain

$$-c^2 + 2(1-b) < \sqrt{(c^2 + 4)(c^2 - 4b)}. \quad (2.3.41)$$

If the number on the left hand side of inequality (2.3.41) is negative, I have

$$c^2 > 2(1 - b) \quad (2.3.42)$$

and

$$c \equiv c_1 > \sqrt{2(1 - b)} > c_2^* \quad (2.3.43)$$

for $0 < b < 1/3$. If the number on the left hand side of inequality (2.3.41) is nonnegative, then

$$c \equiv c_2 \leq \sqrt{2(1 - b)}. \quad (2.3.44)$$

Once again, I square both sides of inequality (2.3.41) to get

$$c_2 > c_2^*. \quad (2.3.45)$$

From inequalities (2.3.44) and (2.3.45), I require

$$\sqrt{2(1 - b)} > c_2^* = \frac{1 + b}{\sqrt{2(1 - b)}}, \quad (2.3.46)$$

which holds for $0 < b < 1/3$. From the above, I have shown that speed $c = c_2^*$ in equation (2.3.39) obtained from $A_1 = 0$ is the minimum speed (see Figure 2.4) and the slowest heteroclinic connection is

$$u(z) = \begin{cases} \frac{1}{2}e^{-\sqrt{\frac{1-b}{2}}z}, & z \geq 0, \\ 1 - \frac{1}{2}e^{\sqrt{\frac{1-b}{2}}z}, & z \leq 0, \end{cases} \quad (2.3.47)$$

for $0 < b < 1/3$.

Equation (2.3.30) for the speed of a sufficiently weak Allee case, $1/3 \leq b < 1$, is the same as the formula that results from linearization. In contrast,

Strong Allee effect	$b < 0$	$c = \frac{1+b}{\sqrt{2(1-b)}}$
Weak Allee effect	$0 < b < \frac{1}{3}$	$c \geq c^* = \frac{1+b}{\sqrt{2(1-b)}}$
	$\frac{1}{3} \leq b < 1$	$c \geq c^* = 2\sqrt{b}$

Table 2.1: Wave speeds c and minimum speeds c^* for population growth rate (2.2.2)

equation (2.3.39) for the speed of an insufficiently weak Allee effect, $0 < b < 1/3$, is the same as equation (2.3.20) for the speed of the strong Allee case, $b < 0$. The latter was not obtained by linearization. Thus, linearization may or may not give the correct speed of invasion for this simple example of a weak Allee effect, depending on the exact strength of the effect.

Table 2.1 shows wave speeds c and minimum speeds c^* for various choices of b .

2.4 General case

In this section, I consider the reaction-diffusion equation

$$n_t = f(n) + Dn_{xx}, \quad (2.4.1)$$

with the general growth rate

$$f(n) = \begin{cases} bn, & 0 \leq n \leq a, \\ 1-n, & a < n < 1, \end{cases} \quad (2.4.2)$$

Strong Allee Effect	$b < 0$	$c = [(1 - a)^2 + ba^2] \sqrt{\frac{D}{a(1-a)(1-a-ab)}}$
Weak Allee Effect	$0 < b < \frac{(1-a)^2}{a(2-a)}$	$c \geq c^* = [(1 - a)^2 + ba^2] \sqrt{\frac{D}{a(1-a)(1-a-ab)}}$
	$\frac{(1-a)^2}{a(2-a)} \leq b < \frac{1-a}{a}$	$c \geq c^* = 2\sqrt{bD}$

Table 2.2: Minimum speeds c^* and possible speeds c for population growth rate (2.4.1)

where D is the diffusion coefficient and

$$0 < a < 1, \quad b < \frac{1}{a} - 1. \quad (2.4.3)$$

The function $f(n)$ has a strong Allee effect if

$$b < 0, \quad (2.4.4)$$

and a weak Allee effect if

$$0 < b < \frac{1}{a} - 1. \quad (2.4.5)$$

Notice that there is no Allee effect for $b \geq 1/a - 1$ and the minimum speed is thus $c^* = 2\sqrt{bD}$. Table 2.2 shows minimum speeds c^* and possible speeds c for different values of b . Traveling wave solutions u and the slowest heteroclinic connections u^* are shown in Table 2.3.

Figure 2.7A shows the effect of a on the minimum speed c^* for different net reproductive rates b , while Figure 2.7B shows the effect of net reproductive rate b on the minimum speed c^* for various choices of a .

<p>Strong Allee Effect $b < 0$</p>	$u(z) = \begin{cases} ae^{-\sqrt{a(1-a-ab)}/[D(1-a)]z}, & z \geq 0 \\ 1 + (a-1)e^{\sqrt{a(1-a-ab)}/[D(1-a)]z}, & z \leq 0 \end{cases}$
<p>Weak Allee Effect $b < \frac{(1-a)^2}{a(2-a)}$</p>	$u^*(z) = \begin{cases} ae^{-\sqrt{a(1-a-ab)}/[D(1-a)]z}, & z \geq 0 \\ 1 + (a-1)e^{\sqrt{a(1-a-ab)}/[D(1-a)]z}, & z \leq 0 \end{cases}$ $u(z) = \begin{cases} A_1 e^{-\frac{c+\sqrt{c^2-4bD}}{2D}z} + A_2 e^{-\frac{c-\sqrt{c^2-4bD}}{2D}z}, & z \geq 0 \\ 1 + (a-1)e^{-\frac{c+\sqrt{c^2+4D}}{2D}z}, & z \leq 0 \end{cases}$ $A_1 = \frac{a\sqrt{c^2-4bD} - (1-a)\sqrt{c^2+4D} + c}{2\sqrt{c^2-4bD}}$ $A_2 = \frac{a\sqrt{c^2-4bD} + (1-a)\sqrt{c^2+4D} - c}{2\sqrt{c^2-4bD}}$
<p>Weak Allee Effect $\frac{(1-a)^2}{a(2-a)} \leq b < \frac{1-a}{a}$</p>	$u^*(z) = \begin{cases} ae^{-\sqrt{\frac{b}{D}}z} + \left[(a-1)\sqrt{\frac{b+1}{D}} + \sqrt{\frac{b}{D}} \right] ze^{-\sqrt{\frac{b}{D}}z}, & z \geq 0 \\ 1 + (a-1)e^{\left(\frac{\sqrt{b+1}-\sqrt{b}}{\sqrt{D}}\right)z}, & z \leq 0 \end{cases}$ $u(z) = \begin{cases} A_1 e^{-\frac{c+\sqrt{c^2-4bD}}{2D}z} + A_2 e^{-\frac{c-\sqrt{c^2-4bD}}{2D}z}, & z \geq 0 \\ 1 + (a-1)e^{-\frac{c+\sqrt{c^2+4D}}{2D}z}, & z \leq 0 \end{cases}$ $A_1 = \frac{a\sqrt{c^2-4bD} - (1-a)\sqrt{c^2+4D} + c}{2\sqrt{c^2-4bD}}$ $A_2 = \frac{a\sqrt{c^2-4bD} + (1-a)\sqrt{c^2+4D} - c}{2\sqrt{c^2-4bD}}$

Table 2.3: Traveling wave solutions u and the slowest heteroclinic connections u^* for (2.4.1)

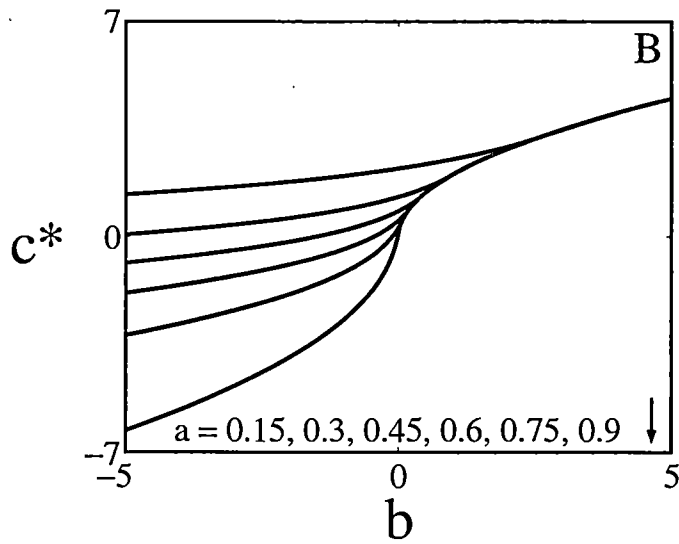
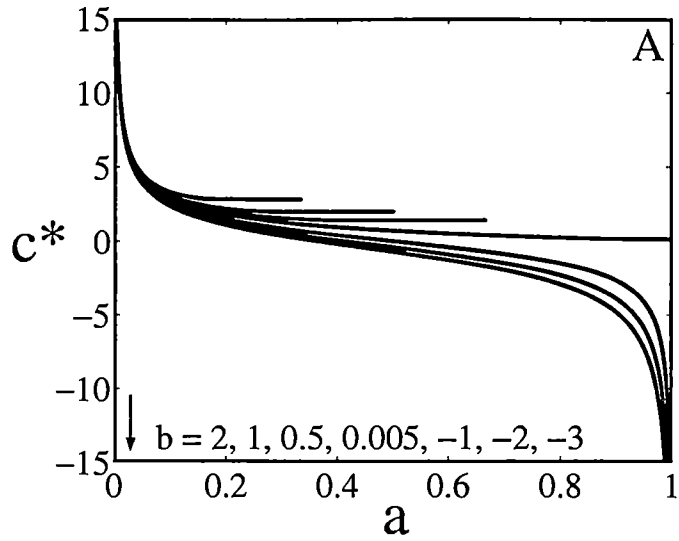


Figure 2.7: The minimum speed c^* as a function of the parameter a (b) for various choices of b (a)
 Note: The minimum speed c^* for each curve in subfigure A decreases as a increases. For each curve in subfigure B, the minimum speed c^* decreases as b decreases.

2.5 Conclusion and discussion

Allee [1, 2] observed increases in the per capita growth rate at low population densities, but did not name this phenomenon. Odum [80] named this phenomenon “Allee’s principle” and showed a representative figure [80] that emphasizes the positive effect of population size on per capita growth rates. This figure is an example of a weak Allee effect. At about the same time, Odum and Allee [81] displayed two different survival-density curves that characterize a positive (cooperative) relationship between specific survival rate (specific growth rate, per capita growth rate) and density. I use the terms “strong Allee effect” for the one with a negative survival rate at low densities and “weak Allee effect” for the one that has a positive survival rate at minimum densities.

To date, most models for Allee effects have misused the definition of the effect or have focused on a limited range of phenomena that involve population thresholds. It is clear, from Allee’s original investigations and Odum’s definition, that Allee effects can be strong or weak. I have formalized these terms in section 2.1.

In sections 2.2 and 2.3, I computed the speeds of invasion and solved for the exact traveling wave solutions for a piecewise-linear population growth rate. This function shows all the important properties of more general Allee growth rates and exhibit a full range of strong and weak Allee effects. My results show that the minimum speed of invasion for a sufficiently weak Allee

effect may be derived by linearization, while the formula for the minimum wave speed for an insufficiently weak Allee effect is the same as that for a strong Allee effect. This implies that the absence of an Allee effect is a sufficient, but not a necessary condition for linearization. Haderler and Rothe [35, 92] calculated the minimum wave speed for a cubic or bistable [54] population growth rate. They determined speeds for a range of Allee effects, but did not highlight weak Allee effects. Their results support my contention that linearization may still work for sufficiently weak Allee effects. They could not, however, determine the shape of the traveling front for the weakest Allee effects.

In section 2.4, I generalized the model of section 2; my results are found in Table 2.2, Table 2.3, and Figure 2.7. Allee effects can slow down the traveling wave solution of reaction-diffusion equations [66]. Figure 2.7B shows that, for fixed a , the minimum wave speed c^* decreases as b decreases: the stronger the Allee effect, the slower the wave speed. Notice that the number a is a population threshold for $b < 0$.

Growth rate (2.4.2) is a modified form of the linear-constant, Allee growth rate [102] that I previously used in a study of integrodifference equations [102]. I examined this linear-constant growth rate and introduced a numerical scheme to estimate the speed of traveling wave solutions for integrodifference equations. I did not, however, obtain exact analytic expressions for the traveling wave solutions or for the minimum wave speeds. My results in this chapter are analytical. I hope to extend the work of Wang et al [102]

analytically in future research.

Chapter 3

Integrodifference Equations and Competition Models, I

3.1 Introduction

The history of modeling competition interactions started with the studies of Lotka [68] and Volterra [101]. They independently suggested a continuous-time two-species competition model. Although there has been extensive work on multispecies systems of reaction-diffusion equations [12, 24, 31, 47, 48, 50, 51, 52, 53, 83], there has relatively little work on multispecies systems of IDEs. A discrete-time growth and continuous-space dispersal model for the invasion of an annual plant that is subject to competition from an established annual was derived under integrodifference formulation by Hart and Gardner [39]. Hart and Gardner restricted their model so that the problem could be reduced to that of one species. They actually solved a one-species problem instead of solving the two-species problem directly. Their approach cannot be applied to other general cases. In contrast, Allen et al. [3] considered a quite general

two-species system of IDEs with competition and dispersal, but gave only numerical investigations. In this chapter, I analytically study a two-species competition problem based on the integrodifference formulation, from both a mathematical and a biological point of view.

My analyses are based on linearization. However, Hosono [47, 48] has shown that the speed derived by linearization may underestimate the true speed for a reaction-diffusion system because of a weak Allee effect. I also find this effect takes place in my IDE model. My objective is to obtain a formula for the speed of invasion by analyzing traveling wave solutions and to discuss the behavior of the traveling wave. I will also try to estimate the speed of invasion under a weak Allee effect by a linear-constant approximation to the growth function.

3.2 The model

Recall the single-species IDE that I introduced in chapter 1:

$$N_{t+1}(x) = \int_{-\infty}^{+\infty} k(x-y)f(N_t(y)) dy, \quad (3.2.1)$$

where $N_t(x)$ is the population density, in space, of a species at generation t . The life cycle is composed of two distinct processes: sedentary and dispersal stages. All growth happens in the sedentary stage, all movement occurs in the dispersal stage.

For the sedentary stage, $f(N_t(x))$ represents the growth of the species.

Examples include the compensatory growth function [14]

$$f(N_t(x)) = \frac{\lambda N_t(x)}{1 + [(\lambda - 1)N_t(x)/K]}, \quad (3.2.2)$$

and the overcompensatory growth function [90]

$$f(N_t(x)) = N_t(x) \exp \left[r \left(1 - \frac{N_t(x)}{K} \right) \right]. \quad (3.2.3)$$

K is the carrying capacity of the environment. The parameters $\lambda = e^r$ and r are the geometric and intrinsic rates of increase, respectively. The function f is assumed to be nonnegative and to satisfy

$$f(N) \leq f'(0)N, \quad (3.2.4)$$

which means that there is no Allee effect [1, 2]. For nonlinear integrodifference equations without an Allee effect, the asymptotic velocity of scalar equation (3.2.1) can be derived from the linear IDE

$$N_{t+1}(x) = f'(0) \int_{-\infty}^{+\infty} k(x-y) N_t(y) dy, \quad (3.2.5)$$

(see [60, 103, 104]).

For the dispersal stage, I assume that k is a probability density function.

If k is symmetric, then

$$k(x-y) = k(y-x). \quad (3.2.6)$$

Examples include the Gaussian distribution

$$k(x) = \frac{1}{\sqrt{2\pi\alpha^2}} \exp\left(-\frac{x^2}{2\alpha^2}\right) \quad (3.2.7)$$

and the leptokurtic Laplace kernel

$$k(x) = \frac{\alpha}{2} e^{-\alpha|x|}. \quad (3.2.8)$$

In this chapter, I generalize one-species IDE (3.2.1) to a two-species model,

$$U_{t+1}(x) = \int_{-\infty}^{+\infty} k_1(x-y) f(U_t(y), V_t(y)) dy, \quad (3.2.9a)$$

$$V_{t+1}(x) = \int_{-\infty}^{+\infty} k_2(x-y) g(U_t(y), V_t(y)) dy, \quad (3.2.9b)$$

where $U_t(x)$ and $V_t(x)$ are the population densities, in space, of the first and second species, respectively, at generation t ; $k_1(x-y)$ and $k_2(x-y)$ are the kernels; $f(U_t(y), V_t(y))$ and $g(U_t(y), V_t(y))$ are the growth functions for the first and second species. I am particularly interested in competition.

To formulate a competition model based on IDEs, I first look at the system of difference equations for a discrete-time competition model [40]

$$U_{t+1} = \frac{\lambda_1 U_t}{1 + [(\lambda_1 - 1)/K_1](U_t + \alpha_{12} V_t)}, \quad (3.2.10a)$$

$$V_{t+1} = \frac{\lambda_2 V_t}{1 + [(\lambda_2 - 1)/K_2](V_t + \alpha_{21} U_t)}, \quad (3.2.10b)$$

where

$$\lambda_1 > 1, \lambda_2 > 1, \alpha_{12} > 0, \alpha_{21} > 0. \quad (3.2.10c)$$

U_{t+1} and V_{t+1} are the densities at generation t for the first and second species. The parameter λ_i is the net reproductive rate in the limit of small populations; K_i is the carrying capacity. Index $i = 1$ represents the first species,

index $i = 2$ represents the second species. I define

$$u_t \equiv \frac{U_t}{K_1}, \quad v_t \equiv \frac{V_t}{K_2}, \quad (3.2.11)$$

so that system (3.2.10) may be reduced to

$$u_{t+1} = f(u_t, v_t) = \frac{\lambda_1 u_t}{1 + (\lambda_1 - 1)(u_t + \beta_{12} v_t)}, \quad (3.2.12a)$$

$$v_{t+1} = g(u_t, v_t) = \frac{\lambda_2 v_t}{1 + (\lambda_2 - 1)(v_t + \beta_{21} u_t)}, \quad (3.2.12b)$$

where

$$\beta_{12} \equiv \alpha_{12} \frac{K_2}{K_1}, \quad \beta_{21} \equiv \alpha_{21} \frac{K_1}{K_2}. \quad (3.2.12c)$$

I now turn model (3.2.12) into a system of IDEs for a discrete-time, continuous-space competition model by introducing spatial coordinates and dispersal kernels. In order to examine the speed of invasion for an organism subject to competition, I analyze the system

$$u_{t+1}(x) = \int_{-\infty}^{+\infty} k_1(x-y) f(u_t(y), v_t(y)) dy, \quad (3.2.13a)$$

$$v_{t+1}(x) = \int_{-\infty}^{+\infty} k_2(x-y) g(u_t(y), v_t(y)) dy, \quad (3.2.13b)$$

where $f(u_t(y), v_t(y))$ and $g(u_t(y), v_t(y))$ are defined as

$$f(u_t(y), v_t(y)) = \frac{\lambda_1 u_t(y)}{1 + (\lambda_1 - 1)[u_t(y) + \beta_{12} v_t(y)]}, \quad (3.2.13c)$$

$$g(u_t(y), v_t(y)) = \frac{\lambda_2 v_t(y)}{1 + (\lambda_2 - 1)[v_t(y) + \beta_{21} u_t(y)]}, \quad (3.2.13d)$$

with

$$\lambda_1 > 1, \quad \lambda_2 > 1. \quad (3.2.13e)$$

I assume that both redistribution kernels have moment generating functions,

$$M_i(\lambda) \equiv \int_{-\infty}^{+\infty} k_i(x) e^{\lambda x} dx, \quad i = 1, 2, \quad (3.2.14)$$

and two-sided Laplace transforms

$$L_i(s) \equiv \int_{-\infty}^{+\infty} k_i(x) e^{-sx} dx, \quad i = 1, 2, \quad (3.2.15)$$

that are well-defined for some intervals of λ and s about zero.

Difference equations (3.2.12) and IDEs (3.2.13) possess four equilibria, corresponding to (i) extinction of both species, $(u_t, v_t) = (0, 0)$; (ii) extinction of the first species and survival of the second species at its carrying capacity, $(u_t, v_t) = (0, 1)$; (iii) extinction of the second species and survival of the first species at its carrying capacity, $(u_t, v_t) = (1, 0)$; (iv) coexistence of both species, $(u_t, v_t) = (u^*, v^*)$, where

$$u^* = \frac{1 - \beta_{12}}{1 - \beta_{12}\beta_{21}}, \quad v^* = \frac{1 - \beta_{21}}{1 - \beta_{12}\beta_{21}}. \quad (3.2.16)$$

The equilibrium (u^*, v^*) exists provided that

$$(1 - \beta_{12})(1 - \beta_{21}) > 0. \quad (3.2.17)$$

In this chapter, I consider the case

$$\beta_{12} < 1, \quad \beta_{21} > 1, \quad (3.2.18)$$

in which the first species is invading a resource that is dominated by the second species.

3.3 Traveling waves

I will solve IDEs (3.2.13) by looking for a traveling wave solution,

$$u_{t+1}(x) = u_t(x - c), \quad v_{t+1}(x) = v_t(x - c). \quad (3.3.1)$$

This solution corresponds to a heteroclinic connection from $(1, 0)$ to $(0, 1)$.

The wave solutions satisfy

$$u(x - c) = \int_{-\infty}^{+\infty} k_1(x - y) f(u(y), v(y)) dy, \quad (3.3.2a)$$

$$v(x - c) = \int_{-\infty}^{+\infty} k_2(x - y) g(u(y), v(y)) dy. \quad (3.3.2b)$$

I have taken the liberty of dropping the subscripts on the u_t 's and v_t 's.

It is very difficult to prove the existence of the heteroclinic connection from $(1, 0)$ to $(0, 1)$. If this connection does exist, I may determine the speed of the wave.

3.3.1 The front and the speed of the wave

I will look at the front of the wave by linearizing near the equilibrium $(u, v) = (0, 1)$. If I let

$$\tilde{u}(x) \equiv u(x), \quad \tilde{v}(x) \equiv v(x) - 1, \quad (3.3.3)$$

the linearization near $(0, 1)$ is

$$\tilde{u}(x - c) = \int_{-\infty}^{+\infty} k_1(x - y) \left[\frac{\lambda_1}{1 + (\lambda_1 - 1)\beta_{12}} \right] \tilde{u}(y) dy, \quad (3.3.4a)$$

$$\tilde{v}(x - c) = \int_{-\infty}^{+\infty} k_2(x - y) \left[- \left(1 - \frac{1}{\lambda_2} \right) \beta_{21} \tilde{u}(y) + \frac{1}{\lambda_2} \tilde{v}(y) \right] dy. \quad (3.3.4b)$$

Since exponential functions are eigenfunctions for both the translation operator on the left hand side of equations (3.3.4) and for the integral operator on the right hand side of equations (3.3.4), it is natural to look for an exponential solution,

$$\tilde{u}(x) = u_0 e^{-\lambda x}, \quad \tilde{v}(x) = v_0 e^{-\lambda x}, \quad (3.3.5)$$

for $\lambda > 0$. The change of variable $z \equiv x - y$ gives me

$$u_0 e^{\lambda c} = \left[\frac{\lambda_1}{1 + (\lambda_1 - 1)\beta_{12}} u_0 \right] \int_{-\infty}^{+\infty} k_1(z) e^{\lambda z} dz, \quad (3.3.6a)$$

$$v_0 e^{\lambda c} = \left[- \left(1 - \frac{1}{\lambda_2} \right) \beta_{21} u_0 + \frac{1}{\lambda_2} v_0 \right] \int_{-\infty}^{+\infty} k_2(z) e^{\lambda z} dz. \quad (3.3.6b)$$

The characteristic equation at $(0, 1)$ may now be written as

$$u_0 e^{\lambda c} = \left[\frac{\lambda_1}{1 + (\lambda_1 - 1)\beta_{12}} u_0 \right] M_1(\lambda), \quad (3.3.7a)$$

$$v_0 e^{\lambda c} = \left[- \left(1 - \frac{1}{\lambda_2} \right) \beta_{21} u_0 + \frac{1}{\lambda_2} v_0 \right] M_2(\lambda), \quad (3.3.7b)$$

where $M_1(\lambda)$ and $M_2(\lambda)$ are the two moment generating functions

$$M_i(\lambda) \equiv \int_{-\infty}^{+\infty} k_i(z) e^{\lambda z} dz, \quad i = 1, 2. \quad (3.3.8)$$

System (3.3.7) can be written in the matrix form

$$\begin{bmatrix} \frac{e^{\lambda c}}{M_1(\lambda)} - \frac{\lambda_1}{1 + (\lambda_1 - 1)\beta_{12}} & 0 \\ - \left(1 - \frac{1}{\lambda_2} \right) \beta_{21} & \frac{1}{\lambda_2} - \frac{e^{\lambda c}}{M_2(\lambda)} \end{bmatrix} \begin{bmatrix} u_0 \\ v_0 \end{bmatrix} = \begin{bmatrix} 0 \\ 0 \end{bmatrix}. \quad (3.3.9)$$

In order to get nontrivial solutions to system (3.3.9), the leading matrix must be singular,

$$\begin{vmatrix} \frac{e^{\lambda c}}{M_1(\lambda)} - \frac{\lambda_1}{1 + (\lambda_1 - 1)\beta_{12}} & 0 \\ - \left(1 - \frac{1}{\lambda_2} \right) \beta_{21} & \frac{1}{\lambda_2} - \frac{e^{\lambda c}}{M_2(\lambda)} \end{vmatrix} = 0. \quad (3.3.10)$$

There are two transcendental equations for the eigenvalues. The roots of the first equation,

$$\frac{1}{\lambda_2} = \frac{e^{\lambda c}}{M_2(\lambda)}, \quad (3.3.11)$$

have an eigenvector $(0, 1)$ that will not lead to invasion of the first species.

The second equation is

$$\frac{e^{\lambda c}}{M_1(\lambda)} = \frac{\lambda_1}{1 + (\lambda_1 - 1)\beta_{12}}, \quad (3.3.12)$$

which gives an estimate of the speed of the traveling wave.

Since the number of the invading species must remain nonnegative (both mathematically and biologically), I need a wave speed that is sufficiently large to give monotonic (rather than oscillatory) wave fronts and real (rather than complex) roots λ . Real roots emerge as double roots at the second order contact that is given by rewriting equation (3.3.12) as

$$e^{\lambda c} = \frac{\lambda_1}{1 + (\lambda_1 - 1)\beta_{12}} M_1(\lambda) \quad (3.3.13)$$

and differentiating equation (3.3.13) with respect to λ ,

$$c e^{\lambda c} = \frac{\lambda_1}{1 + (\lambda_1 - 1)\beta_{12}} M_1'(\lambda). \quad (3.3.14)$$

By combining the above two equations, I obtain a minimal wave speed c^* that may be expressed parametrically as

$$c^* = \frac{M_1'(\lambda^*)}{M_1(\lambda^*)}, \quad \frac{\lambda_1}{1 + (\lambda_1 - 1)\beta_{12}} = \frac{e^{\lambda^* \frac{M_1'(\lambda^*)}{M_1(\lambda^*)}}}{M_1(\lambda^*)}. \quad (3.3.15)$$

Notice that c^* is positive for symmetric kernels.

Example 3.3.1. Consider IDEs (3.2.13) with

$$k_i(x) = \frac{1}{2}\alpha_i e^{-\alpha_i|x|}, \quad i = 1, 2 \quad (3.3.16)$$

and moment generating functions

$$M_i(\lambda) = \frac{\alpha_i^2}{\alpha_i^2 - \lambda^2}, \quad |\lambda| < \alpha_i, \quad i = 1, 2. \quad (3.3.17)$$

I have

$$M'_1(\lambda) = \frac{2\alpha_1^2\lambda}{(\alpha_1^2 - \lambda^2)^2}. \quad (3.3.18)$$

It then follows from parametric equations (3.3.15) that

$$c^* = \frac{2\lambda^*}{\alpha_1^2 - \lambda^{*2}}. \quad (3.3.19)$$

and

$$\frac{\lambda_1}{1 + (\lambda_1 - 1)\beta_{12}} = \left(1 - \frac{\lambda^{*2}}{\alpha_1^2}\right) e^{2\lambda^{*2}/(\alpha_1^2 - \lambda^{*2})}. \quad (3.3.20)$$

Figure 3.1 shows c^* as a function of $\lambda_1/[1 + (\lambda_1 - 1)\beta_{12}]$.

For the case

$$\lambda_1 = \lambda_2 = 1.5, \quad \beta_{12} = 0.25, \quad \beta_{21} = 1.25, \quad \alpha_1 = 7.0 \quad \alpha_2 = 5.0, \quad (3.3.21)$$

the predicted speed obtained from parametric equations (3.3.19) and (3.3.20)

is

$$c^* = 0.16315 \quad (3.3.22)$$

and the speed obtained by simulating the traveling wave solution is

$$\bar{c} = 0.1587 \quad (3.3.23)$$

(see Figure 3.2A). For the case

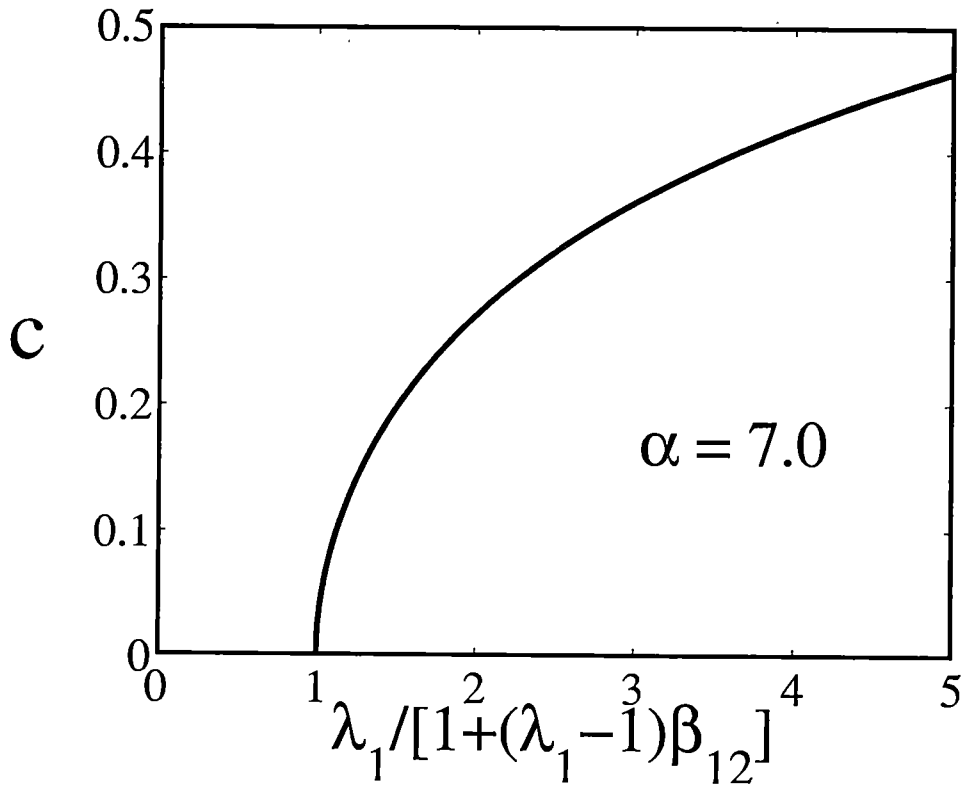


Figure 3.1: The speed c^* as a function of $\lambda_1/[1+(\lambda_1-1)\beta_{12}]$ for IDEs (3.2.13) with the Laplace kernels (3.3.16)

Using parametric equations (3.3.19) and (3.3.20), the speed c^* can be written as a function of $\lambda_1/[1+(\lambda_1-1)\beta_{12}]$.

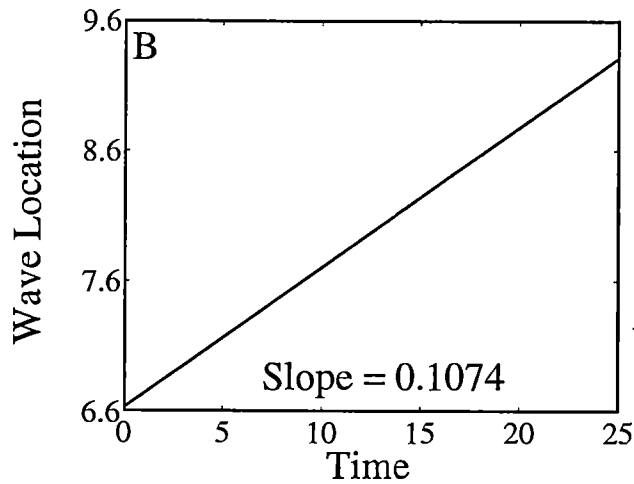
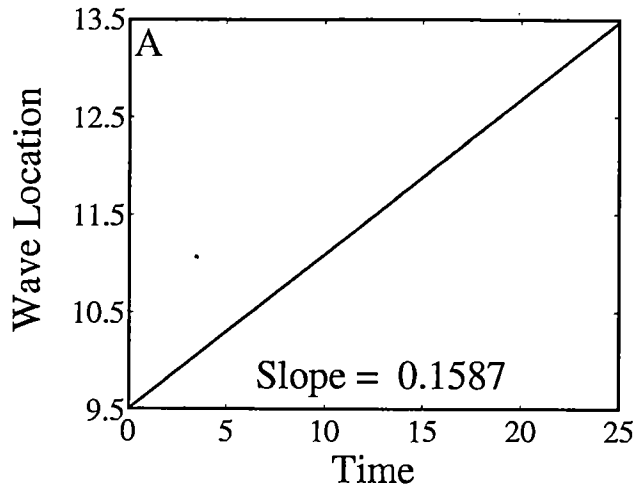


Figure 3.2: The observed speed \bar{c} for IDEs (3.2.13) with the Laplace kernels (3.3.16)

The observed speed \bar{c} was obtained by simulating the traveling wave solution of IDEs (3.2.13) with Laplace kernels (3.3.16). The population was fixed to obtain the location of the wave for each generation t . The slope of the location of the wave with respect to the generation t is the observed speed \bar{c} . The parameters were chosen as A: $\lambda_1 = \lambda_2 = 1.5$, $\beta_{12} = 0.25$, $\beta_{21} = 1.25$, $\alpha_1 = 7.0$, $\alpha_2 = 5.0$, and B: $\lambda_1 = 1.2$, $\lambda_2 = 1.5$, $\beta_{12} = 0.2$, $\beta_{21} = 1.2$, $\alpha_1 = \alpha_2 = 7.0$.

$$\lambda_1 = 1.2, \lambda_2 = 1.5, \beta_{12} = 0.2, \beta_{21} = 1.2, \alpha_1 = \alpha_2 = 7.0, \quad (3.3.24)$$

the predicted speed is

$$c^* = 0.11173 \quad (3.3.25)$$

and the speed obtained by simulating the traveling wave solution is

$$\bar{c} = 0.1074 \quad (3.3.26)$$

(see Figure 3.2B). □

Example 3.3.2. Consider IDEs (3.2.13) with

$$k_1(x) = \frac{1}{2}\alpha_1 e^{-\alpha_1|x|} \quad (3.3.27)$$

and

$$k_2(x) = \begin{cases} \alpha_2 e^{-\alpha_2 x}, & \text{if } x > 0, \\ 0, & \text{if } x \leq 0, \end{cases} \quad (3.3.28)$$

Since the first kernel is a Laplace kernel, equations (3.3.19) and (3.3.20) give the parametric equations for speed c^* . For the case

$$\lambda_1 = \lambda_2 = 2, \beta_{12} = 0.25, \beta_{21} = 1.25, \alpha_1 = 7, \alpha_2 = 5, \quad (3.3.29)$$

the predicted speed is

$$c^* = 0.2155. \quad (3.3.30)$$

The speed obtained by simulating the traveling wave solution is

$$\bar{c} = 0.2116 \quad (3.3.31)$$

(see Figure 3.3). □

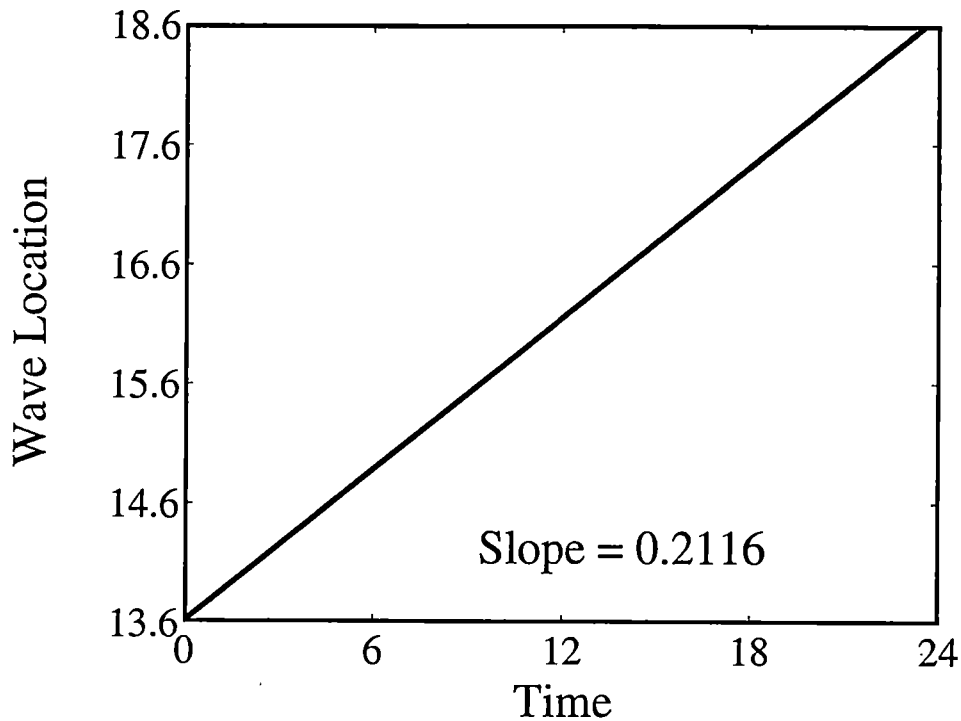


Figure 3.3: The observed speed \bar{c} for IDEs (3.2.13) with kernels (3.3.27) and (3.3.28)

The observed speed \bar{c} was obtained by simulating the traveling wave solution of IDEs (3.2.13) with kernels (3.3.27) and (3.3.28). The population was fixed to obtain the location of the wave for each generation t . The slope of the location of the wave with respect to the generation t is the observed speed \bar{c} . The parameters were chosen as $\lambda_1 = \lambda_2 = 2$, $\beta_{12} = 0.25$, $\beta_{21} = 1.25$, $\alpha_1 = 7.0$, $\alpha_2 = 5.0$.

The above analysis is customarily based on linearization. However, Hosono [47, 48] has proved that the minimal speed derived by linearization may underestimate the true wave speed for a reaction-diffusion system because of the introduction of a weak Allee effect. I find that this effect may also affect my estimation of the wave speed.

Weak Allee effect

Let us now consider a special case that causes a weak Allee effect in competition model (3.2.13). For this special case, I define

$$k_2(x - y) = \delta(x - y), \quad (3.3.32)$$

where $\delta(x)$ is the Dirac delta function so that IDE (3.2.13) is rewritten as

$$u_{t+1}(x) = \int_{-\infty}^{+\infty} k_1(x - y) f(u_t(y), v_t(y)) dy, \quad (3.3.33a)$$

$$v_{t+1}(x) = g(u_t(x), v_t(x)), \quad (3.3.33b)$$

where

$$f(u_t(y), v_t(y)) = \frac{\lambda_1 u_t(y)}{1 + (\lambda_1 - 1)[u_t(y) + \beta_{12} v_t(y)]}, \quad (3.3.33c)$$

$$g(u_t(y), v_t(y)) = \frac{\lambda_2 v_t(y)}{1 + (\lambda_2 - 1)[v_t(y) + \beta_{21} u_t(y)]}, \quad (3.3.33d)$$

$$\lambda_1 > 1, \quad \lambda_2 > 1. \quad (3.3.33e)$$

The traveling wave solution,

$$u_{t+1}(x) = u_t(x - c), \quad v_{t+1}(x) = v_t(x - c) \quad (3.3.34)$$

satisfies

$$u_t(x - c) = \int_{-\infty}^{+\infty} k_1(x - y) f(u_t(y), v_t(y)) dy, \quad (3.3.35a)$$

$$v_t(x - c) = \frac{\lambda_2 v_t(x)}{1 + (\lambda_2 - 1)[v_t(x) + \beta_{21} u_t(x)]}. \quad (3.3.35b)$$

As λ_2 goes to ∞ , equation (3.3.35b) implies that

$$v_t(x - c) = \lim_{\lambda_2 \rightarrow +\infty} \frac{\lambda_2 v_t(x)}{1 + (\lambda_2 - 1)[v_t(x) + \beta_{21} u_t(x)]} \quad (3.3.36)$$

$$= \frac{v_t(x)}{v_t(x) + \beta_{21} u_t(x)}. \quad (3.3.37)$$

I thus have

$$\frac{\lambda_2 v_t(x)}{1 + (\lambda_2 - 1)[v_t(x) + \beta_{21} u_t(x)]} = \frac{v_t(x)}{v_t(x) + \beta_{21} u_t(x)} \quad (3.3.38)$$

or

$$v_t(x)[1 - v_t(x) - \beta_{21} u_t(x)] = 0 \quad (3.3.39)$$

as λ_2 goes to ∞ .

In light of equation (3.3.39), I can define $v_t(x)$ as

$$v_t(x) = \begin{cases} 0, & \frac{1}{\beta_{21}} < u_t(x) < 1, \\ 1 - \beta_{21} u_t(x), & 0 < u_t(x) < \frac{1}{\beta_{21}}, \end{cases} \quad (3.3.40)$$

so that two-species competition problem (3.2.13) reduces to the single-species problem

$$u_{t+1}(x) = \int_{-\infty}^{+\infty} k_1(x - y) F(u_t(y)) dy, \quad (3.3.41a)$$

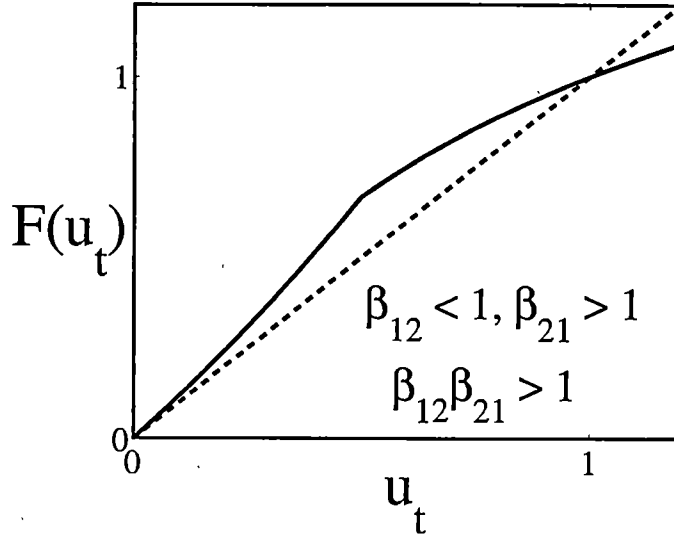


Figure 3.4: Weak Allee growth rate (3.3.41c)

Function (3.3.41c) is the growth rate of the resulting single-species IDE (3.3.41a) of IDEs (3.2.13) using kernel (3.3.32) for the second species. This growth rate exhibits a weak Allee effect.

where

$$F(u_t(y)) = f(u_t(y), v_t(y)) \quad (3.3.41b)$$

$$= \begin{cases} \frac{\lambda_1 u_t(y)}{1 + (\lambda_1 - 1)u_t(y)}, & \frac{1}{\beta_{21}} < u_t(y) < 1, \\ \frac{\lambda_1 u_t(y)}{1 + (\lambda_1 - 1)[u_t(y)(1 - \beta_{21}\beta_{12}) + \beta_{12}]}, & 0 < u_t(x) < \frac{1}{\beta_{21}} \end{cases} \quad (3.3.41c)$$

(see Figure 3.4).

Notice that $F(u_t(y))$ is nonnegative and

$$F'(0) = \frac{\lambda_1}{1 + (\lambda_1 - 1)\beta_{12}} > 1. \quad (3.3.42)$$

In addition, I have

$$F(u_t(y)) > F'(0)u_t(y) \text{ for } 0 < u_t(y) < \frac{1}{\beta_{21}} \quad (3.3.43)$$

if

$$\beta_{12}\beta_{21} > 1. \quad (3.3.44)$$

These imply that the reduced single species problem has a weak Allee effect if (3.3.44) holds and c^* may underestimate the true minimal speed for the original two-species problem.

Since single-species IDE (3.3.41) has a weak Allee effect, linearization may fail to give the correct speed for the traveling wave solution. However, I will estimate the speed of the wave under this weak Allee effect by means of a linear-constant approximation $F^*(u_t)$ to the growth function $F(u_t)$. The function F^* has the same form as the one that appears in equation (1.3.1)

$$F^*(u_t) = \begin{cases} \lambda u_t, & 0 < u_t < a, \\ 1, & a \leq u_t < 1, \end{cases} \quad (3.3.45)$$

where

$$1 < \lambda \leq \frac{1}{a}, \quad 0 < a < 1. \quad (3.3.46)$$

I define

$$A(a) \equiv \int_0^a \lambda u \, du + \int_a^1 1 \, du - \frac{1}{2} = \frac{\lambda a^2}{2} - a + \frac{1}{2}, \quad (3.3.47)$$

as the area bounded by the 45° line and $F^*(u_t)$ and

$$B \equiv \int_0^{\frac{1}{\beta_{21}}} \frac{\lambda_1 u}{1 + (\lambda_1 - 1)[(1 - \beta_{12}\beta_{21})u + \beta_{12}]} \, du + \int_{\frac{1}{\beta_{21}}}^1 \frac{\lambda_1 u}{1 + (\lambda_1 - 1)u} \, du - \frac{1}{2}, \quad (3.3.48)$$

as the area bounded by the 45° line and $F(u_t)$. For F^* , function (3.3.45), the parameter λ is chosen as the slope of F at $u_t = 0$,

$$\lambda = F'(0) = \frac{\lambda_1}{1 + (\lambda_1 - 1)\beta_{12}} \quad (3.3.49)$$

and the parameter a is the a^* that makes $A(a)$ as close as possible to B ,

$$|A(a^*) - B| = \min_{0 < a \leq \frac{1}{\lambda}} |A(a) - B| = \min_{0 < a \leq \frac{1}{\lambda}} \left| \frac{\lambda a^2}{2} - a + \frac{1}{2} - B \right|. \quad (3.3.50)$$

I approximate the wave speed of IDE (3.3.43) by estimating the speed for the system

$$u_{t+1}(x) = \int_{-\infty}^{+\infty} k_1(x-y)F^*(u_t(y)) dy, \quad (3.3.51)$$

where $F^*(u_t)$ is defined as Allee growth function (3.3.45) and the parameters λ and a^* are defined by equations (3.3.49) and (3.3.50), respectively. Applying iterative scheme (1.3.11) to (3.3.51), I solve for c as a function of λ numerically.

Example 3.3.3. Consider IDEs (3.2.13) with

$$k_1(x) = \frac{1}{2}\alpha e^{-\alpha|x|}, \quad k_2(x) = \delta(x), \quad (3.3.52)$$

and

$$\lambda_1 = 2.0, \quad \lambda_2 = \infty, \quad \beta_{12} = 0.75, \quad \alpha = 7.0. \quad (3.3.53)$$

If I choose $\beta_{21} = 1.5$, I have by definitions (3.3.49) and (3.3.50) that

$$\lambda = 1.1429, \quad a^* = 0.8180447. \quad (3.3.54)$$

The predicted speed obtained from parametric equations (3.3.15) is $c^* = 0.10771$, the approximated speed obtained by iterative scheme (1.3.11) is $\bar{c} = 0.1040$, and the speed obtained by simulating the traveling wave solution is $\bar{c} = 0.1064$ (see Figure 3.5A).

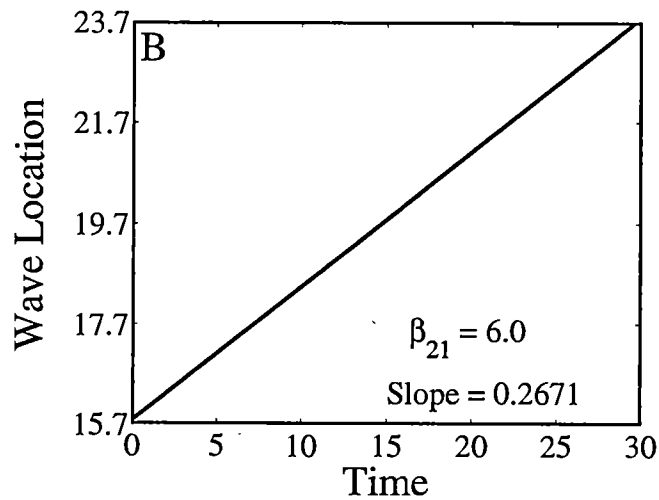
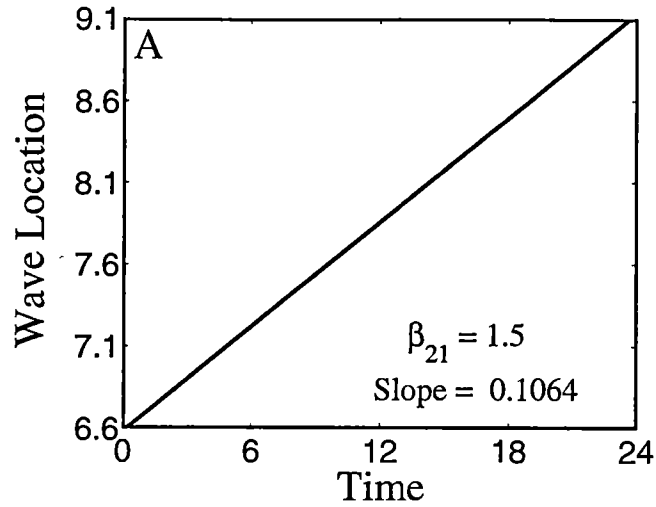


Figure 3.5: The observed speed \bar{c} of IDEs (3.2.13) with kernels (3.3.52)

The observed speed \bar{c} was obtained by simulating the traveling wave solution of IDEs (3.2.13) with kernels (3.3.52). The population was fixed to obtain the location of the wave for each generation t . The slope of the location of the wave with respect to the generation t is the observed speed \bar{c} . The parameters were chosen as $\lambda_1 = 2.0$, $\lambda_2 = \infty$, $\beta_{21} = 1.5$ (A) and 6.0 (B), $\beta_{12} = 0.75$, $\alpha = 7.0$.

If I choose $\beta_{21} = 6$, I have by definitions (3.3.49) and (3.3.50) that

$$\lambda = 1.1429, \quad a^* = 0.5889. \quad (3.3.55)$$

The predicted speed obtained from parametric equations (3.3.15) is $c^* = 0.10771$, the approximated speed obtained by iterative scheme (1.3.11) is $\tilde{c} = 0.1068$, and the speed obtained by simulating the traveling wave solution is $\bar{c} = 0.2671$ (see Figure 3.5B). Figure 3.6 shows the graphs of the resulting functions F and F^* . \square

Even though the two choices of β_{21} in the above example both satisfy $\beta_{12}\beta_{21} > 1$, c^* is quite close to \tilde{c} for $\beta_{21} = 1.5$, not for $\beta_{21} = 6.0$. Once again, I conclude that linearization may give the correct speed of invasion for a sufficiently weak Allee effect and may fail to give the correct speed of invasion for an insufficient weak Allee effect. On the other hand, the linear-constant approximation provide a good estimate of the wave speed for $\beta_{21} = 1.5$, but not for $\beta_{21} = 6.0$.

3.3.2 The behavior behind the wave

To analyze the behavior behind the wave, I restrict my attention to $c^* > 0$ for symmetric kernels (3.2.6). Even though the speed c^* obtained from linearization may underestimate the true wave speed, it still gives a lower bound of the true speed. This means $c \geq c^* > 0$ provided that $c^* > 0$.

I will look at the back of the wave by linearizing about $(u, v) = (1, 0)$. If I let

$$\tilde{u}(x) = u(x) - 1, \quad \tilde{v}(x) = v(x), \quad (3.3.56)$$

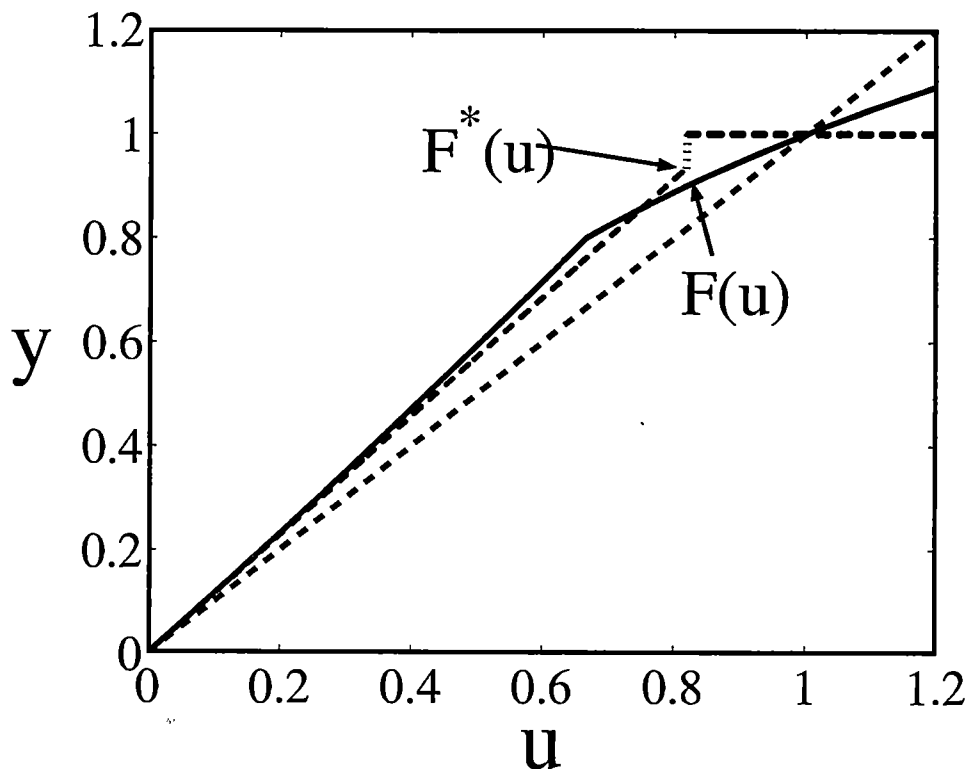


Figure 3.6: Growth function F in (3.3.41c) and its linear-constant approximation F^*

The function F is the growth rate of the resulting single-species IDE (3.3.41a) of IDEs (3.2.13) using kernels (3.3.52). The function F^* is a linear-constant approximation of the growth rate F and is defined as (3.3.45). The parameters were chosen as $\lambda_1 = 2.0$, $\lambda_2 = \infty$, $\beta_{12} = 1.5$, $\beta_{21} = 0.75$, $\alpha = 7.0$. The slope of the linear ramp for the linear-constant approximation is $\lambda = 1.1429$, while the parameter $a^* = 0.8180447$.

the linearization is

$$\tilde{u}(x - c) = \int_{-\infty}^{+\infty} k_1(x - y) \left[\frac{1}{\lambda_1} \tilde{u}(y) - \left(1 - \frac{1}{\lambda_1} \right) \beta_{12} \tilde{v}(y) \right] dy, \quad (3.3.57a)$$

$$\tilde{v}(x - c) = \int_{-\infty}^{+\infty} k_2(x - y) \left[\frac{\lambda_2}{1 + (\lambda_2 - 1)\beta_{21}} \right] \tilde{v}(y) dy. \quad (3.3.57b)$$

For IDEs (3.2.13), I look for an exponentially bounded trailing edge of the traveling wave,

$$\tilde{u}(x) = u_1 e^{sx}, \quad \tilde{v}(x) = v_1 e^{sx} \quad (3.3.58)$$

with $s > 0$. Substituting (3.3.58) into equations (3.3.57) and making the change of variables $z \equiv x - y$, I obtain

$$u_1 e^{-sc} = \left[\frac{1}{\lambda_1} u_1 - \left(1 - \frac{1}{\lambda_1} \right) \beta_{12} v_1 \right] L_1(s), \quad (3.3.59a)$$

$$v_1 e^{-sc} = \frac{\lambda_2}{1 + (\lambda_2 - 1)\beta_{21}} v_1 L_2(s), \quad (3.3.59b)$$

where

$$L_i(s) \equiv \int_{-\infty}^{+\infty} k_i(z) e^{-sz} dz, \quad i = 1, 2, \quad (3.3.60)$$

are the two sided Laplace transforms. System (3.3.59) can be written in the matrix form

$$\begin{bmatrix} \frac{e^{-sc}}{L_1(s)} - \frac{1}{\lambda_1} & \left(1 - \frac{1}{\lambda_1} \right) \beta_{12} \\ 0 & \frac{e^{-sc}}{L_2(s)} - \frac{\lambda_2}{1 + (\lambda_2 - 1)\beta_{21}} \end{bmatrix} \begin{bmatrix} u_1 \\ v_1 \end{bmatrix} = \begin{bmatrix} 0 \\ 0 \end{bmatrix}. \quad (3.3.61)$$

I, once again, impose the condition that the leading matrix is singular to get two transcendental equations. The roots of the first equation,

$$\frac{e^{-sc}}{L_1(s)} - \frac{1}{\lambda_1} = 0, \quad (3.3.62)$$

have eigenvectors for the form $(1, 0)$. This contradicts my assumption that the second species dominates the system and is at its carrying capacity at the beginning of the problem. The second equation can be written as

$$\frac{e^{-sc}}{L_2(s)} = Q, \quad (3.3.63)$$

where

$$Q \equiv \frac{\lambda_2}{1 + (\lambda_2 - 1)\beta_{21}} < 1. \quad (3.3.64)$$

The value of s for the edge behind the traveling wave is given by equation (3.3.63).

To prevent negative population density for the retreating species, I need a monotonic (rather than oscillatory) wave back and positive real (rather than complex) roots s . I also need a positive real root s to get an exponentially bounded wave edge. The existence of a positive real root of equation (3.3.63) will be shown in Lemma 3.3. To prove Lemma 3.3, I first introduce Watson's lemma (Olver, 1974).

Lemma 3.1. (*Watson's lemma*) *Let*

$$I(s) \equiv \int_0^\infty e^{-sz} h(z) dz, \quad (3.3.65)$$

and assume that the following three conditions hold:

1. *$h(z)$ is a real or complex function of the positive real variable z with a finite number of discontinuities and infinities;*
2. *as $z \rightarrow 0^+$,*

$$h(z) \approx \sum_{i=0}^{\infty} a_i z^{\frac{i+\lambda-\mu}{\mu}}, \quad (3.3.66)$$

where μ is a positive constant and λ is a real or complex constant such that the real part of λ is positive;

3. the abscissa of convergence of the integral (3.3.66) is not ∞ .

Then

$$I(s) \approx \sum_{i=0}^{\infty} \Gamma\left(\frac{i+\lambda}{\mu}\right) \frac{a_i}{s^{\frac{i+\lambda}{\mu}}} \quad (3.3.67)$$

as $s \rightarrow \infty$ in the sector

$$|\text{ph } s| \leq \frac{1}{2}\pi - \delta \left(< \frac{1}{2}\pi \right), \quad (3.3.68)$$

where $\text{ph } s$ is defined as the argument of s , δ is an arbitrary constant, and $s^{\frac{i+\lambda}{\mu}}$ has its principle value. \square

Corollary 3.2. There exist real numbers $a_i, b_i, i = 1, 2, \dots$ such that

$$\int_0^{\infty} e^{-sz} k(z) dz \approx \sum_{i=1}^{\infty} \frac{a_i}{s^{i+1}}, \text{ as } s \rightarrow \infty, \quad (3.3.69)$$

and

$$\int_0^{\infty} e^{-sz} zk(z) dz \approx \sum_{i=1}^{\infty} \frac{b_i}{s^{i+2}}, \text{ as } s \rightarrow \infty. \quad (3.3.70)$$

Proof : By Lemma 3.1, if I let

$$h(z) = k(z) \quad (3.3.71)$$

and

$$\lambda = \mu = 1, \quad (3.3.72)$$

then there exist $a_i, i = 1, 2, \dots$ such that (3.3.69) holds. In addition, if I let

$$h(z) = zk(z), \quad (3.3.73)$$

and

$$\lambda = 2, \mu = 1, \quad (3.3.74)$$

then there exist $b_i, i = 1, 2, \dots$ such that (3.3.70) holds. \square

Lemma 3.3. *Let*

$$q(s) = \frac{e^{-sc}}{L(s)} \text{ for } s \geq 0 \text{ and } c > 0 \quad (3.3.75)$$

and given a real number Q , $0 < Q < 1$, *then there exists a positive real number* s^* *such that*

$$q(s^*) = Q. \quad (3.3.76)$$

Proof : Setting $s \equiv 0$ in equation (3.3.76) implies that

$$q(0) = 1. \quad (3.3.77)$$

I assume that $L(s)$ is well-defined on $[0, \bar{\tau})$ ($\bar{\tau}$ can be ∞) and will show that

$$\lim_{s \rightarrow \bar{\tau}^-} q(s) = 0. \quad (3.3.78)$$

Mean Value Theorem guarantees the existence of a positive real number s^* ($0 < s^* < \bar{\tau}$) that satisfies (3.3.78).

Since

$$L(s) = \int_{-\infty}^{+\infty} e^{-sz} k(z) dz > 0, \quad (3.3.79)$$

I have

$$L''(s) = \int_{-\infty}^{+\infty} e^{-sz} k(z) z^2 dz > 0, \quad (3.3.80)$$

which implies that $L(s)$ is a convex function and $L'(s)$ is a strictly increasing function. I will show that asymptotic boundary condition (3.3.78) holds by considering the following two cases:

Case 1 Assume that $L(s)$ is a strictly decreasing function,

$$L'(s) < 0 \text{ for all } s \geq 0. \quad (3.3.81)$$

Assumption (3.3.81) implies that

$$L(s) < L(0) = 1 \text{ for } s > 0 \quad (3.3.82)$$

and $L(s)$ is well-defined on $[0, \infty)$. Assumption (3.3.81) also implies that

$$\lim_{s \rightarrow \infty} L'(s) \leq 0. \quad (3.3.83)$$

By corollary 3.2, I have

$$\lim_{s \rightarrow \infty} L'(s) = \lim_{s \rightarrow \infty} \int_0^{\infty} [(-z)e^{-sz}k(z) + ze^{sz}k(-z)] dz \quad (3.3.84)$$

$$= \lim_{s \rightarrow \infty} \left[\sum_{i=1}^{\infty} \frac{-b_i}{s^{i+2}} + \int_0^{\infty} ze^{sz}k(-z) dz \right] \quad (3.3.85)$$

$$= \lim_{s \rightarrow \infty} \int_0^{\infty} ze^{sz}k(-z) dz \quad (3.3.86)$$

for some real numbers b_i , $i = 1, 2, \dots$. It follows that

$$\lim_{s \rightarrow \infty} \int_0^{\infty} ze^{sz}k(-z) dz \leq 0. \quad (3.3.87)$$

Since z , e^{sz} and $k(-z)$ are all nonnegative on $(-\infty, \infty)$, I conclude that

$$\lim_{s \rightarrow \infty} \int_0^{\infty} ze^{sz}k(-z) dz = 0 \quad (3.3.88)$$

and

$$k(z) = 0 \text{ almost everywhere on } (-\infty, 0). \quad (3.3.89)$$

By (3.3.89) and corollary 3.2, I have

$$\lim_{s \rightarrow \infty} L(s) = \lim_{s \rightarrow \infty} \sum_{i=1}^{\infty} \frac{a_i}{s^{i+1}} + \lim_{s \rightarrow \infty} \int_0^{\infty} e^{sz}k(-z) dz \quad (3.3.90)$$

$$= \lim_{s \rightarrow \infty} \sum_{i=1}^{\infty} \frac{a_i}{s^{i+1}} \quad (3.3.91)$$

for some real numbers a_i , $i = 1, 2, \dots$. Under Assumption (3.3.81) of $L'(s)$, I thus have

$$\lim_{s \rightarrow \infty} q(s) = \lim_{s \rightarrow \infty} \frac{e^{-sc}}{L(s)} = \lim_{s \rightarrow \infty} \frac{e^{-sc}}{\sum_{i=1}^{\infty} \frac{a_i}{s^{i+1}}} = 0. \quad (3.3.92)$$

Case 2 Assume that

$$\exists \bar{s} \geq 0 \text{ s. t. } L'(\bar{s}) \geq 0. \quad (3.3.93)$$

Under this assumption, I have

$$L'(s) > L'(\bar{s}) \geq 0, \text{ for } s > \bar{s} \quad (3.3.94)$$

because $L'(s)$ is a strictly increasing function. Inequality (3.3.93) implies that $L(s)$ is a strictly increasing function for $s \geq \bar{s}$. Since $L(s)$ is defined as a continuous function, there exists a positive number τ such that $L(s)$ is well-defined on $[0, \tau)$ (τ can be ∞) and

$$\lim_{s \rightarrow \tau^{-1}} L(s) = \infty. \quad (3.3.95)$$

Under Assumption (3.3.93), I thus have

$$\lim_{s \rightarrow \tau^{-1}} q(s) = \lim_{s \rightarrow \tau^{-1}} \frac{e^{-sc}}{L(s)} = 0. \quad (3.3.96)$$

The above two cases guarantee the existence of a positive real number s^* that satisfies equation (3.3.76) of q . I conclude that if the heteroclinic connection from $(1, 0)$ to $(0, 1)$ exists and the minimum speed c^* is positive, the wave then has an exponentially bounded tail and there is no oscillation behind the wave.

Example 3.3.4. Consider the kernel

$$k_2(x) = \frac{1}{2}\alpha e^{-\alpha|x|} \quad (3.3.97)$$

with the two-sided Laplace transform,

$$L_2(s) = \frac{\alpha^2}{\alpha^2 - s^2}, \quad |s| < \alpha. \quad (3.3.98)$$

I can show the existence of a positive real number s^* that satisfies equation (3.3.76).

I am done if I can find a positive real root s^* of the equation

$$1 - \frac{s^2}{\alpha^2} = Qe^{sc} \quad (0 < Q < 1). \quad (3.3.99)$$

By plotting $1 - s^2/\alpha^2$ and Qe^{sc} as functions of s on the two dimensional plane, one can see from Figure 3.7 the existence of a positive real root s^* . □

Example 3.3.5. Consider IDEs (3.2.13) with Laplace kernels (3.3.16) in example 3.3.1

Since the Laplace kernel is symmetric for the first species, the minimum speed c^* is positive so that there exists a positive root s^* for equation (3.3.76) of q . Figure 3.8 shows the traveling wave solutions for two different choices of parameters. There is no oscillation behind the wave for the Laplace kernels. □

Example 3.3.6. Consider IDEs (3.2.13) with kernels (3.3.27) and (3.3.28) in example 3.3.2.

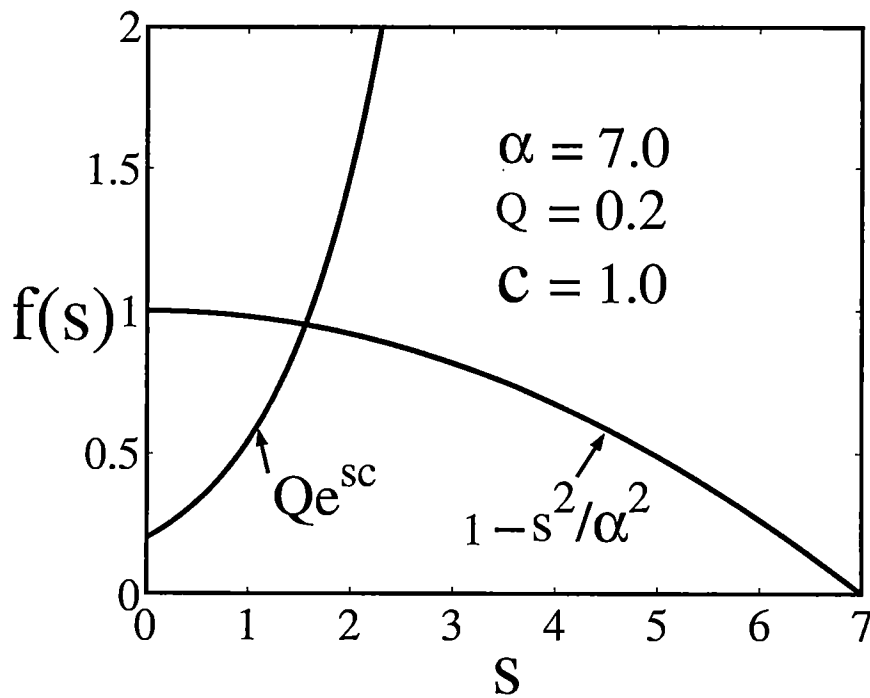


Figure 3.7: The root s^* of equation (3.3.99)

Note: For each real number Q in the interval $(0, 1)$, there exists a positive root s^* of equation (3.3.99) provided that $c \geq 0$.

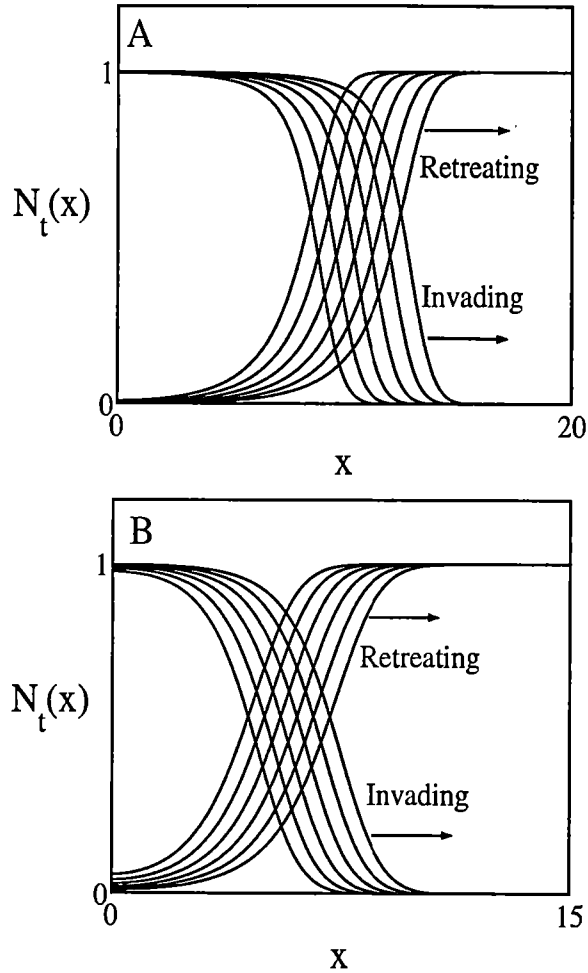


Figure 3.8: The traveling wave solution for IDEs (3.2.13) with Laplace kernels (3.3.16)

The population densities of the two species converge to traveling waves, that are moving to the right for $x > 0$. The first species is the invading species (approaching density 1), while the second species is the retreating species (approaching density 0). The parameters in subfigure A were chosen as $\lambda_1 = \lambda_2 = 1.5$, $\beta_{12} = 0.25$, $\beta_{21} = 1.25$, $\alpha_1 = 7.0$, $\alpha_2 = 5.0$. The parameters in subfigure B were chosen as $\lambda_1 = 1.2$, $\lambda_2 = 1.5$, $\beta_{12} = 0.2$, $\beta_{21} = 1.2$, $\alpha_1 = \alpha_2 = 7.0$. There is no oscillation behind the wave.

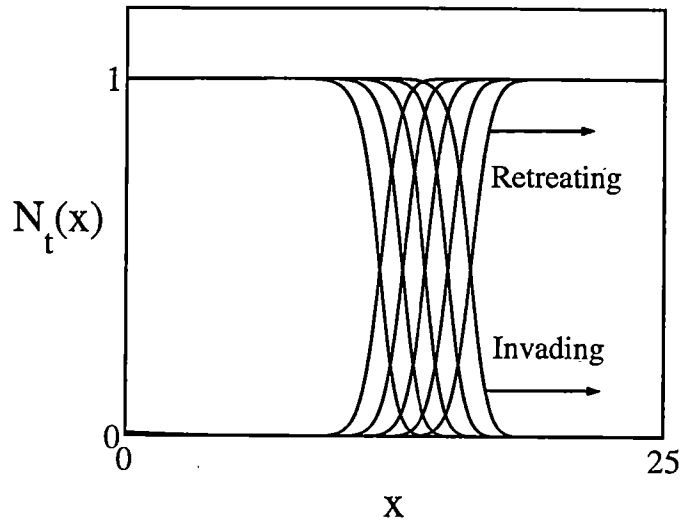


Figure 3.9: The traveling wave solution for IDEs (3.2.13) with kernels (3.3.27) and (3.3.28)

The population densities of the two species converge to traveling waves, that are moving to the right for $x > 0$. The first species is the invading species (approaching density 1), while the second species is the retreating species (approaching density 0). The parameters were chosen as $\lambda_1 = \lambda_2 = 2.0$, $\beta_{12} = 0.25$, $\beta_{21} = 0.5$, $\alpha_1 = 7.0$, and $\alpha_2 = 5.0$. There is no oscillation behind the wave.

Since the Laplace kernel (3.3.27) is symmetric, the minimum speed c^* is positive so that there exists a positive root s^* for equation (3.3.76) of q . Figure 3.9 shows the traveling wave solutions for this example. \square

Chapter 4

Integrodifference Equations and Competition Models, II

In this chapter, I consider competition model (3.2.13) with $\beta_{12} < 1$ and $\beta_{21} < 1$. The analysis of the front of the wave is the same as that of the case in chapter 3. I will focus on the analysis on the back of the wave for $\beta_{12} < 1$ and $\beta_{21} < 1$ in this chapter. Some sufficient conditions that guarantee no oscillation behind the wave are given.

4.1 Traveling waves

In this section, I consider IDEs (3.2.13) for the case

$$\beta_{12} < 1, \beta_{21} < 1, \tag{4.1.1}$$

in which the first species is invading a resource that is dominated by the second species at equilibrium. I also look for traveling wave solutions: the heteroclinic connection from the interior equilibrium (u^*, v^*) to $(0, 1)$, where u^* and v^* are defined as (3.2.16).

The analysis of the front of the wave is the same as that of the case in chapter 3. From section 3.3.1, I know that speed formula (3.3.15) may underestimate the true minimum speed under conditions (3.2.18) and (3.3.46) of β_{12} and β_{21} because of a weak Allee effect. I could not determine whether this result also occurs in case (4.1.1) or not. However, speed formula (3.3.15) gives a lower bound of the minimum wave speed c^* .

4.1.1 The behavior behind the wave

In this subsection, I also restrict my attention to the case $c^* > 0$, which includes the case of symmetric kernels (3.2.6). I analyze the wave back by linearizing near the equilibrium,

$$(u^*, v^*) = \left(\frac{1 - \beta_{12}}{1 - \beta_{12}\beta_{21}}, \frac{1 - \beta_{21}}{1 - \beta_{12}\beta_{21}} \right). \quad (4.1.2)$$

If I let

$$\tilde{u}(x) \equiv u(x) - u^*, \quad \tilde{v}(x) \equiv v(x) - v^*, \quad (4.1.3)$$

the linearization is

$$\begin{aligned} \tilde{u}(x - c) &= \int_{-\infty}^{+\infty} k_1(x - y) \left[\frac{1 + (\lambda_1 - 1)\beta_{12}v^*}{\lambda_1} \right] \tilde{u}(y) dy \\ &+ \int_{-\infty}^{+\infty} k_1(x - y) \left[\frac{-u^*\beta_{12}(\lambda_1 - 1)}{\lambda_1} \right] \tilde{v}(y) dy, \end{aligned} \quad (4.1.4a)$$

$$\begin{aligned} \tilde{v}(x - c) &= \int_{-\infty}^{+\infty} k_2(x - y) \left[\frac{-v^*\beta_{21}(\lambda_2 - 1)}{\lambda_2} \right] \tilde{u}(y) dy \\ &+ \int_{-\infty}^{+\infty} k_2(x - y) \left[\frac{1 + (\lambda_2 - 1)\beta_{21}u^*}{\lambda_2} \right] \tilde{v}(y) dy. \end{aligned} \quad (4.1.4b)$$

For system (4.1.4), I look for an exponential bounded edge of the traveling

wave,

$$\tilde{u}(x) = u_1 e^{sx}, \quad \tilde{v}(x) = v_1 e^{sx} \quad (4.1.5)$$

with $s > 0$. After substituting (4.1.5) into (4.1.4) and making the change of the variables $z \equiv x - y$, I obtain

$$u_1 e^{-sc} = \left[\frac{1 + (\lambda_1 - 1)\beta_{12}v^*}{\lambda_1} \right] u_1 L_1(s) + \left[\frac{-u^*\beta_{12}(\lambda_1 - 1)}{\lambda_1} \right] v_1 L_1(s), \quad (4.1.6a)$$

$$v_1 e^{-sc} = \left[\frac{-v^*\beta_{21}(\lambda_2 - 1)}{\lambda_2} \right] u_1 L_2(s) + \left[\frac{1 + (\lambda_2 - 1)\beta_{21}u^*}{\lambda_2} \right] v_1 L_2(s), \quad (4.1.6b)$$

which can be written as the matrix form,

$$\begin{bmatrix} \frac{e^{-sc}}{L_1(s)} - \frac{1 + (\lambda_1 - 1)\beta_{12}v^*}{\lambda_1} & \frac{u^*\beta_{12}(\lambda_1 - 1)}{\lambda_1} \\ \frac{v^*\beta_{21}(\lambda_2 - 1)}{\lambda_2} & \frac{e^{-sc}}{L_2(s)} - \frac{1 + (\lambda_2 - 1)\beta_{21}u^*}{\lambda_2} \end{bmatrix} \begin{bmatrix} u_1 \\ v_1 \end{bmatrix} = \begin{bmatrix} 0 \\ 0 \end{bmatrix}. \quad (4.1.7)$$

Again, I impose the condition that the leading matrix of (4.1.7) is singular for nontrivial solutions. This leads to the characteristic equation,

$$[p(s) - D][q(s) - E] = B, \quad (4.1.8)$$

or

$$p(s)q(s) - [Dp(s) + Eq(s)] + DE - B = 0, \quad (4.1.9)$$

where

$$p(s) \equiv \frac{e^{-sc}}{L_1(s)}, \quad q(s) \equiv \frac{e^{-sc}}{L_2(s)}, \quad (4.1.10a)$$

$$B \equiv \left(D - \frac{1}{\lambda_1} \right) \left(E - \frac{1}{\lambda_2} \right), \quad (4.1.10b)$$

$$0 < D \equiv \frac{1 + (\lambda_1 - 1)\beta_{12}v^*}{\lambda_1} < \frac{1 + (\lambda_1 - 1)}{\lambda_1} = 1, \quad (4.1.10c)$$

$$0 < E \equiv \frac{1 + (\lambda_2 - 1)\beta_{21}u^*}{\lambda_2} < \frac{1 + (\lambda_2 - 1)}{\lambda_2} = 1, \quad (4.1.10d)$$

$$0 < DE - B = \frac{1 + (\lambda_1 - 1)\beta_{12}v^* + (\lambda_2 - 1)\beta_{21}u^*}{\lambda_1\lambda_2}. \quad (4.1.10e)$$

Special case: equal dispersal

For the case $k_1(x) = k_2(x)$, I have $L_1(s) = L_2(s)$ and $p(s) = q(s)$. I define

$$k(x) \equiv k_1(x) = k_2(x), \quad L(s) \equiv L_1(s) = L_2(s), \quad (4.1.11)$$

so that characteristic equation (4.1.9) reduces to

$$[p(s)]^2 - (D + E)p(s) + DE - B = 0. \quad (4.1.12)$$

It follows that

$$p(s) = \frac{(D + E) + \sqrt{(D - E)^2 + 4B}}{2} \equiv p_1, \quad (4.1.13a)$$

or

$$p(s) = \frac{(D + E) - \sqrt{(D - E)^2 + 4B}}{2} \equiv p_2. \quad (4.1.13b)$$

Since $D + E$ and $DE - B$ are both positive and by definition (4.1.13), p_1 and p_2 are both positive real numbers. In addition, I have

$$1 + DE - D - E - B = \frac{(\lambda_1 - 1)(\lambda_2 - 1)(1 - \beta_{12})(1 - \beta_{21})}{\lambda_1 \lambda_2 (1 - \beta_{12} \beta_{21})} > 0, \quad (4.1.14)$$

which implies that

$$B < 1 + DE - D - E \quad (4.1.15)$$

and leads to

$$p_1 < 1. \quad (4.1.16)$$

On the other hand, I have

$$0 < p_2 = \frac{(D + E) - \sqrt{(D - E)^2 + 4B}}{2} < \frac{D + E - |D - E|}{2} < 1. \quad (4.1.17)$$

For characteristic equation (4.1.12), I have shown from the above that

$$p(s) = p_1 \text{ or } p(s) = p_2, \quad (4.1.18a)$$

where

$$0 < p_1 < 1, \quad 0 < p_2 < 1. \quad (4.1.18b)$$

I now consider the following questions in order to know the behavior behind the wave.

1. Is there any positive real root s of characteristic equation (4.1.12)?
2. Is the smallest positive real root of characteristic equation (4.1.12) smaller than all positive real parts of any complex roots of equation (4.1.12) with positive real parts? (If the answer is yes, then there is no oscillation behind the wave.)

The answer is yes for the first question. I have shown in Lemma 3.3 that there exists at least a positive real root s_j of $p(s) = p_j$ ($j = 1, 2$). This implies that there exist positive real roots s_1 and s_2 of characteristic equation (4.1.12). I assume that s_j^* is the smallest positive real root of $p(s) = p_j$ for $j = 1, 2$.

The answer is yes for the second question if the smallest positive real root s_j^* of $p(s) = p_j$ is smaller than all positive real parts of any complex roots of $p(s) = p_j$ with positive real parts, where $j = 1, 2$.

I will show in Theorem 4.1 and Theorem 4.3 that if the kernel satisfies Condition 4.1 or Condition 4.2, then there is no oscillation behind the wave.

I will also introduce Lemma 4.2 for proving Theorem 4.3.

Condition 4.1.

$$k(x) \leq k(-x) \text{ almost everywhere on } (0, \infty). \quad (4.1.19)$$

Theorem 4.1. *If the kernel satisfies Condition 4.1, then there is no oscillation behind the wave.*

Proof : Under Condition 4.1, I show in appendix A that the positive real root s_j is smaller than all positive real parts of any complex roots of $p(s) = p_j$ with positive real parts, where $j = 1, 2$. This implies that the smallest positive real root (s_1^* or s_2^*) of characteristic equation (4.1.12) is smaller than all positive real parts of any complex roots of equation (4.1.12) with positive real parts. □

Condition 4.2.

$$L'(s) + cL(s) > 0 \text{ for } c > 0 \text{ and } s \geq 0. \quad (4.1.20)$$

Lemma 4.2. *Define*

$$p(s) \equiv \frac{e^{-sc}}{L(s)}. \quad (4.1.21)$$

If the kernel satisfies Condition 4.2, then $p(s)$ is a strictly decreasing function of s for $s \geq 0$ and $c > 0$. Furthermore, the following inequality holds

$$|p(\beta + i\omega)| \geq |p(\beta)| \text{ for any } \beta \geq 0. \quad (4.1.22)$$

Proof : Differentiating equation (4.1.21) with respect to s , I obtain

$$p'(s) = \frac{-ce^{-sc}L(s) - e^{-sc}L'(s)}{[L(s)]^2} < 0 \text{ for } s \geq 0 \text{ and } c > 0, \quad (4.1.23)$$

which implies $p(s)$ is a strictly decreasing function of s for $s \geq 0$ and $c > 0$.

On the other hand, I have for any $\beta \geq 0$ that

$$|p(\beta+i\omega)| = \frac{|e^{-c(\beta+i\omega)}|}{|L(\beta+i\omega)|} = \frac{e^{-\beta c}}{|\int_{-\infty}^{\infty} k(z)e^{-(\beta+i\omega)z} dz|} \quad (4.1.24)$$

$$\geq \frac{e^{-\beta c}}{\int_{-\infty}^{\infty} |k(z)||e^{-(\beta+i\omega)z}| dz} = \frac{e^{-\beta c}}{\int_{-\infty}^{\infty} k(z)e^{-\beta z} dz} = p(\beta). \quad (4.1.25)$$

□

Theorem 4.3. *If the kernel satisfies Condition 4.2, then there is no oscillation behind the wave.*

Proof : I am done if I can show that under Condition 4.2, the smallest positive real root of characteristic equation (4.1.12) is smaller than all positive real parts of any complex roots of equation (4.1.12) with positive real parts.

By Lemma 3.3, there exists at least one positive real root of $p(s) = p_j$, $j = 1, 2$. Since $p(s)$ is strictly decreasing (by Lemma 4.2) under Condition 4.2, there exists at most one positive real root of $p(s) = p_j$, $j = 1, 2$. I thus conclude that there exists exactly one positive real root s_j^* of $p(s) = p_j$, ($j = 1, 2$) under Condition 4.2.

Suppose $\beta_j + i\omega$, $j = 1, 2$ is a complex root of $p(s) = p_j$ with $\beta_j > 0$, I have by appendix A (Lemma A.1) that

$$\beta_j \neq s_j^*. \quad (4.1.26)$$

If $\beta_j < s_j^*$, I have by Lemma 4.2 that

$$p_j = |p(\beta_j + i\omega)| \geq p(\beta_j) > p(s_j^*) = p_j, \quad (4.1.27)$$

which is a contradiction. Therefore,

$$s_j^* < \beta_j. \quad (4.1.28)$$

Since $p(s)$ is decreasing (by Lemma 4.2) and $p_1 > p_2$, I have

$$s_1^* < s_2^*. \quad (4.1.29)$$

It follows that

$$s_1^* < s_2^* < \beta_2, \quad s_1^* < \beta_1 \quad (4.1.30)$$

for any complex roots $\beta_j + i\omega$ of $p(s) = p_j$ with $\beta_j > 0$, where $j = 1, 2$.

This implies that the smallest positive real root s_1^* of characteristic equation (4.1.12) is smaller than all positive real parts of any complex roots of (4.1.12) with positive real parts. \square

Notice that if $k(x)$ satisfies Condition 4.1, then it satisfies Condition 4.2 because $L'(s) > 0$ under Condition 4.1.

Example 4.1.1. Consider IDEs (3.2.13) with the Laplace kernels

$$k(x) = k_1(x) = k_2(x) = \frac{1}{2}\alpha e^{-\alpha|x|}, \quad (4.1.31)$$

and the two sided Laplace transform

$$L(s) = L_1(s) = L_2(s) = \frac{\alpha^2}{\alpha^2 - s^2}, \quad \text{where } |s| < \alpha. \quad (4.1.32)$$

1. Is there any positive real root of

$$\frac{e^{-sc}}{L(s)} = p, \quad 0 < p < 1? \quad (4.1.33)$$

2. Is the smallest positive real root s_1 smaller than all positive real parts of any complex roots of equation (4.1.12) with positive real parts?

The kernel in this example is symmetric, hence it satisfies Condition 4.1 and Condition 4.2.

Figure 3.8). The root s_1 satisfies

$$e^{-s_1 c} \left(1 - \frac{s_1^2}{\alpha^2}\right) = p. \quad (4.1.35)$$

Let $\beta + i\omega$ ($\omega \neq 0$) be a complex root of equation (4.1.34) with $\beta > 0$ such that

$$1 - \frac{(\beta + i\omega)^2}{\alpha^2} = pe^{(\beta + i\omega)c}, \quad (4.1.36)$$

which implies that

$$1 - \frac{\beta^2 - \omega^2}{\alpha^2} = pe^{\beta c} \cos \omega c, \quad -\frac{2\beta\omega}{\alpha^2} = pe^{\beta c} \sin \omega c. \quad (4.1.37)$$

Equations (4.1.37) give me

$$e^{-\beta c} \left(1 - \frac{\beta^2 - \omega^2}{\alpha^2}\right) \leq e^{-s_1 c} \left(1 - \frac{s_1^2}{\alpha^2}\right). \quad (4.1.38)$$

I now consider the following two cases:

Case 1: Assume that $s_1 = \beta$.

In this case, equation (4.1.38) implies that

$$e^{-\beta c} \left(1 - \frac{\beta^2 - \omega^2}{\alpha^2}\right) \leq e^{-\beta c} \left(1 - \frac{\beta^2}{\alpha^2}\right). \quad (4.1.39)$$

This will lead to a contradiction that

$$\omega^2 \leq 0. \quad (4.1.40)$$

Case 2: Assume that $s_1 > \beta > 0$.

Under this assumption, I have

$$s_1^2 > \beta^2, \quad e^{-\beta c} > e^{-s_1 c}. \quad (4.1.41)$$

Equations (4.1.38) and (4.1.39) imply that

$$1 - \frac{\beta^2 - \omega^2}{\alpha^2} \leq 1 - \frac{s_1^2}{\alpha^2} \quad (4.1.42)$$

and lead to a contradiction that

$$\omega^2 \leq \beta^2 - s_1^2 < 0. \quad (4.1.43)$$

I have shown there exists a positive real root of (4.1.12) and the smallest positive real root s_1 is smaller than all positive real parts of any complex roots of equation (4.1.12) with positive real parts, i.e., there is no oscillation behind the wave for the Laplace kernel (see Figure 4.1). \square

Example 4.1.2. Consider IDEs (3.2.13) with the kernels

$$k(x) = k_1(x) = k_2(x) = \begin{cases} \alpha e^{-\alpha x}, & \text{if } x > 0, \\ 0, & \text{if } x \leq 0, \end{cases} \quad (4.1.44)$$

the two sided Laplace transform

$$L(s) = L_1(s) = L_2(s) = \frac{\alpha}{\alpha + s}, \quad (4.1.45)$$

and the moment generating function

$$M(\lambda) = M_1(\lambda) = M_2(\lambda) = \frac{\alpha}{\alpha - \lambda}, \quad \lambda < \alpha, \quad (4.1.46)$$

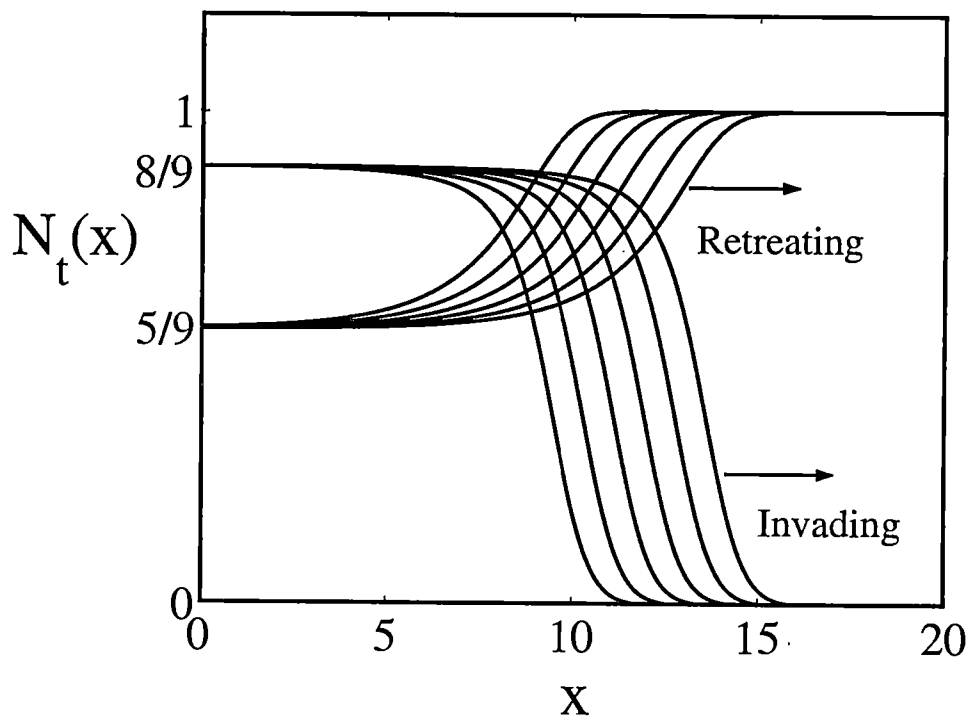


Figure 4.1: The traveling wave solution for IDEs (3.2.13) with two same Laplace kernels (4.1.31)

The population densities of the two species converge to traveling waves, that are moving to the right for $x > 0$. The first species is the invading species (approaching density $8/9$), while the second species is the retreating species (approaching density $5/9$). The parameters were chosen as $\lambda_1 = 1.2$, $\lambda_2 = 1.5$, $\beta_{12} = 0.2$, $\beta_{21} = 0.5$, $\alpha = 7.0$. The interior equilibrium is $(u^*, v^*) = (8/9, 5/9)$. There is no oscillation behind the wave.

By speed formula (3.3.15),

$$c \geq c^* = \frac{1}{\alpha - \lambda}; \quad (4.1.47)$$

which means the wave speed is positive. Since

$$L'(s) + cL(s) > \frac{\alpha(\lambda + s)}{(\alpha + s)^2(\alpha - \lambda)} \quad (4.1.48)$$

for $s \geq 0$, kernel (4.1.44) satisfies Condition 4.2. I thus conclude that if the heteroclinic connection from (u^*, v^*) to $(0, 1)$ exists, there is no oscillation behind the wave (see Figure 4.2). \square

Notice that kernel (4.1.44) does not satisfies Condition 4.1. This means that Condition 4.1.1 is only a sufficient, not a necessary condition that guarantees no oscillation behind the wave.

Unequal dispersal

In the case of unequal dispersal,

$$k_1(x) \neq k_2(x), \quad (4.1.49)$$

I define

$$F(s) \equiv [p(s) - D][q(s) - E] - B, \quad (4.1.50)$$

so that characteristic equation (4.1.8) is rewritten as

$$F(s) = 0. \quad (4.1.51)$$

I derive Condition 4.3 that guarantees no oscillation behind the wave.

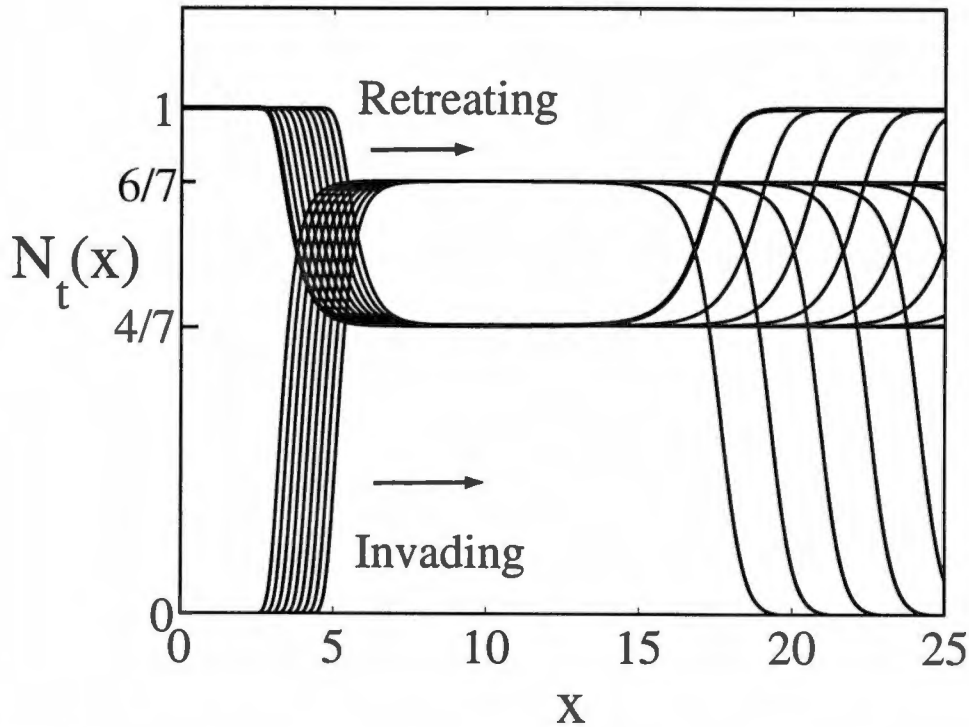


Figure 4.2: The traveling wave solution for IDEs (3.2.13) with kernels (4.1.44)

The population densities of the two species converge to right-moving traveling waves. The first species is the invading species (approaching density $6/7$), while the second species is the retreating species (approaching density $4/7$). The parameters were chosen as $\lambda_1 = \lambda_2 = 2.0$, $\beta_{12} = 0.25$, $\beta_{21} = 0.5$, $\alpha = 7.0$. The interior equilibrium is $(u^*, v^*) = (6/7, 4/7)$. There is no oscillation behind the wave.

Condition 4.3.

$$L'_i(s) + cL_i(s) > 0 \text{ for } s \geq 0, i = 1, 2. \quad (4.1.52)$$

Lemma 4.4. *If $k_1(x)$ and $k_2(x)$ satisfy Condition 4.3, then there exists at least a positive real root of the characteristic equation (4.1.8).*

Proof : By definition of $F(s)$, I have

$$F(0) = \frac{(\lambda_1 - 1)(\lambda_2 - 1)(1 - \beta_{12})(1 - \beta_{21})}{\lambda_1 \lambda_2 (1 - \beta_{12} \beta_{21})} > 0, \quad (4.1.53)$$

and

$$F'(s) = p'(s)[q(s) - D] + [p(s) - C]q'(s). \quad (4.1.54)$$

I have shown in Lemma 3.3 that if $L_1(s)$ is well-defined on $[0, \tau_1)$ and $L_2(s)$ is well-defined on $[0, \tau_2)$ (τ_1, τ_2 can be ∞), then

$$\lim_{s \rightarrow \tau_1^-} p(s) = 0 \quad \lim_{s \rightarrow \tau_2^-} q(s) = 0. \quad (4.1.55)$$

Without loss of generosity, I assume

$$\tau \equiv \min(\tau_1, \tau_2) = \tau_1 \quad (\tau_1 \geq \tau_2) \quad (4.1.56)$$

so that

$$\lim_{s \rightarrow \tau^-} p(s) = 0. \quad (4.1.57)$$

I can show there exists at least a positive real root of characteristic equation (4.1.51) by considering the following two cases:

Case 1: Assume that

$$\lim_{s \rightarrow \tau^-} F(s) < 0. \quad (4.1.58)$$

Applying Mean Value Theorem to (4.1.53) and (4.1.58), I know there exists a positive real number $s_1 \in (0, \tau)$ such that

$$F(s_1) = 0. \quad (4.1.59)$$

Case 2: Assume that

$$\lim_{s \rightarrow \tau^-} F(s) \geq 0. \quad (4.1.60)$$

Under this assumption, I have by equation (4.1.57) that

$$\lim_{s \rightarrow \tau^-} F(s) = \lim_{s \rightarrow \tau^-} [p(s) - D][q(s) - E] - B \quad (4.1.61)$$

$$= \lim_{s \rightarrow \tau^-} (-D)[q(s) - E] - B \geq 0, \quad (4.1.62)$$

which implies

$$\lim_{s \rightarrow \tau^-} [q(s) - E] < 0. \quad (4.1.63)$$

Under Condition 4.3, if I differentiate equations (4.1.10) of p and g with respect to s , I obtain

$$p'(s) = \frac{-ce^{-sc}L_1(s) - e^{-sc}L_1'(s)}{[L_1(s)]^2} < 0, \text{ for } s \geq 0, \quad (4.1.64)$$

and

$$q'(s) = \frac{-ce^{-sc}L_2(s) - e^{-sc}L_2'(s)}{[L_2(s)]^2} < 0, \text{ for } s \geq 0. \quad (4.1.65)$$

In particular, I have

$$p'(0) < 0, \quad q'(0) < 0, \quad (4.1.66)$$

and

$$F'(0) = p'(0)(1 - E) + (1 - D)q'(0) < 0. \quad (4.1.67)$$

Therefore, I have by (4.1.57), (4.1.63), (4.1.64), (4.1.65) that

$$\lim_{s \rightarrow \tau^-} F'(s) = \lim_{s \rightarrow \tau^-} \{p'(s)[q(s) - E] + [p(s) - D]q'(s)\} \quad (4.1.68)$$

$$= \lim_{s \rightarrow \tau^-} \{p'(s)[q(s) - E] - Dq'(s)\} > 0. \quad (4.1.69)$$

Applying Mean Value Theorem to (4.1.67) and (4.1.69), I know there exists $s_2 \in (0, \tau)$ such that

$$F'(s_2) = 0. \quad (4.1.70)$$

I will show by Lemma 4.5 that

$$F(s_2) < 0. \quad (4.1.71)$$

Applying Mean Value Theorem to equation (4.1.53) of $F(0)$ and equation (4.1.71), I show that there exists a positive real number $s_3 \in (0, s_2)$ such that

$$F(s_3) = 0. \quad (4.1.72)$$

□

Lemma 4.5. *Assume that $F'(\hat{s}) = 0$ for some $\hat{s} > 0$, then I have $F(\hat{s}) < 0$ under Condition 4.3.*

Proof : Under Condition 4.3, I have particularly by equation (4.1.64) of p' and equation (4.1.65) of q' that

$$p'(\hat{s}) < 0, \quad q'(\hat{s}) < 0. \quad (4.1.73)$$

By assumption, I have

$$F'(\hat{s}) = p'(\hat{s})[q(\hat{s}) - E] + [p(\hat{s}) - D]q'(\hat{s}) = 0. \quad (4.1.74)$$

It follows that

$$[p(\hat{s}) - D][q(\hat{s}) - E] \leq 0 \quad (4.1.75)$$

and

$$F(\hat{s}) = [p(\hat{s}) - D][q(\hat{s}) - E] - B \leq -B < 0. \quad (4.1.76)$$

□

In order to show that the smallest positive real root of characteristic equation (4.1.51) is smaller than all positive real parts of any complex roots of equation (4.1.51) with positive real parts, I first introduce Lemma 4.6.

Lemma 4.6. *Suppose s^* is the smallest positive real root of characteristic equation (4.1.51), I have*

$$F'(s^*) < 0, \quad (4.1.77)$$

$$p(s^*) - D > 0, \quad q(s^*) - E > 0 \quad (4.1.78)$$

under Condition 4.3

Proof : Since $F(s^*) = 0$, I have by Lemma 4.5 that

$$F'(s^*) \neq 0. \quad (4.1.79)$$

If I assume

$$F'(s^*) > 0, \quad (4.1.80)$$

and apply Mean Value Theorem to (4.1.67) of $F'(0)$ and (4.1.80), I know there exists a real number \bar{s} , $0 < \bar{s} < s^*$ such that

$$F'(\bar{s}) = 0 \quad (4.1.81)$$

Applying Lemma 4.5 to equation (4.1.81), I obtain

$$F(\bar{s}) < 0. \quad (4.1.82)$$

Applying Mean Value Theorem to equation (4.1.53) of $F(0)$ and equation (4.1.82), I know there exists a real number \hat{s} ($0 < \hat{s} < \bar{s}$) such that

$$F(\hat{s}) = 0. \quad (4.1.83)$$

This is a contradiction to the assumption that s^* is the smallest positive real root of characteristic equation (4.1.51). I thus conclude that

$$F'(s^*) < 0. \quad (4.1.84)$$

Since

$$F(s^*) = [p(s^*) - D][q(s^*) - E] - B = 0, \quad (4.1.85)$$

I have either

$$[p(s^*) - D] > 0, [q(s^*) - E] > 0 \quad (4.1.86)$$

or

$$[p(s^*) - D] < 0, [q(s^*) - E] < 0. \quad (4.1.87)$$

By inequality (4.1.84), I have

$$F'(s^*) = p'(s^*)[q(s^*) - E] + q'(s^*)[p(s^*) - D] < 0 \quad (4.1.88)$$

where

$$p'(s^*) < 0, \quad q'(s^*) < 0. \quad (4.1.89)$$

particularly by equation (4.1.64) of p' and equation (4.1.65) of q' . It follows that

$$[p(s^*) - D] > 0, \quad [q(s^*) - E] > 0. \quad (4.1.90)$$

Theorem 4.7. *Under Condition 4.3, s^* is smaller than all positive real parts of any complex roots of characteristic equation (4.1.51) with positive real parts.*

Proof : Consider any complex number $\delta = \beta + i\omega$ with $0 < \beta \leq s^*$, I am done if I can show that δ is not a root of characteristic equation (4.1.51).

By Lemma 4.2, I have

$$|p(\delta)| \begin{cases} > p(s^*), & \text{if } \beta < s^*, \\ \geq p(s^*), & \text{if } \beta = s^*. \end{cases} \quad (4.1.91)$$

and

$$|q(\delta)| \begin{cases} > q(s^*), & \text{if } \beta < s^*, \\ \geq q(s^*), & \text{if } \beta = s^*. \end{cases} \quad (4.1.92)$$

In addition, I have by (4.1.91), (4.1.92), and Lemma 4.6 that

$$|p(\delta)| - D \geq p(s^*) - D > 0, \quad |q(\delta)| - E \geq q(s^*) - E > 0. \quad (4.1.93)$$

It follows that

$$|F(\delta)| = |[p(\delta) - D][q(\delta) - E] - B| \quad (4.1.94a)$$

$$\geq |p(\delta) - D||q(\delta) - E| - B \quad (4.1.94b)$$

$$\geq ||p(\delta)| - D||q(\delta)| - E| - B \quad (4.1.94c)$$

$$= [|p(\delta)| - D][|q(\delta)| - E] - B \quad (4.1.94d)$$

$$\begin{cases} > [p(s^*) - D][q(s^*) - E] - B = F(s^*) = 0, & \text{if } \beta < s^*, \\ \geq [p(s^*) - D][q(s^*) - E] - B = F(s^*) = 0, & \text{if } \beta = s^*. \end{cases} \quad (4.1.94e)$$

I now consider the following two cases:

Case 1: Assume that

$$\beta < s^*. \quad (4.1.95)$$

In this case, I have by (4.1.94e) that

$$|F(\delta)| > 0, \quad (4.1.96)$$

which implies

$$F(\delta) \neq 0. \quad (4.1.97)$$

and δ is not a root of equation (4.1.54) of F' .

Case 2: Assume that

$$\beta = s^*. \quad (4.1.98)$$

If $F(\delta) = F(\beta + i\omega) = 0$, then “=” hold on (4.1.94b), (4.1.94c), and (4.1.94e). Since “=” holds on (4.1.94e) for $\beta = s^*$, I have

$$|p(\delta)| = p(s^*) \text{ and } |q(\delta)| = q(s^*). \quad (4.1.99)$$

In addition, I have

$$|p(\delta) - D| = |p(\delta)| - D \text{ and } |q(\delta) - E| = |q(\delta)| - E \quad (4.1.100)$$

because “=” hold on (4.1.94c) and (4.1.94e). This implies

$$p(\delta) \in R, q(\delta) \in R, \text{ and } p(\delta) > 0, q(\delta) > 0. \quad (4.1.101)$$

(4.1.99), (4.1.101) imply that

$$|p(\delta)| = p(\delta) = p(\beta + i\omega) = p(s^* + i\omega) = p(s^*) \in R, \quad (4.1.102)$$

which is a contradiction to appendix A (Lemma A.1) that

$$\text{if } p(\beta + i\omega) = p(s^*) \in R, \text{ then } \beta \neq s^*. \quad (4.1.103)$$

I have shown from above that s^* is smaller than all positive real parts of any complex roots of characteristic equation (4.1.51) with positive real parts.

Lemma 4.4 and Theorem 4.7 imply that there is no oscillation behind the wave under Condition 4.3.

Example 4.1.3. Consider

$$k_1(x) = \frac{1}{2}\alpha_1 e^{-\alpha_1|x|} \quad (4.1.104)$$

and

$$k_2(x) = \begin{cases} \alpha_2 e^{-\alpha_2 x}, & \text{if } x > 0, \\ 0, & \text{if } x \leq 0, \end{cases} \quad (4.1.105)$$

with the two sided Laplace transform

$$L_1(s) = \frac{\alpha_1^2}{\alpha_1^2 - s^2}, \quad L_2(s) = \frac{\alpha_2}{\alpha_2 + s}, \quad (4.1.106)$$

where $|s| < \alpha_1$.

Since kernels (4.1.104) and (4.1.105) satisfies Condition 4.3. I thus conclude that if the heteroclinic connection from (u^*, v^*) to $(0, 1)$ exists, there is no oscillation behind the wave (see Figure 4.3).

Notice that the method shown in this section for unequal dispersal can also be applied to the special case of equal dispersal.

4.2 Discussion

In chapter 3 and chapter 4, I analyzed the traveling wave solution for a two-species competition model based on IDEs. I derived the speed of invasion by linearized near the equilibrium at the front of the wave. I also analyzed the behavior behind the wave and derived some sufficient conditions that

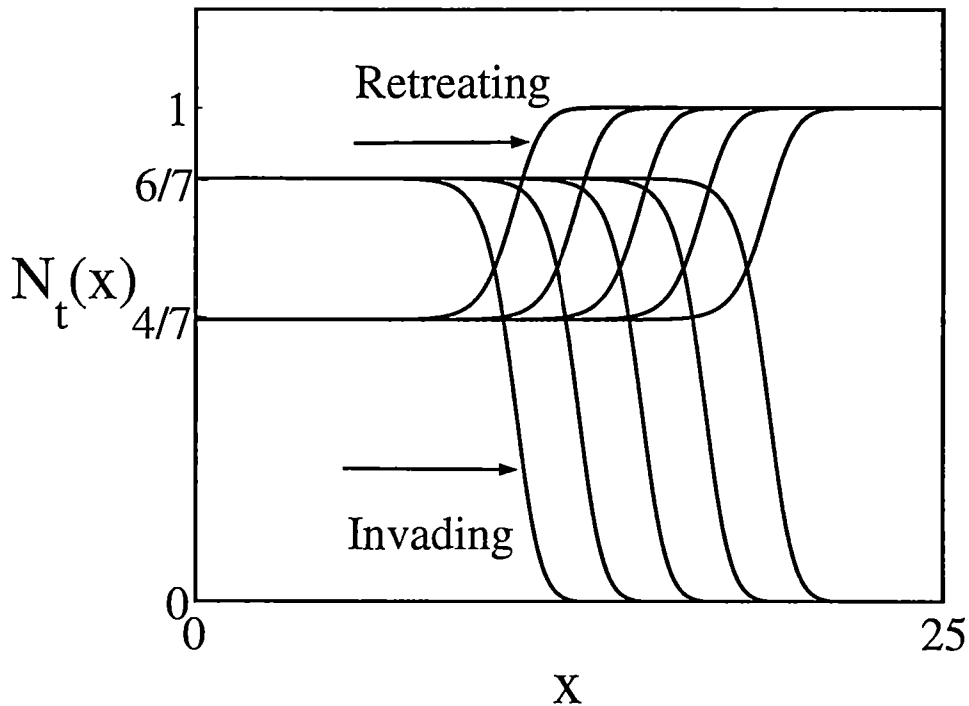


Figure 4.3: The traveling wave solution for IDEs (3.2.13) with kernels (4.1.104) and (4.1.105)

The population densities of the two species converge to traveling waves, that are moving to the right for $x > 0$. The first species is the invading species (approaching density $6/7$), while the second species is the retreating species (approaching density $4/7$). The parameters were chosen as $\lambda_1 = \lambda_2 = 2.0$, $\beta_{12} = 0.25$, $\beta_{21} = 0.5$, $\alpha_1 = 7.0$, and $\alpha_2 = 5.0$. The interior equilibrium is $(u^*, v^*) = (6/7, 4/7)$. There is no oscillation behind the wave.

guarantee no oscillation behind the wave. However, I have shown by an example that linearization may not give the correct spread rate because of a weak Allee effect.

In chapter 2, I considered a reaction-diffusion equation with a weak Allee effect. I concluded that linearization may still give the correct spread rate for a sufficiently weak Allee effect and may fail to give the correct speed for an insufficiently weak Allee effect. I also found that this result applied to two-species models based on IDEs. However, I could not determine the sufficient or necessary conditions for the linearization to be valid for my competition model. I hope to complement this in future research.

Bibliography

Bibliography

- [1] Allee, W. C., *Animal Aggregations*, The University of Chicago Press, Illinois, 1931.
- [2] Allee, W. C., *The Social Life of Animals*, W. W. Norton and Co., New York, 1938.
- [3] Allen, E. J., Allen, L. J. S., and Gilliam, X., Dispersal and competition models for plants, *J. Math. Biol.*, **34** (1996), 445-481.
- [4] Allison, T. D., Pollen production and plant density affect pollination and seed production in *Taxus Canadensis*, *Ecology*, **71** (1990), 516-522.
- [5] Alvarez, L. H. R., Optimal harvesting under stochastic fluctuations and critical depensation, *Math. Biosci.*, **152** (1998), 63-85.
- [6] Andersen, M., Properties of some density-dependent integrodifference-equation population models, *Math. Biosci.*, **104** (1991), 135-157.
- [7] Anselone, P. M., and Sloan, I. H., Numerical solutions of integral equations on the half line II: the Wiener-Hopf case, *J. Integ. Eqs. Appl.*, **1** (1988), 203-225.

- [8] Apostol, T. M., *Mathematical Analysis*, Addition-Wesley Publishing Company, Inc., 1974.
- [9] Aronson, D. G., and H. F. Weinberger, Nonlinear diffusion in population genetics, combustion, and nerve pulse propagation, in: J. A. Goldstein, (Ed.), *Partial Differential Equations and Related Topics, Lecture Notes in Mathematics*, 446, Springer, New York, 1975, pp. 5-49.
- [10] Aronson, D. G., and H. F. Weinberger, Multidimensional nonlinear diffusion arising in population genetics, *Adv. Math.*, **30** (1978), 33-76.
- [11] Atkinson, K., The numerical solution of integral equations on the half-line, *SIAM J. Numer. Anal.*, **6** (1969), 375-397.
- [12] Auger, P., Bravo De La Parra, R., and Sanchez, E., Hawk-Dove game and competition dynamics, *Math. Comput. Modeling*, **27** (1988), 89-98.
- [13] Banks, R. B., *Growth and Diffusion Phenomena: Mathematical Frameworks and Applications*, Springer-Verlag, Berlin, Germany, 1994.
- [14] Beverton, R. J. H., and Holt, S. J., On the dynamics of exploited fish populations, *Fish. Invest. Lond., ser. 2*, **19** (1957),
- [15] Brewster, C. C., and Allen, J. C., Spatiotemporal model for studying insect dynamics in large-scale cropping systems, *Environ. Entomol.*, **26** (1997), 473-482.

- [16] Brewster, C. C., Allen, J. C., Schuster, D. J., and Stansly, P. A., Simulating the dynamics of *Bemisia argentifoli* (Homoptera: Aleyrodidae) in an organic cropping system with a spatiotemporal model, *Environ. Entomol.*, **26** (1997), 603–616.
- [17] Britton, N. F., *Reaction-Diffusion Equations and their Applications to Biology*, Academic Press, London, 1986.
- [18] Chapman, R. N., The quantitative analysis of environmental factors, *Ecology*, **9** (1928), 111–122.
- [19] Clark, C. W., *Mathematical Bioeconomics: The Optimal Management of Renewable Resource*, John Wiley and Sons, New York, 1990.
- [20] Clark, J. S., Why trees migrate so fast: confronting theory with dispersal biology and the paleorecord, *Am. Nat.*, **152** (1998), 204–224.
- [21] Cruickshank, I., Gurney, W. S. C., and Veitch, A. R., The characteristics of epidemics and invasions with thresholds, *Theor. Pop. Biol.*, **56** (1999), 279–292.
- [22] Dennis, B., Allee effects: population growth, critical density, and the chance of extinction, *Nat. Res. Model.*, **3** (1989), 481–538.
- [23] Drake, J. A. Mooney, H. A., di Castri, F., Groves, R. H., Kruger, F. J., Rejmanek, M., and Williamson, M., *Biological Invasions: A Global Perspective*, John Wiley and Sons, Chichester, UK, 1989.

- [24] Eilbeck, J. C., and Lopez-Gomez, J., On the periodic Lotka–Volterra competition model, *J. Math. Anal. Appl.*, **210** (1997), 58–87.
- [25] Feinsinger, P., and Tiebout III, H. M., Do tropical bird-pollinated plants exhibit density-dependent interactions? Field experiments, *Ecology*, **72** (1991), 1953–1963.
- [26] Fife, P. C., and Mcleod, S. B., The approach of solutions of nonlinear diffusion equations to travelling front solutions, *Arch. Rat. Mech. Anal.*, **65** (1975), 335–361.
- [27] Fife, P. C., *Mathematical Aspects of Reacting and Diffusing Systems*, Springer, Berlin, 1979.
- [28] Fisher, R. A., The wave of advance of advantageous genes, *Ann. Eugen.*, **7** (1937), 353–369.
- [29] Fowler, C. W., and Baker, J. D., A review of animal population dynamics at extremely reduced population levels, *Rep. Int. Whal. Commn.*, **41** (1991), 545–554.
- [30] Friedman, A., *Foundations of Modern Analysis*, Holt, Rinehart, and Winston, Inc., New York, 1970.
- [31] Gardner, R. A., Existence and stability of traveling wave solutions of competition models: a degree theoretic approach, *J. Diff. Eqns.*, **44** (1982), 343–364.

- [32] Gohberg, I. C., and Fel'dman, I. A., *Convolution Equations and Projection methods for their solution*, American Mathematical Society, Providence, Rhode Island, 1974.
- [33] Groom, M. J., Allee effects limit population viability of an annual plant, *Am. Nat.*, **151** (1998), 487–496.
- [34] Gruntfest, Y., Arditi, R., and Dombrovsky, Y., A fragmented population in a varying environment, *J. Theor. Biol.*, **185** (1997), 539–547.
- [35] Hadeler, K. P., Rothe, F., Travelling fronts in nonlinear diffusion equations, *J. Math. Biol.*, **2** (1975), 251–263.
- [36] Hardin, D. P., Takac, P., and Webb, G. F., A comparison of dispersal strategies for survival of spatially heterogeneous populations, *SIAM J. Appl. Math.*, **48** (1988a), 1396–1423.
- [37] Hardin, D. P., Takac, P., and Webb, G. F., Asymptotic properties of a continuous-space discrete-time population model in a random environment, *J. Math. Biol.*, **26** (1988b), 361–374.
- [38] Hardin, D. P., Takac, P., and Webb, G. F., Dispersion population models discrete in time and continuous in space, *J. Math. Biol.*, **28** (1990), 1–20.
- [39] Hart, D. R., and Gardner, R. H., A spatial model for the spread of invading organisms subject to competition, *J. Math. Biol.*, **35** (1997), 935–948.

- [40] Hassell, M. P., and Comins, H. N., Discrete time models for two-species competition, *Theor. Pop. Biol.*, **9** (1976), 202–221.
- [41] Hastings, A., and Higgins, K., Persistence of transients in spatially structured ecological models, *Science*, **263** (1994), 1133–1136.
- [42] Hengeveld, R., *Dynamics of Biological Invasions*, Chapman and Hall, London, UK, 1990.
- [43] Hochstadt, H., *Integral Equations*, John Wiley and Sons, Inc. New York, 1973.
- [44] Hoog, F. D., and Sloan I. H., The finite-section approximation for integral equations on the half-line, *J. Austral. Math. Soc. Ser.*, **B 28** (1987), 415–434.
- [45] Hopf, F. A., and Hopf, F. W., The role of the Allee effect in species packing, *Theor. Pop. Biol.*, **27** (1985), 27–50.
- [46] Hopper, K. R., and Roush, R. T., Mate finding, dispersal, number released, and the success of biological control introductions, *Ecol. Entomol.*, **18** (1993), 321–331.
- [47] Hosono, Y., Traveling waves for a diffusive Lotka–Volterra competition model II: a geometric approach, *Forma*, **10** (1995), 235–257.
- [48] Hosono, Y., The minimal speed of traveling fronts for a diffusive Lotka–Volterra competition model, *Bull. Math. Biol.*, **60** (1998), 435–448.

- [49] Jones, D. S., and Sleeman, B. D., *Differential Equations and Mathematical Biology*, G. Allen and Unwin, London, UK, 1983.
- [50] Kanel, J. I., and Zhou, L., Existence of wave front solutions and estimates of wave speed for a competition-diffusion system, *Nonlin. Anal. TMA.*, **27** (1996), 579–587.
- [51] Kan-on Y., Instability of stationary solutions for a Lotka–Volterra competition model with diffusion, *J. Math. Anal. Appl.*, **208** (1997), 158–170.
- [52] Kan-on Y., Bifurcation structure of stationary solutions of a Lotka–Volterra competition model with diffusion, *SIAM J. Math. Anal.*, **29** (1998), 424–436.
- [53] Kan-on Y., Existence of positive traveling waves for generic Lotka–Volterra competition model with diffusion, *Dynamics of Continuous, Discrete and Impulsive System*, **6** (1999), 345–365.
- [54] Keener, J., and Sneyd, J., *Mathematical Physiology*, Springer-Verlag, New York, 1998.
- [55] King, C. E., and Dawson, P. S., Population biology and the *Tribolium* model, In: T. Dobzhansky, M. K. Hecht, W. C. Steere, (Ed.), *Evolutionary Biology*, **5** New York, 1972, pp. 133–227.

- [56] Kolmogorov, A., Petrovsky, I., and Piscounoff, N., Etude de l'équation de la diffusion avec croissance de la quantité de matière et son application à un problème biologique, *Mosc. Univ. Bull. Math.*, **1** (1937), 1–25.
- [57] Kot, M., Diffusion-driven period-doubling bifurcations, *Biosystems*, **22** (1989), 279–287.
- [58] Kot, M., Discrete-time traveling waves: ecological examples, *J. Math. Biol.*, **30** 413–436 (1992)
- [59] Kot, M., and Schaffer, W. M., Discrete-time growth-dispersal models. *Math. Biosci.*, **80** (1986), 109–136.
- [60] Kot, M., Lewis, M. A., and van den Driessche, P., Dispersal data and the spread of invading organisms, *Ecology*, **77** (1996), 2027–2042.
- [61] Kunin, W. E., Density and reproductive success in wild populations of *Diplotaxis eruroides* (Brassicaceae), *Oecologia*, **91** (1992), 129–133.
- [62] Kunin, W. E., Sex and the single mustard: population density and pollinator behavior effects on seed-set, *Ecology*, **74** (1993), 2145–2160.
- [63] Kuussaari, M., Saccheri, I., Camara, M., and Hanski, I., Allee effect and population dynamics in the Glanville fritillary butterfly, *Oikos*, **82** (1998), 384–392.

- [64] Lamont, B. B., Klinkhamer, P. G. L., and Witkowski, E. T. F., Population fragmentation may reduce fertility to zero in *Banksia goodii* — a demonstration of the Allee effect, *Oecologia*, **94** (1993), 446–450.
- [65] Latore, J., Gould P., and Mortimer, A. M., Spatial dynamics and critical patch size of annual plant populations. *J. Theor. Biol.*, **190** (1998), 277–285.
- [66] Lewis, M. A., and Kareiva, P., Allee dynamics and the spread of invading organisms, *Theor. Pop. Biol.*, **43** (1993), 141–158.
- [67] Lewis, M. A., and P. van den Driessche, Waves of extinction from sterile insect release, *Math. Biosci.*, **116** (1993), 221–247.
- [68] Lotka, A. J., *Elements of Physical Biology*, Williams and Wilkins, Baltimore, 1925.
- [69] Ludwig, D., Management of stocks that may collapse, *Oikos*, **83** (1998), 397–402.
- [70] Lui, R., A nonlinear integral operator arising from a model in population genetics, I. Monotone initial data, *SIAM J. Math. Anal.*, **13** (1982a), 913–937.
- [71] Lui, R., A nonlinear integral operator arising from a model in population genetics, II. Initial data with compact support, *SIAM J. Math. Anal.*, **13** (1982b), 938–953.

- [72] Lui, R., Existence and stability of traveling wave solutions of a nonlinear integral operator, *J. Math. Biol.*, **16** (1983), 199–220.
- [73] Maclagan, D. S., The effect of population density upon rate of reproduction with special reference to insects, *Proc. R. Soc. London*, **B 111** (1932), 437–454.
- [74] McCarthy, M. A., The Allee effect, finding mates and theoretical models. *Ecol. Model.*, **103** (1997), 99–102.
- [75] Mollison, D., Dependence of epidemics and population velocities on basic parameters, *Math. Biosc.*, **107** (1991), 255–287.
- [76] Mooney, H. A., and Drake, J. A., *Ecology of Biological Invasions of North America and Hawaii.*, Springer-Verlag, New York, 1986.
- [77] Neubert, M. G., Kot, M., and Lewis, M. A., Dispersal and pattern formation in a discrete-time predator-prey model, *Theor. Pop. Biol.*, **48** (1995), 7–43.
- [78] Neubert, M. G., A simple population model with qualitatively uncertain dynamics, *J. Theor. Biol.*, **189** (1997), 399–411.
- [79] Neubert, M. G., and Caswell, H., Dispersal and demography: calculation and sensitivity analysis of invasion speeds for stage-structured populations, *Ecology.*, In press, 2000.

- [80] Odum, E. P., *Fundamentals of Ecology*, W. B. Saunders Co., Philadelphia, 1971.
- [81] Odum, H. T., and W. C. Allee, A note on the stable point of populations showing both intraspecific cooperation and disoperation, *Ecology*, **35** (1954), 95–97.
- [82] Okubo, A., *Diffusion and Ecological Problems: Mathematical Models*, Springer, Berlin, 1980.
- [83] Okubo, A., Maini, P. K., Williamson, M. H., and Murray, J. D., On the spatial spread of the grey squirrel in Britain, *Proc. R. Soc. Lond. B* **238** (1989), 113–125.
- [84] Olver, A., *Asymptotic and Special functions*, 1974.
- [85] Padrón, V., and Trevisan, M. C., Effect of aggregating behavior on population recovery on a set of habitat islands, *Math. Biosci.*, **165** (2000), 63–78.
- [86] Park, T., Studies in population physiology: The relation of numbers to initial population growth in the flour beetle *tribolium confusum* duval, *Ecology*, **8** (1932), 172–181.
- [87] Petersen, W., The relation of density of population to rate of reproduction in *Paramecium caudatum*, *Physiol. Zool.*, **2** (1929), 221–254.

- [88] Pipkin, A. C., *A Course on Integral Equations*. Springer-Verlag, New York, 1991.
- [89] Press, W. H., Flannery B. P., Teukolsky, S. A., and Vetterling, W. T., *Numerical recipes: The Art of Scientific Computing*, Cambridge University Press, Cambridge, 1986.
- [90] Ricker, W. E., Stock and recruitment. *J. Fish. Res. Board. Can.*, **11** (1954), 559-623.
- [91] Robertson, T. B., Experimental studies on cellular reproduction. II, The influence of mutual contiguity upon redproductive rate in Infusoria, *Ibid.*, **15** (1921), 612-619.
- [92] Rothe, F., Convergence to pushed fronts, *Rocky Mountain J. Math.*, **11** (1981), 617-633.
- [93] Sánchez-Garduño, F., and P. H. Maini, Travelling wave phenomena in non-linear diffusion degenerate Nagumo equations, *J. Math. Biol.*, **35** (1997), 713-728.
- [94] Shigesada, N., and Kawasaki, K., *Biological Invasions: Theory and Practice*, Oxford University Press, Oxford, UK, 1997.
- [95] Skellam, J. G., Random dispersal in theoretical populations, *Biometrika.*, **38**(1951), 196-218.

- [96] Sloan, I. H., and Spence, A., Integral Equations on the half-line: a modified finite-section approximation, *Math. Comp.*, **47** (1986), 589–595.
- [97] Turchin, P., and Kareiva, P., Aggregation in *Aphis Varians*: An effective strategy for reducing predation risk, *Ecology*, **70** (1989), 1008–1016.
- [98] van den Bosch, F., Metz, J. A. J., and Diekmann, O. The velocity of population spatial expansion. *J. Math. Biol.*, **28** (1990), 529–565.
- [99] Van Kirk, R. W., and Lewis, M. A., Integrodifference models for persistence in fragmented habitats, *Bull. Math. Biol.*, **59** (1997), 107–138.
- [100] Veit, R. R., and Lewis, M. A., Dispersal, population growth, and the Allee effect, Dynamics of the House Finch invasion of eastern North America, *Am. Nat.*, **148** (1996), 255–274.
- [101] Volterra, V., Variazioni e fluttuazioni del numero d'individui in specie animali conviventi, *Mem. Acad. Lincei.*, **2** (1926), 31–113.
- [102] Wang, M. H., Kot, M., and Neubert, M. G., Integrodifference equations, Allee effects, and invasions, *J. Math. Biol.*, (2000), In review.
- [103] Weinberger, H. F., Asymptotic behavior of a model of population genetics, In, Chadam, J. (Ed.), *Nonlinear Partial Differential Equations and Applications*, Lecture Notes in Mathematics, **648** (1978), 47–98.

- [104] Weinberger, H. F., Long-time behavior of a class of biological models,
SIAM J. Math. Anal., **13** (1982),353–396.
- [105] Wheeden, R. L., and Zygmund, A., *Measure and Integral: An Introduction to Real Analysis*, Marcel Dekker, Inc. New York, 1977.

Appendix

Appendix A

Suppose s_1 is a positive real root and $s = \beta + i\omega$ ($\beta > 0$) is a complex root of the equation

$$p(s) \equiv \frac{e^{-sc}}{L(s)} = p. \quad (\text{A.1})$$

The objective of this appendix is to show that $s_1 \neq \beta$ and that if the kernel satisfies Assumption A.1, then $s_1 < \beta$.

Equation (A.1) can be rewritten as

$$\frac{1}{p} = L(s)e^{sc}, \quad (\text{A.2})$$

where

$$\begin{aligned} L(s) &\equiv \int_{-\infty}^{\infty} k(z)e^{-sz} dz \\ &= \int_{-\infty}^0 k(z)e^{-sz} dz + \int_0^{\infty} k(z)e^{-sz} dz \\ &= \int_0^{\infty} k(-z)e^{sz} dz + \int_0^{\infty} k(z)e^{-sz} dz \\ &= \int_0^{\infty} [k(z)e^{-sz} + k(-z)e^{sz}] dz. \end{aligned} \quad (\text{A.3})$$

Therefore,

$$L(\beta + i\omega) = \int_0^{\infty} k(z)e^{-(\beta+i\omega)z} + k(-z)e^{(\beta+i\omega)z} dz. \quad (\text{A.4})$$

Since s_1 is a positive real root of equation (A.1), s_1 satisfies

$$L(s_1)e^{s_1c} = \frac{1}{p}, \quad (\text{A.5})$$

or

$$e^{s_1 c} \int_0^{\infty} [k(z)e^{-s_1 z} + k(-z)e^{s_1 z}] dz = \frac{1}{p}. \quad (\text{A.6})$$

For complex root $s = \beta + i\omega$ of equation (A.1) with $\beta > 0$, I have

$$L(\beta + i\omega)e^{(\beta+i\omega)c} = \frac{1}{p}, \quad (\text{A.7})$$

or

$$e^{(\beta+i\omega)c} \left\{ \int_0^{\infty} [k(z)e^{-(\beta+i\omega)z} + k(-z)e^{(\beta+i\omega)z}] dz \right\} = \frac{1}{p}. \quad (\text{A.8})$$

Equation (A.8) can be written as

$$e^{\beta c} \left\{ \int_0^{\infty} [k(z)e^{-\beta z} e^{i\omega(c-z)} + k(-z)e^{\beta z} e^{i\omega(c+z)}] dz \right\} = \frac{1}{p}. \quad (\text{A.9})$$

Lemma A.1 shows that $s_1 \neq \beta$.

Lemma A. 1. $s_1 \neq \beta$, where $s_1 > 0$ and $\beta > 0$.

Proof : If $s_1 = \beta$, equations (A.6) and (A.9) imply that

$$\begin{aligned} & e^{s_1 c} \int_0^{\infty} [k(z)e^{-s_1 z} + k(-z)e^{s_1 z}] dz \\ &= e^{\beta c} \int_0^{\infty} [k(z)e^{-\beta z} + k(-z)e^{\beta z}] dz \end{aligned} \quad (\text{A.10})$$

$$\begin{aligned} &= e^{\beta c} \int_0^{\infty} k(z)e^{-\beta z} \cos \omega(z-c) dz \\ &+ e^{\beta c} \int_0^{\infty} k(-z)e^{\beta z} \cos \omega(z+c) dz. \end{aligned} \quad (\text{A.11})$$

Deleting $e^{\beta c}$ terms and redistributing equation (A.11), I obtain

$$\begin{aligned} & \int_0^{\infty} k(z)e^{-\beta z} [1 - \cos \omega(z-c)] dz \\ &= \int_0^{\infty} k(-z)e^{\beta z} [\cos \omega(z+c) - 1] dz. \end{aligned} \quad (\text{A.12})$$

Since

$$\int_0^{\infty} k(z)e^{-\beta z}[1 - \cos \omega(z - c)]dz \geq 0 \quad (\text{A.13})$$

and

$$\int_0^{\infty} k(-z)e^{\beta z}[\cos \omega(z + c) - 1]dz \leq 0, \quad (\text{A.14})$$

equation (A.12) guarantees that

$$\int_0^{\infty} k(z)e^{-\beta z}[1 - \cos \omega(z - c)]dz = 0, \quad (\text{A.15})$$

and

$$\int_0^{\infty} k(-z)e^{\beta z}[\cos \omega(z + c) - 1]dz = 0. \quad (\text{A.16})$$

It follows that $\cos \omega(z + c) = 1$ almost everywhere for z in $(0, \infty)$ and leads to a contradiction that $\omega = 0$. I thus conclude that $s_1 \neq \beta$.

Assumption A. 1. $k(z) \leq k(-z)$ almost everywhere for z in $(0, \infty)$.

Lemma A. 2. Under Assumption A.1, I have $\beta > s_1$ for $s_1 > 0$ and $\beta > 0$.

Proof : I have shown from Lemma A.1 that $s_1 \neq \beta$.

If $\beta < s_1$, I have

$$e^{\beta c} < e^{s_1 c}. \quad (\text{A.17})$$

In addition, equations (A.6) and (A.9) give me

$$\begin{aligned} & e^{s_1 c} \int_0^{\infty} [k(z)e^{-s_1 z} + k(-z)e^{s_1 z}]dz \\ &= e^{\beta c} \int_0^{\infty} [k(z)e^{-\beta z} \cos \omega(z - c) + k(-z)e^{\beta z} \cos \omega(z + c)] dz. \end{aligned} \quad (\text{A.18})$$

It follows that

$$\begin{aligned} & \int_0^{\infty} [k(z)e^{-s_1z} + k(-z)e^{s_1z}]dz \\ < \int_0^{\infty} [k(z)e^{-\beta z} \cos \omega(z-c) + k(-z)e^{\beta z} \cos \omega(z+c)] dz, \end{aligned} \quad (\text{A.19})$$

which reduces to

$$\begin{aligned} & \int_0^{\infty} k(-z)[e^{s_1z} - e^{\beta z} \cos \omega(z+c)]dz \\ < \int_0^{\infty} k(z)[e^{-\beta z} \cos \omega(z-c) - e^{-s_1z}]dz. \end{aligned} \quad (\text{A.20})$$

Since $-1 \leq \cos \omega(z-c) \leq 1$ and $-1 \leq \cos \omega(z+c) \leq 1$, I have

$$\int_0^{\infty} k(z)[e^{-\beta z} \cos \omega(z-c) - e^{-s_1z}]dz \leq \int_0^{\infty} k(z)[e^{-\beta z} - e^{-s_1z}]dz, \quad (\text{A.21})$$

and

$$\int_0^{\infty} k(-z)[e^{s_1z} - e^{\beta z}]dz \leq \int_0^{\infty} k(-z)[e^{s_1z} - e^{\beta z} \cos \omega(z+c)]dz. \quad (\text{A.22})$$

It follows that

$$\int_0^{\infty} k(-z)[e^{s_1z} - e^{\beta z}]dz < \int_0^{\infty} k(z)[e^{-\beta z} - e^{-s_1z}]dz. \quad (\text{A.23})$$

Moreover, I have for $z \geq 0$ that

$$e^{-\beta z} - e^{-s_1z} - e^{s_1z} + e^{\beta z} = e^{-\beta z}[1 - e^{(\beta-s_1)z}] - e^{\beta z}[e^{(s_1-\beta)z} - 1] \quad (\text{A.24})$$

$$< e^{-\beta z}[1 - e^{(\beta-s_1)z}] - e^{-\beta z}[e^{(s_1-\beta)z} - 1]$$

$$= (-e^{-\beta z})[e^{(\beta-s_1)z} - 2 + e^{(s_1-\beta)z}]$$

$$= (-e^{-\beta z})[e^{\frac{(\beta-s_1)z}{2}} + e^{\frac{(s_1-\beta)z}{2}}]^2 < 0. \quad (\text{A.25})$$

This implies that

$$e^{-\beta z} - e^{-s_1 z} < e^{s_1 z} - e^{\beta z}. \quad (\text{A.26})$$

By Assumption A.1 and (A.26), I thus have

$$\int_0^\infty k(z)[e^{-\beta z} - e^{-s_1 z}]dz \leq \int_0^\infty k(-z)[e^{s_1 z} - e^{\beta z}]dz, \quad (\text{A.27})$$

which is a contradiction to inequality (A.23). I have shown from the above that $s_1 < \beta$.

From the above discussion, I conclude that $s_1 \neq \beta$. Under Assumption A.1, I have $s_1 < \beta$, which means that the positive real root s_1 is smaller than all positive real parts of any complex roots of equation (A.1) with positive real parts.

Vita

Mei-Hui Wang was born in Taichung, Taiwan on November 29, 1969. She graduated from The First Taichung Girl's High School in June, 1988. The following September, she entered National Tsing-Hua University, Hsinchu, Taiwan, where she received a Bachelor of Science degree in Applied Mathematics in June, 1992 and a Master's degree in Applied Mathematics in June, 1994. During her study at National Tsing-Hua University, she was awarded Chinese Culture and National Science Scholarship (1989), Mr. Chang Bai-Chin Memorial Scholarship (1989 and 1990), Mr. Hu Memorial Scholarship (1990 and 1991), Mr. Chow of Academic Sinica Memorial Scholarship (1992), and the Ministry of Education Graduate Fellowship (1992-1994). In January, 1994, Mei-hui was elected as a Phi Tau Phi Scholar of Phi Tau Phi Scholars Association of the Republic of China. In August, 1994, she entered the University of Tennessee, where in May, 1996 she received a Master's degree in Mathematics and continued her study toward a Doctoral degree with a major in Mathematics.